

LS-40

November 21, 1985

Magnetic Field Measurements and Analysis
For an Aladdin Dipole Magnet

by

Kenneth M. Thompson
Electromagnetic Technology Program
Argonne National Laboratory
Argonne, IL 60439

	<u>Page</u>
Summary	i
A. Introduction.....	1
1. Magnet Description	1
2. Measuring System	1
3. Data Descriptions	3
B. Equipment	5
1. Probe Positioning System	5
a. Description	5
b. Calibration	7
2. Field Probe	7
a. Calibration	8
b. Probe Center	9
1. Method	9
2. Repeatability	9
c. Hall Gaussmeter Parameters	10
3. Auxiliary Probes	10
4. Optical Alignment Equipment	13
5. Power Supply	13
6. Magnet Cooling Water System	14
7. Support	14
a. Magnet	14
b. Manipulator	14
C. Coordinate Systems.....	17
1. Magnet (Absolute)	17
2. Measuring System	19
D. Alignment of Magnet and Manipulator.....	21
1. Magnet	21
a. Installation	21
b. Level	21
c. Horizontal Orientation	23
2. Manipulator	23
a. Level	23
b. Primary Reference Point	24
c. Rotation Angle	24
d. Probe Location	25
E. Gap measurements.....	27
1. Pole Faces	27
a. Level	27
b. Gap Height and Geometrical Midplane	28
2. Gap Height vs Current	28
F. Vertical Field Measurements.....	31

1. Turn-On, Turn-Off, and Warm-Up Procedures	31
2. Data Taking Details	31
a. Geometries	31
1. Universe	31
2. Scan Lines	32
b. Multiple Readings	34
c. Readings Taken During a Scan	34
1. Parameters Measured	34
2. Repeatability of Vertical Field Measurements	35
d. Reference Checks	35
e. Storage Media and Data Files	36
f. Estimated Measurement Error	37
G. Data Analysis Programs.....	41
1. Data Presentation	41
a. Tabular Listings	41
1. Field, and X, Y, Z Coordinates	41
2. Logged Readings of Auxiliary Probes	42
b. 3D Plots of Field Values	42
2. Normalize, Match, and Merge	42
3. Field Integration	43
4. Least Squares Fitting	44
5. Harmonic Field Coefficients	45
6. Vertical Midplane	46
H. Results	47
1. Field vs Current	47
2. Field Integrals	49
3. Effective Lengths	52
4. Harmonic Field Coefficients	54
a. Estimated Measurement Error	54
b. Radial Scan Length Used	54
c. Degree of Polynomial Used	55
d. Harmonic Coefficient Values	56
1. Representative Coefficient Errors	56
2. Representative Relative Strengths of Harmonics	57
3. Central Gap vs the Gap Ends	58
4. Left Side vs Both Sides	59
5. Coefficient Lists	60
6. Coefficients vs Y (vertical)	61
7. Coefficients vs Z (axial)	63
5. Vertical Midplane	66
I. Magnetostatic Field Calculation.....	69
J. Discussions.....	73
Acknowledgments and References.....	80
Appendices Index.....	81

Summary

In January 1985, the task of measuring the vertical magnetic fields in one of the dipole magnets built for the Aladdin ring at the University of Wisconsin began at Argonne National Laboratory. The primary goal of this effort was to determine the harmonic field coefficients for the magnet; a secondary goal was to determine the location of the magnetic midplane.

There already existed at Argonne most of the major parts of the measuring system that was used for this work; some modifications and additions had to be made, however, in the hardware and software components to accommodate the specific requirements of this magnet. Only the vertical component of the magnetic field at each point in the scan geometry was measured using a Hall probe. The field values were measured on seven horizontal planes each containing up to 2037 points extending across the gap between ± 7.62 cm with respect to the gap center and to about 41.73 cm from each end of the magnet core. The points were located on lines parallel to the X-axis, called "radial" lines, and on axial lines that were at fixed distances from the center path through the scan geometry. The elevations of the planes extended over ± 1.727 cm with respect to the geometrical midplane. The factors contributing to the measurement errors for the field values were determined mostly through explicit measurements. The estimated measurement errors were 4.7 Gauss (0.04%) for runs with central field values between 1.2 and 1.6 T and 2.4 Gauss (0.16%) for central fields around 0.15 T.

The dependency of the central field on the magnet current was determined. Since the magnet has a C-core, the gap height decreases with increasing current. This variation was measured from 0A to 1.2 kA; the total change in the gap height at the magnet center (0,0) at an excitation of 1000 MeV (1018 A) was found to be $153 \mu\text{m} \pm 28 \mu\text{m}$.

The vertical field values were measured at three excitations corresponding to circulating electron beam energies of 1000 MeV, 800 MeV, and 100 MeV. The most complete measurements were done at 1000 MeV. The next most complete data was taken for 100 MeV, the injection energy and only a few representative runs were done for 800 MeV, the current operating energy of the ring. These vertical field values were integrated along axial paths through the geometry. The integrals for paths located at distances between ± 5.08 cm from the center of the gap were found and the results were used to calculate the harmonic coefficients.

A representative set of coefficient values and the associated standard errors are shown in Table i.

Table i

Harmonic Coefficients for 1000 MeV and Y = 0

Type	i	b_i		
Dipole	0	$1.7563 \pm 5 \times 10^{-6}$	T-m	
Quadrupole	1	0.0783 ± 0.0005	T-m/m ²	
Sextupole	2	-7.53 ± 0.05	T-m/m ³	
Octupole	3	$100. \pm 8.$	T-m/m ⁴	
Decapole	4	$-10700. \pm 550.$		

The primary harmonic coefficients of interest are the quadrupole and sextupole. Variations in these values were obtained on the different planes that were covered. At 1000 MeV, these coefficients had the largest magnitudes on the geometrical midplane and decreased by about 4 to 6% at $Y = \pm 0.64$ cm and by 15 to 35% at $Y = \pm 1.73$ cm. The dipole coefficients had corresponding increases of $< 0.01\%$ and 0.04 to 0.1% over these ranges.

The field integrals were also used to determine the effective lengths of the magnet. At 1000 MeV for the integral path on the geometrical midplane, $Y = 0$, and along the center of the gap, $X = 0$, the effective length was found to be 1.127 m; at 100 MeV the corresponding value was 1.141 m. The locations of the effective edges at both ends of the magnet were also found for the 1000 MeV, $Y = 0$ data. This showed that the magnet has an effective wedge angle of $3.5^\circ \pm 0.1^\circ$ at 1000 MeV.

In addition to the harmonic coefficients found for the field integrals, the coefficients were also found for the midplane scans at 1000 MeV and 100 MeV for the field values on each "radial" line through the scan geometry. Plots of the quadrupole and sextupole coefficients were shown in Fig. 1 for 1000 MeV at $Y = 0$.

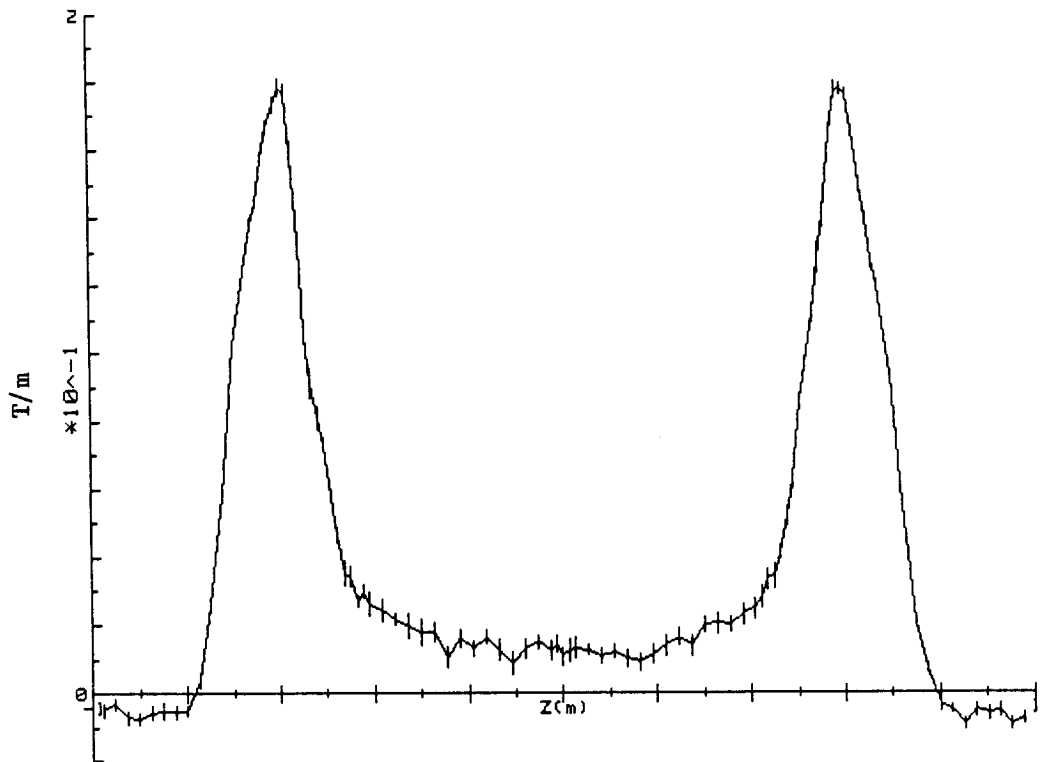


Fig. i.a. Quadrupole harmonic Coefficient vs Z for 1000 MeV at $Y = 0$.

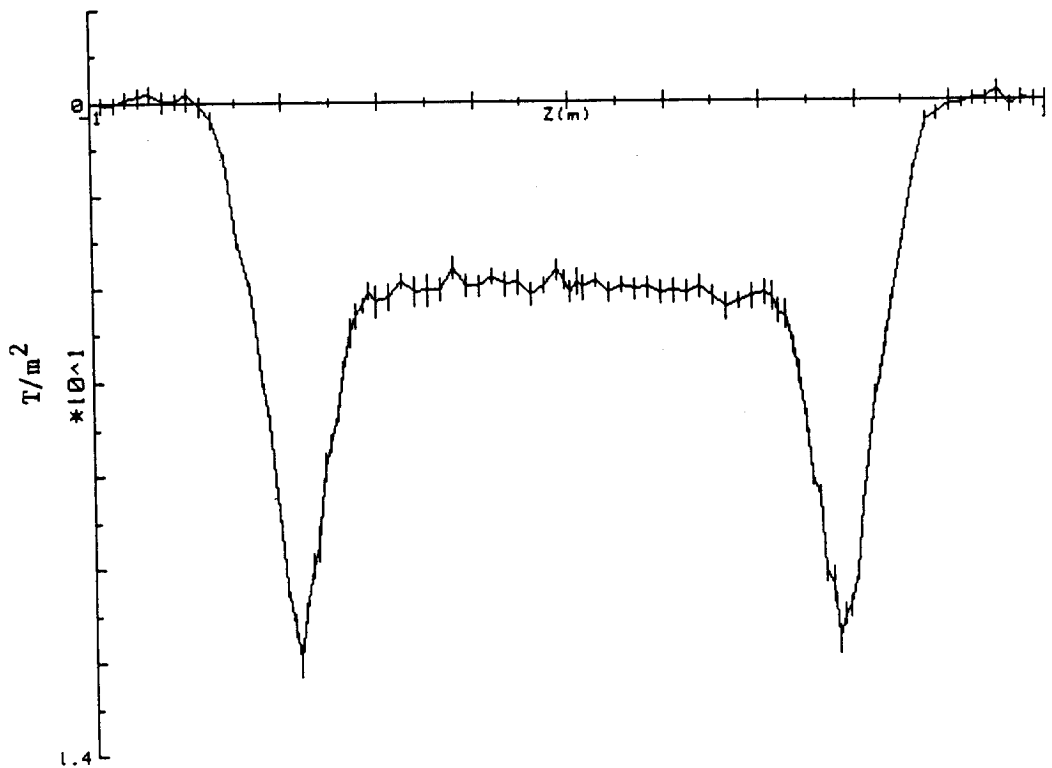


Fig. i.b. Sextupole harmonic coefficient vs Z for 1000 MeV at $Y = 0$.

The measured vertical field values were also used to define the location of the magnetic midplane at each of 2037 points in the scan geometry for 1000 MeV and 100 MeV. The location of the magnetic midplane is relative to the geometrical midplane $Y = 0$. The average elevation inside the magnet gap at 1000 MeV was determined to be at $Y = + 1.8$ mm and the average slope of the magnetic midplane in the transverse, X, direction was $- 2.3 \times 10^{-3}$ mm/mm. This slope corresponds to a total variation of 0.23 mm across the 10 cm wide useable gap. The elevation at 100 MeV, however, is much less than the positioning errors in the Z direction and is, therefore, not significantly different from 0.0.

The above is only a brief description of the major areas addressed by these measurements and the associated analysis. Some of the results presented here are only representative of the values determined. The following sections of this report, however, contain the details of the measurements, and a complete listing of the resulting parameters.

A. Introduction

The following report describes the measurements and corresponding analyses of the vertical magnetic fields of an Aladdin dipole magnet. The primary goal was to measure the vertical magnetic fields and to extract the harmonic field coefficients. A secondary goal was to get information concerning the location of the magnetic midplane. In order for the reader to have confidence in the accuracy of the results, many of the procedures used to calibrate the system and check the repeatability of the measurements are also included.

A.1. Magnet Description

The dipole magnet measured is BM03 according to the Aladdin designation. It has a C-core made from parallel-stacked mm thick laminations each 2.3 mm thick and composed of C. R. steel. The core was assembled from five separate substacks each 21.56 cm long. The front (outside radius) edge of each of these blocks has an angle of 0°, 6°, or 12° with respect to a square edge depending on its location in the assembled magnet. The nominal radius of curvature of the magnet gap is 208.3 cm. The gap height was measured to be 5.702 cm \pm .004 (2.245 inches \pm 0.0017). The pole tip is 17.8 cm (7 in) wide and contains edge shims .15 x 1.27 cm (.060 x .5 inches) in size. These shims leave an accessible gap height of only 5.4 cm.

The coil on each pole is assembled from four, double-layer pancakes and is attached to the core through two stainless steel bars, one located only at each end of the core. The sketches in Figs. A.1 and A.2 show a cross sectional view and a plan sectional view of the magnet with the dimensions of interest. The electrical and water connections are made to each coil on the outside radius edge resulting in a more symmetric shape for the magnetic field at each end of the gap. Note the asymmetry in the upper and lower coil thicknesses.

A.2. Measuring System

The measuring system¹ used was originally designed and built to measure the magnetic fields in prototype sector magnets for a proposed electron microtron at Argonne. It contains a probe positioning manipulator with the two horizontal axes driven with DC servo motors and a manually adjusted vertical axis.

The methods used to calibrate the manipulator and to find measuring center of the Hallprobe will be briefly described below and the resulting

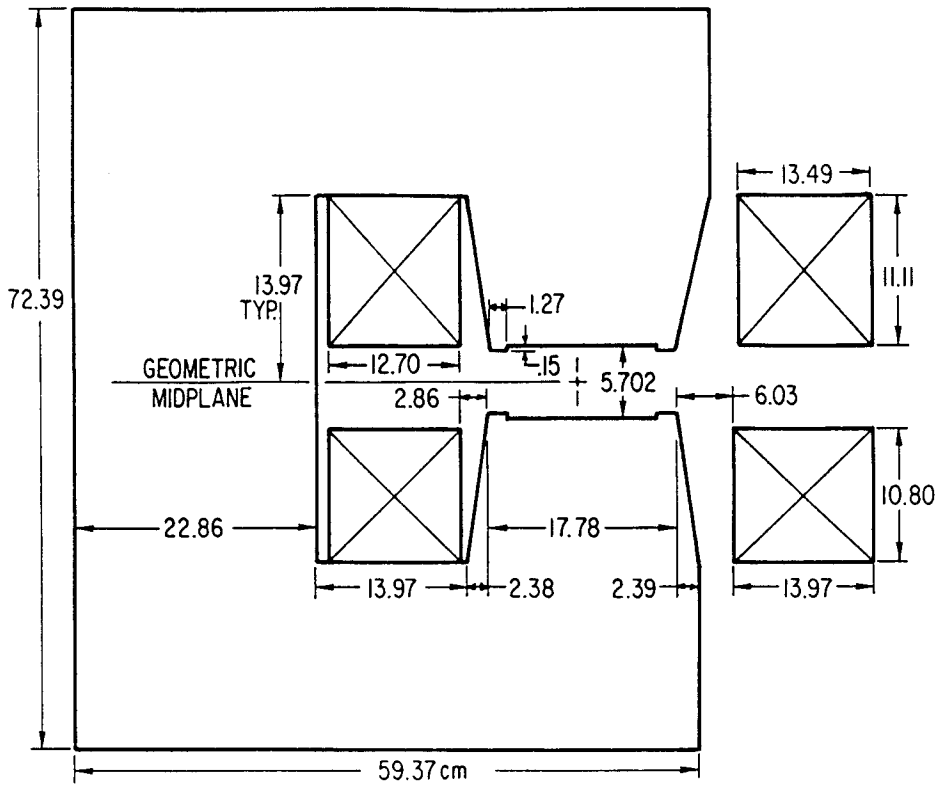


Figure A.1 Cross section of Aladdin dipole as built.
Dimensions in cm.

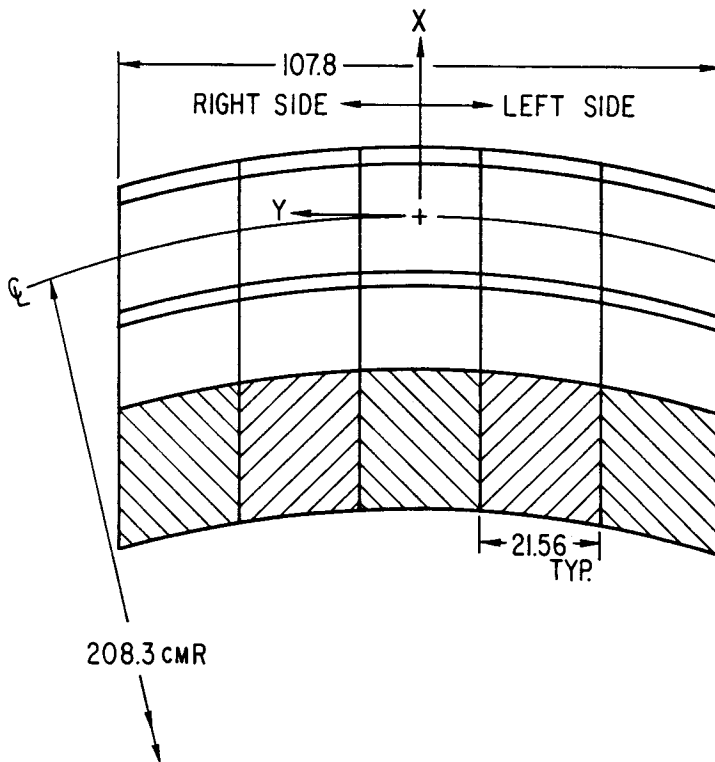


Figure A.2 Plan sectional view of Aladdin dipole.
Dimensions in cm.

positioning uncertainties will be listed. The measuring system contained a Hall probe to measure the vertical components of the magnetic fields. Other probes, called auxiliary probes, were also used to measure a reference field (NMR) and various voltages and temperatures associated with the magnet environment during the measurements. The calibration of the Hall probe will be described below. The results of repeatability checks will also be presented. The measuring system was controlled with a Hewlett Packard 9845 desk top computer programmed in BASIC. The analysis programs were also contained in the data taking software which facilitated the on line analysis of the data during the data taking processes.

A.3. Data Descriptions

The results described in this report are for central field and gap height measurements versus excitation current as well as the vertical field measurements at excitations corresponding to 1000 MeV, 800 MeV, and 100 MeV and at elevations of 0, ± 0.635 , ± 1.27 , and ± 1.7272 cm with respect to the geometrical midplane. All combinations of energy and vertical position were not covered, however, but measurements were concentrated at 1000 MeV and 100 MeV. A representative set of tabulated data is contained in the Appendices to show the form of the data that is available.

The raw data was stored on magnetic tapes compatible with the Hewlett Packard computer and the HEP/VAX at Argonne. The data after being normalized and merged, where appropriate, are called unified data and were also placed in files accessible to the HEP/VAX. These contained the data used to calculate the integral field values and the subsequent field coefficients. The analysis of the data described here was done using the HP 9845 computer with the programs described below. The results presented are primarily related to the field integrals. Effective lengths were extracted as a function of excitation and vertical position. Considering the horizontal distribution of the integrals gave the integrated strengths of the harmonic fields as a function of excitation and vertical position. The location of the magnetic midplane within the magnet gap was also determined.

The probe positioning manipulator covered only an area about 1 m long and as a result each side of the magnet was measured separately. Data was concentrated on the left side as viewed from the open side of the yoke. A full set of data was taken at the left side for only the 1000 MeV and 100 MeV excitations and only near the midplane for the 800 MeV excitation.

The right side data was taken for all planes at only the 1000 MeV excitation, and at 800 and 100 MeV data was taken only on the geometric midplane.

Finally, the results of a magnetic field calculation using the program PE2D⁵ will be presented. The primary area of concern here was the effect of vertical asymmetries in the coil locations on the position of the magnetic midplane.

As a final note, some suggestions are made as to what might be done to improve these existing magnets and how the measurements could be expedited if ever there was a future need.

B. Equipment

The equipment setup that was used for these measurements is shown in Fig. B.1. The primary elements in this system are described below along with some of the procedures used to calibrate or otherwise test their operation.

B.1. Probe Positioning System

B.1.a. Description

The probe positioning system, manipulator, is part of a magnet measuring system designed and built to measure prototype sector magnets for an electron microtron.¹ The manipulator consists of three orthogonal drives called X, Y, and Z, which are used to position the probe at points within the accessible volume. The two horizontal axes are called X and Y and the vertical axis is called Z. These names are not consistent with the usual nomenclature used for bending magnets; i.e., Z along the beam direction, Y vertical, and X horizontal and perpendicular to Y and Z. The choice is, however, a common, right-handed system with Z being vertical. This more generic choice was used because the manipulator was designed to measure a variety of magnets and the final relative orientation of the manipulator could not be assumed beforehand. The following discussions of manipulator axes refer to this internal set of coordinates but all references to the magnet coordinate system in section H. use the more common choice (Y vertical).

The X and Y axes are motor driven and are controlled by the data taking computer. The Z axis can only be changed manually. The Y axis is 1.0 m long, the X axis 0.5 m, and the Z axis 0.1 m. The alignment of the axes is reasonably accurate but slight variations in the ways can cause much larger errors at the probe position usually located at the end of a probe boom which is often longer than 1 m. Because of the multiplying effect of this boom, the control program makes corrections for every destination point. The amounts of the corrections are determined with an algorithm which was derived by a calibration procedure. The standard errors for the probe location after the corrective algorithm was applied are shown in Table B.1 for a probe located on a boom approximately the length used during the measurements of the magnet.

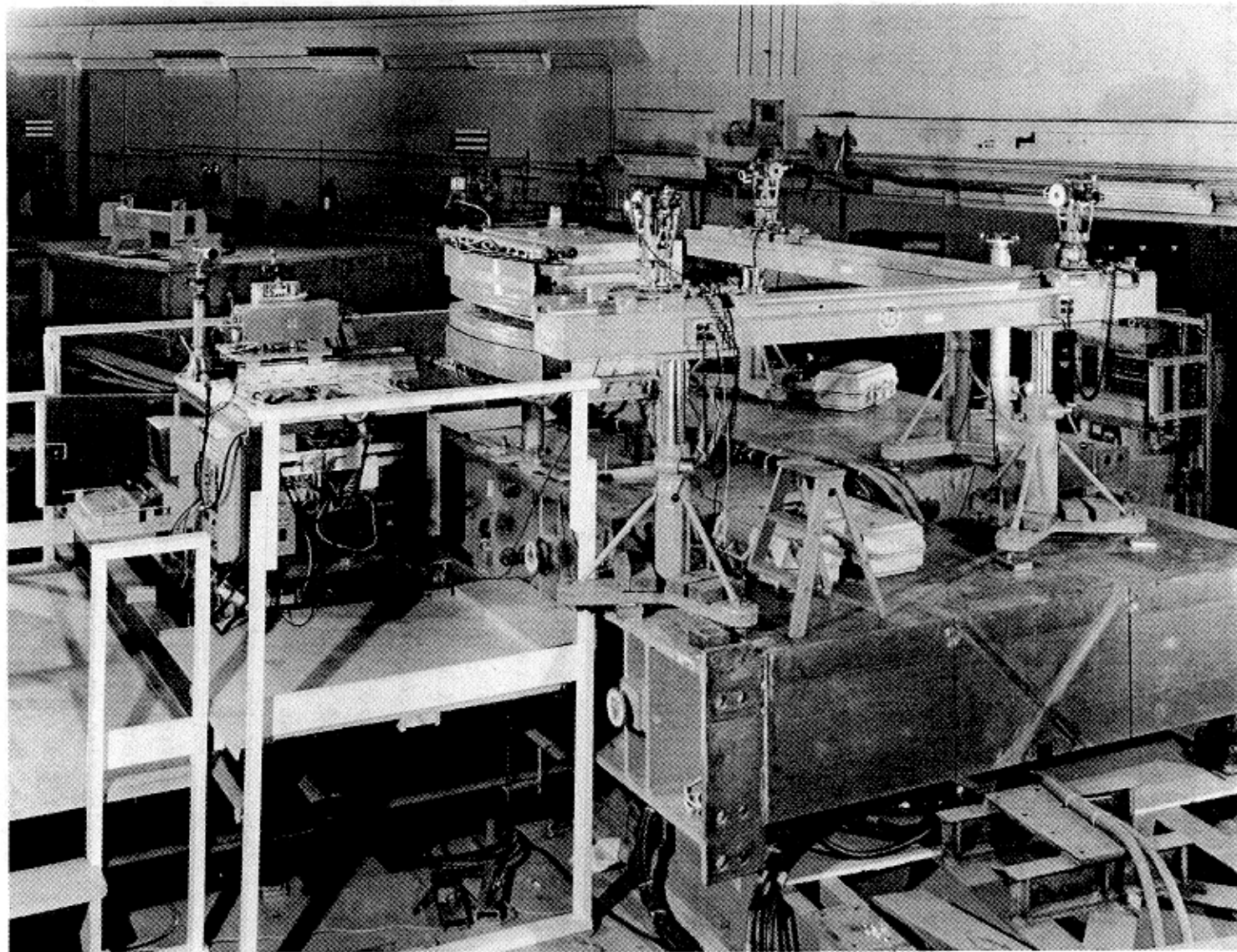


Figure B.1 Equipment setup used to take magnetic field measurements.

Table B.1

Standard Positioning Errors for a 0.924 m
Probe Boom Length

Axis	Standard Error (μm)
X	38 (76)*
Y	64 (178)
Z	190 (305)

*Maximum error over entire accessible area.

B.1.b. Calibration

To calibrate the manipulator, an optical square was assembled from tooling bars. The components and setup of this device were very similar to those used in the magnet measuring system described in sections B.4 and C.1. The manipulator was set so that the long, horizontal axis, Y, was parallel to one side of the square. The four corners of the manipulator were then leveled and targets were mounted on the probe boom at a radius of 0.924 m from the support center; the location was about equal to the location of the Hall probe used for the actual field measurements described in this report. The probe was then positioned at points at 10 cm spacings for both the X and Y axes over the entire accessible area. At each point, the X, Y, and Z locations were found for the associated targets. The differences of the measured values and the values as defined by the tooling bar scales and optical level were the errors. The RMS values of these errors were then used as the standard errors for the manipulator.

B.2. Field Probe

The movable magnetic field probe was a Hall probe supplied by F. W. Bell, Inc. The probe was a Model STL80402 used with a Model 811AR meter unit with a 4 1/2 digit DVM. The probe was calibrated by Bell to determine its temperature coefficients and verify its operational characteristics.

B.2.a. Calibration

The Hall probe was also calibrated at Argonne as a complete system. The probe was placed at the point (0,0,0) at the center of the magnet gap and the NMR probe was placed directly under it at (0,0, - 1.7 cm). Moving the NMR by ± 0.6 cm in X and Y did not change the NMR reading by more than 1 gauss with a central field of about 1.55 T.

The meter was zeroed as per the Bell instructions except that a custom built zero-gauss chamber was used (spiral wound Mu-metal with mylar between layers, 2 cm inside x 6 cm outside x 10 cm long) in order to fit around the probe when it was mounted at the end of the manipulator boom. The magnetic field was raised to 1.25 T and the Hall probe was rotated about the boom axis in order to maximize the reading; a 5 1/2 digit meter was connected to the analog output signal on the Bell meter to get higher resolution. The calibration constant was adjusted to obtain the same reading on the Hall meter as appeared on the NMR.

The above adjustment was done after the meter had been on for over four hours. Besides this obvious precaution, however, the measuring system was totally energized and put into a state that was equal to that during the measurement process; i.e., all electrical components of the system had to be turned on and warmed up. Of particular interest it was found that the computer not only had to be turned on but it had to read the Hall meter at least one time. Not doing so could inject an error of up to 2 gauss.

The Hall probe and NMR meter readings were taken by the computer using the probe reading program. Ten readings were taken at each field setting and RMS differences were calculated. Readings were taken for field values between about 0.35 and 15.5 T. The standard error assigned to this calibration process was derived by finding the RMS value of the RMS differences at the measured values.

B.2.b. Probe Center

B.2.b.1. Method

To locate the effective center of the Hall probe, a localized bump was created in the magnetic field near the center of the magnet gap operating at central field strengths from 1.0 to 1.2 T. The bump was created by a pair of 0.635 cm diameter pins with points having 30° included angles and 0.5 mm flat ends at the tip. The flat ends were incorporated to prevent tip damage during use. These pins were made from SAE 1010 steel and were mounted in an aluminum frame which located the pins concentrically about a common vertical axis with the points facing and separated by 8.5 mm.

The technique used to locate the probe center for a given axis, X, Y, or Z, involved moving the probe across the bump only along the desired direction and measuring the field values at a number of points. A central field strength was also measured with an NMR probe at the same time as the Hall probe measurements were taken at each point. These values were used to normalize the Hall readings so that the deleterious effects of the fluctuations in the central field could be eliminated for scans that have total variations of as little as a few gauss. A least squares procedure was then used to fit a polynomial of degree 2 to the normalized field values, and the coordinate value at which the calculated curve had an extreme was determined. The probe was then moved to this location and the offset value between the calculated point and the original starting point was returned.

B.2.b.2. Repeatability

To determine the repeatability of the bump searching procedure, repeat searches were initiated after an initial run had placed the probe at the calculated location of the extreme value. Of course, a perfect machine would give a zero offset for repeated run, but in reality non-zero offsets resulted. This check was actually done for only the X and Y axes. The repeatability of the Z

axis was assumed to be the average of the X and Y values.
The RMS fluctuations are listed in Table B.2.

Table B.2

RMS Fluctuations in Probe Center Definition

Axis	σ (μm)
X	8
Y	18
Z	13

B.2.c. Hall Gaussmeter Parameters

Some of the parameters for the Hall Gaussmeter system are listed in Table B.3.

Table B.3

Hall Gaussmeter Parameters

Probe serial number	150667
Sensing element diameter	1.0 mm
Meter digits	4 1/2
Meter resolution at 2.0 T FS	1 gauss
Temperature coefficient (20 - 40° C) at 1.52 T	-0.003%/°C
Calibration standard error (0.35 - 1.55 T)	2.9 gauss

B.3. Auxiliary Probes

Besides the Hall probe used to measure the vertical component of the magnetic field at the points in the scan geometry, there were other probes used to monitor a variety of parameters in the measuring environment during the scan process.

B.3.a. NMR Magnetometer

This probe was a Sentec Type 1000 magnetometer used with a #5 probe during the field scan operations at 1000 and 800 MeV. This unit can automatically track a slowly changing field. The parameters for this unit were assumed to be those quoted in the published specifications and some are listed in Table B.4.

Table B.4

NMR Magnetometer Parameters

Meter digits	7
Meter resolution	0.01 gauss
Absolute accuracy at 1.5 T	0.1 gauss

B.3.b. Temperature

In order to determine various temperatures in the measuring environments, an Ultra-7 thin film, platinum resistance device made by Hy-Cal Engineering was used. A number of different types of sensing elements are available but only one was used for the present set of data. Some of the parameters for the sensor and associated amplifier are listed in Table B.5.

Table B.5

Temperature Probe Parameters

Probe Type	RTS-5760-B-U-240
Probe Resistance	1000 Ω
Probe Size (mm)	4.8 wide x 7.9 long x 1.27 thick
Amplifier Type	BA-507-B
Output	0 - 10 volts
Range	10 - 40° C
Accuracy	$\pm 0.025^\circ$ C

B.3.c. Analog to Digital Converter

In order to measure various voltages in the measuring environment, two 12-bit ADC's were available in the measuring system. The units were type AD363K made by Analog Devices. Each also included a 16-channel multiplexer on the input which could be used as eight differential channels. The specifications for these units were assumed to be the published values and some are listed in Table B.6.

Table B.6

12-Bit ADC Parameters

Resolution	12 Bits
Relative accuracy	0.025% FSR
Temperature coefficient	0.004%/°C Max.
Throughput rate, full rated accuracy	25 kHz

B.4. Optical Alignment Equipment

The primary elements of the optical alignment system were transits, optical levels, and tooling bars.

B.4.a. Transits

These transits were Brunson, Type 75 units containing optical micrometers capable of resolving one reading to about 12 μm . There were fluctuations, however, that were demonstrated when readings were repeated. There were also conditions that made the targets hard to see. The total error in establishing the location of a target was, therefore, assumed to be $\pm 50 \mu\text{m}$ (± 0.002 inches) which would result in a standard error of about 18 μm .

Three of these transits were used to establish an optical square. Two of them had autocollimating mirrors on the horizontal axis and the third had a telescope mounted concentrically with the horizontal axis of rotation.

B.4.b. Optical Level

A type N3 optical level, made by Wild, was used to level the magnet and probe manipulator. Using optical scales, it was possible to make repeated readings with total variations of less than or equal to $\pm 25 \mu\text{m}$.

B.4.c. Tooling Bars

The three transits were mounted on two 3.0 m long tooling bars as shown in Fig. B.1. These bars were made by Brunson and contained provisions for mounting precision scales under the transits with a good source of illumination. This permitted the scopes to be located to within a total error of about $\pm 25 \mu\text{m}$.

B.5. Power Supply

The power supply used to excite the magnet was originally designed to operate a 30 ton prototype magnet for another project.² The current and voltage ratings were suitable for the Aladdin dipole but the filter and regulator were not properly matched to the Aladdin magnet. This caused some electrical noise to be imposed on the magnet coils when the supply was operated in the current regulated mode. This caused the NMR probe to be unable to maintain a stable tune. As a result, the power supply was operated in a voltage regulated mode. This caused only minor inconveniences during the measurements since the NMR or current transducer readings were used to normalize the data. There were interlocks installed to

protect the magnet from water shortages, and excess temperatures and to protect the operators from ground faults.

A precision current transductor was incorporated in this supply. This was a type 1000 SH made by Hazemeyer (Holland) and specified to be accurate to better than $\pm 0.01\%$.

B.6. Magnet Cooling Water System

Low conductivity water was used to cool the magnet coils. The water was supplied by a 5 hp pump which could maintain a pressure gradient of 50 psi across the magnet giving a flow in excess of 15 gpm. The temperature of the water supply in this system was maintained at 26.7°C (80°F) $\pm 2^{\circ}\text{C}$.

B.7. Support

B.7.a. Magnet Support

The magnet was mounted on top of about 30 Tons of solid steel. The magnet rested on three points and was supported with the same hardware components that are used for the dipoles located in the Aladdin ring. Directly under the center, (0,0), point in the magnet is a conical pocket. A steel ball bearing, 3.810 cm in diameter sits in this pocket and in a similar pocket on the top of a rigid post. There are two pads at the back corners of the magnet that can slide on the smooth, bottom plate of the magnet. Each of these pads rests on a ball bearing which rests on top of the stem of a 25 T worm screw jack. There were also pusher screws at the pad at the corner which were used to rotate the magnet about the front support point.

B.7.b. Manipulator Support

The measuring system, probe manipulator rested on four steel casters. The two casters located on the side next to the magnet contained V-grooves. These casters rested on the tops of two I-beams, one of which had a V-track. The manipulator could be easily rolled from one end of the magnet to the other. When in a spot where measurements were to be made, four 15 cm high screw jacks were placed between the I-beams and the bottom of the manipulator and were used to raise the manipulator off the wheels and to subsequently level it. To increase the rigidity of this support, small jacks were placed between the bottoms of the I-beams and the floor. This support allowed operators to move around the system during the time when measurements were being taken without causing any vibrations in the

probe that were larger than 0.1 mm. To minimize even these vibrations, however, during the measurements, movements were restricted only to those places which caused NO vibrations. This did allow access to the control computer.

C. Coordinate Systems

There were actually two coordinate systems in the measuring environment. The most important is called the absolute system, which is defined by the optical alignment system. This is the system to which all coordinates are referred. The second system is the one used internally in the control program which coordinates the movements of the probe through the scan geometry.

C.1. Magnet (absolute)

All coordinate values listed in this report are referenced to the absolute coordinate system. This system is defined by an optical alignment system. The nomenclature and target locations for this system are shown in Fig. C.1. The first step in the set-up of this system was to

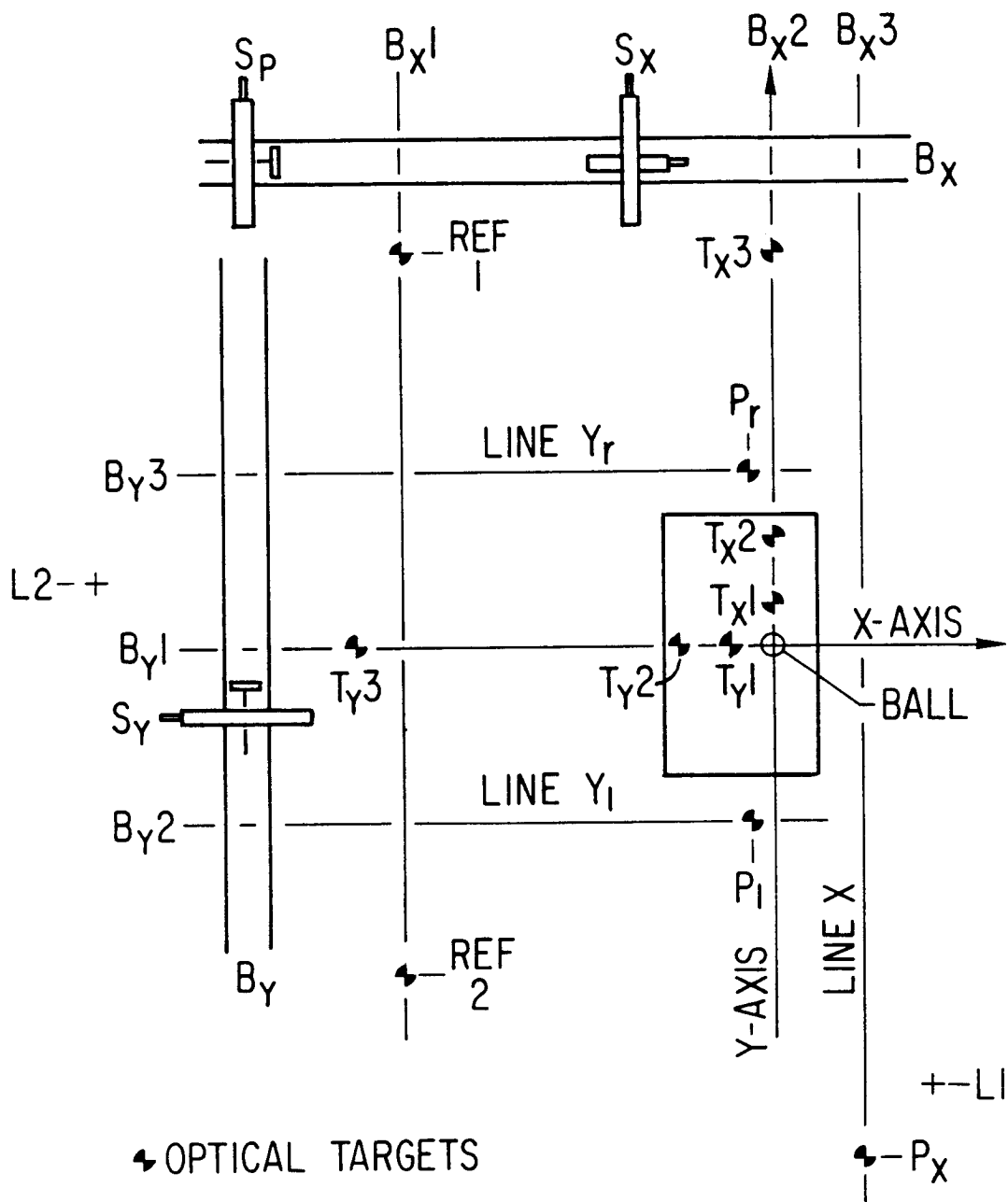


Figure C.1. Absolute coordinate system nomenclature and target locations.

place targets, REF1 and REF2, on the top of the steel foundation blocks on which the magnet and optical square would rest. These targets were placed at spots that would be observable after all other parts had been installed. They were placed so that they were well separated in the Y direction and were approximately parallel to the track on which the manipulator rode when it was moved from one end of the magnet to the other. A 3 m tooling bar, Bx, was then leveled, with a precision, bubble level (Starret #199) and set perpendicular to the line REF1-2. With the scope Sx aligned on REF1-2 and leveled, the tooling bar scale reading directly under the scope was determined for future reference. The horizontal axis scope in Sx was then used to set the pivot scope, Sp, of the optical square to be parallel to scope Sx. The second tooling bar was then set so that it was centered along the line of sight of scope Sp and to be level. Now scope Sy was adjusted to be perpendicular to scope Sp. The two scopes, Sx and Sy, were often moved during the measuring procedures. Whenever they were, they were always readjusted with respect to the fixed, pivot scope, Sp.

At this point, the magnet support was securely bolted to the foundation blocks. A 3.810 cm diameter, steel ball bearing, was placed in the pocket on top of the fixed column. This ball was located, by definition, at the origin of the absolute coordinate system. Its center was located in the X and Y directions by sighting the two corresponding edges with the Sx and Sy scopes. The differences of the edge readings were within 76 μm of the 3.810 cm. The midpoint between the edge readings was then the origin ($\pm 38 \mu\text{m}$). Each scope was moved to the corresponding origin location and aligned to Sp.

The X and Y axis lines were transferred to the base plate by placing targets at Tx1, Tx2, Ty1, and Ty2. A third target, Tx3 or Ty3, was placed on each line but on the foundation block surface.

C.2. Measuring System

The measuring system coordinate system is defined by the mechanical components of the manipulator - the slides, drive screws and motors, and the computer program used to control the moves. The effective result is a coordinate system with straight and perpendicular axes.

D. Alignment of Magnet and Manipulator

D.1. Magnet

D.1.a. Installation

Before the magnet was placed on the support, the scopes, S_x and S_y , were set at the corresponding origins and aligned with S_p . The scopes were then sighted on the corresponding axis targets near the edges of the support base plate, T_{x2} and T_{y2} . The magnet was then carefully placed on the support with the 3.180 cm ball at the origin seated in the conical pocket on the bottom surface of the magnet.

The alignment of the scopes with the targets T_{x2} and T_{y2} was checked and verified that the magnet support had not been accidentally moved during magnet installation. Further verification was made by sighting the target at T_{y1} , which was just within sight of scope S_y , and seeing that it too had not been moved.

D.1.b. Level

The magnet was leveled using a prevision bubble level (Starrett #199). This unit was 38 cm long and had graduations of 8.6 arc secs ($42 \mu\text{m/m}$). Since the top surface of the magnet was machined in the same setup as the pole surfaces, the top surface should be a good reference surface for leveling. The top surface was cleaned of any loose particles. The level was placed between the ball cups 1 and 3 (see Fig. D.1), which were used to locate an alignment fixture for the Aladdin ring. The screw jack under cup 3 as adjusted to make the magnet level. The level was reversed and moved over the surface a little to make sure of a correct reading. The same process was repeated for the level placed between cups 1 and 4. The process was repeated and resulted in final readings of the level well within one division ($42 \mu\text{m/m}$) for both locations.

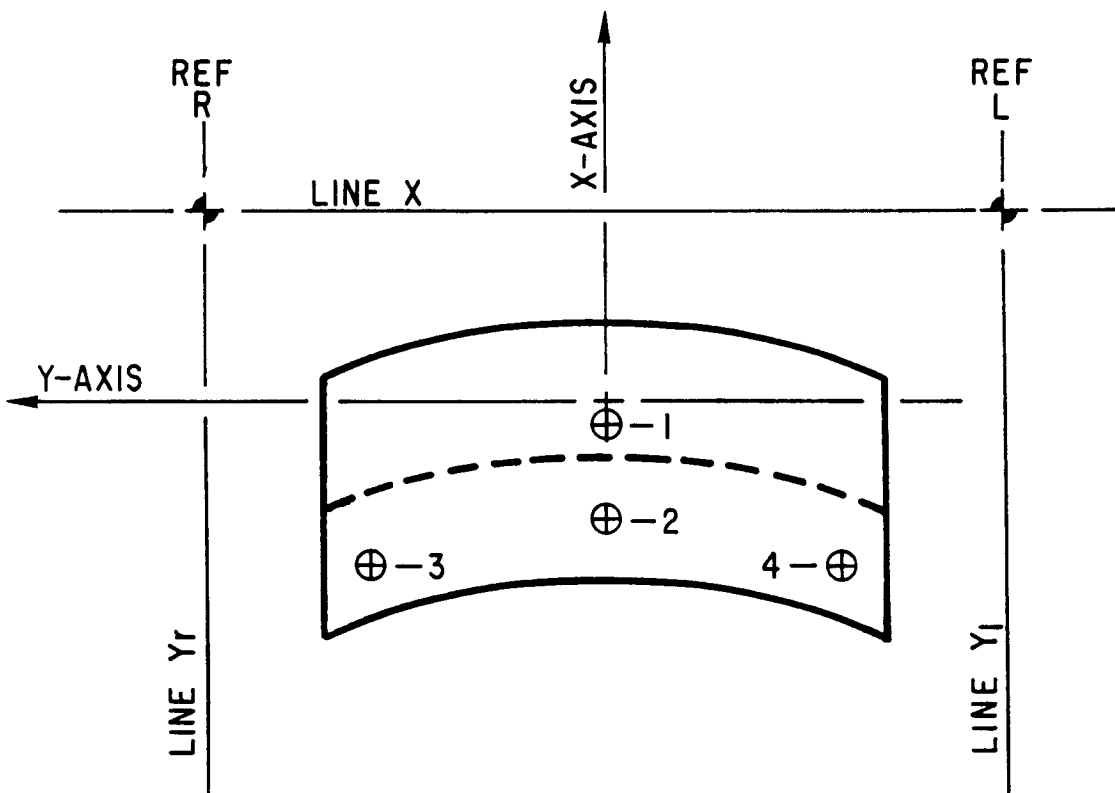


Figure D.1. Top view of magnet core showing ball cups for Aladdin alignment fixture and important reference lines defined in the absolute coordinate system.

D.1.c. Horizontal Orientation

The origin of the absolute coordinate system is locked to the magnet gap center point by the ball and socket coupling to the support. After the magnet was leveled, optical scales were used to measure the distances from an arbitrary line parallel with the Y axis to the back yoke edges of the last lamination at each end of the magnet. These measurements were estimated to be accurate to only about ± 0.1 mm since the yoke surfaces were not flat and they were painted. The rotation angle of the magnet was adjusted to make the two distances the same. For future reference, the locations of the four ball cups on the top of the magnet were located. The X and Y coordinates are relative to the absolute coordinate system. The Z coordinates are with respect to the geometrical midplane of the gap. A 19.05 mm diameter ball was used to locate all three coordinates for each cup. This ball was precisely ground to a hemisphere (± 12.5 μ m) and lines were scribed to cross exactly at its center. A Wild N3 optical level was used at location L1 to obtain the Z coordinates. The total errors are estimated to be ± 0.1 mm for the X and Y coordinates and ± 50 μ m for the Z coordinate. The cup center coordinates are listed in Table D.1. The cup numbers are defined in Fig. D.1.

Table D.1

Coordinates for the Ball Cups on Magnet Top

Ball No.	X (cm)	Y (cm)	Z (cm)
1	-0.363	-0.008	38.301
2	-25.672	0.0076	38.301
3	-43.711	-43.068	38.257
4	-43.442	43.355	38.158

D.2. Manipulator

D.2.a. Level

There are steel pads at each corner of the manipulator table. These were ground during the original system calibration so that they are coplanar to the plane of access as defined by the center of the top, moveable, manipulator platform. Whenever the manipulator was moved, these pads were first leveled. This was done by placing a Wild N3 optical level at location L1, Fig. C.1, and

sighting a single optical scale, moved from pad to pad. The screw jacks under the manipulator table were used to make the required adjustments. The final, total variations at the four corners were always $\leq 50 \mu\text{m}$.

D.2.b. Primary Reference Points

A primary reference point is one at which the absolute coordinates exactly equal the non-rotated coordinates of the measuring system. There were two such points, REF R and REF L, defined for this magnet and are shown in Fig. D.1. These are located at the intersections of the three lines - Yl, Yr, and X. The line X lies along the $X = 31.674 \text{ cm}$ line and is just beyond the front of the magnet; it corresponds to the scale reading Bx3 on the Bx tooling bar. There was also a check target placed on the surface of a 15 Ton steel block located at $Y \approx -490 \text{ cm}$. The line Yl lies along the $Y = -82.875 \text{ cm}$ line and is just beyond the left end of the magnet; it corresponds to the scale reading By2 on the By tooling bar. There is also a check target, Pl, for this line located at $X = -12.7 \text{ cm}$. Similarly the line Yr lies at $Y = +82.875 \text{ cm}$, corresponds to target By3 and has a check target, Pr, at $X = -12.7 \text{ cm}$. The check targets were defined at a time when the optical square had just been set up. They were often used during the measurements to quickly validate the scope positions.

D.2.c. Rotation Angle

The rotation angle of the measuring system coordinate system around a primary reference point and with respect to the absolute coordinate system had to be defined each time the manipulator table was moved. This process was done under computer control. It was defined by first setting the probe under manual control on the primary reference point of interest. The probe was moved under computer control to a point, a secondary reference point, along the line X and near the end of the accessible travel. This move was made with all corrections incorporated in the drive logic. The optical micrometer on the Sx scope was then used to measure the actual offset of the probe target in the X direction from the line X. The probe was then moved back to the primary reference point. The measured offset was then converted to an error angle which was used to correct the rotation angle used during the move from the primary reference

point. The resulting rotation angle was then used for all computer directed moves done until the manipulator was moved to a different location.

D.2.d. Probe Location

The probe could not be fully extracted from under the shadow of the coils and set on the line X. Reference targets were, therefore, placed on the top and two sides of the probe boom about 8.2 cm back from the probe center. These targets were used to set the probe on the primary and secondary reference points. The corresponding location of the probe measuring center, however, still had to be defined in the absolute coordinate system. The location (X_r , Y_r) could be estimated from external measurements at the beginning.

To get a more exact location, however, a magnetic bump was created near the center of the magnet; this procedure is described in section B.2.b.1. The steel pin support structure was mounted on a 3.2 mm thick aluminum plate. This plate was large enough to permit targets to be placed on it and viewed by the scopes S_x and S_y which were set to locate the primary reference point. The optical square was used to locate the geometrical center axis of the pins relative to the two targets. The plate was placed in the magnet gap with one of the targets centered on the primary reference point and the other one on the line X. The installation and subsequent extraction of the pins from the magnet was always done with the magnet turned off. Doing so with the magnet turned on caused unreproducible shifts in the magnetic center of the pin structure. Now the location of the pins was defined (X_p , Y_p) in the absolute coordinate system. The probe was then moved by the computer from the estimated location, (X_r , Y_r), corresponding to the primary reference point to the bump location at (X_p , Y_p). A bump search was done to determine the offsets required in X and Y to move the probe to the axis of the pins. These offset values were used to adjust the values of (X_r , Y_r) giving the effective location of the probe center corresponding to the primary reference point.

The effective Z coordinate of the probe center was found by a semiautomatic procedure. The geometrical midplane of the magnetic pin assembly was placed near the geometrical midplane of the magnet gap. The Wild N3 level located at L1, Fig. C.1, was used to measure

the actual location. It was assumed that the magnetic midplane of the pin structure coincided with the geometric midplane. The Hall probe was placed about 0.13 cm away from the axis of the pins. The probe was moved manually in the Z direction in steps of 0.25 mm over a range of about ± 1.5 mm and the coordinate value was entered into the computer after each move was completed. The computer then took the Hall probe and NMR probe readings. After all the desired points had been entered, the computer calculated the coordinate of the peak value and the offset between this and the starting value. The Hall probe was then moved by the calculated offset distance and the elevation of the side target near the probe was determined. This gave the distance between the effective vertical center point of the Hall probe and the side target. The probe was then moved to the geometrical midplane of the magnet and then to the primary reference location. This is the point at which the probe is initially located at the start of each run. The elevation of the probe target was then recorded as that reading of the Wild level scale that corresponded to the placement of the probe on the geometrical midplane of the magnet at (0,0).

E. Gap Measurements

E.1 Pole Faces

After the magnet was leveled with a bubble level, section D.1.b., and before it was turned on for the first time, measurements of the levelness of the two pole faces were made with the Wild N3 optical level located at point L1, Fig. C.1.

E.1.a. Level

The Wild level was set at a height to make an arbitrary reference elevation near midrange to be about at the height of the geometrical midplane of the gap. A single 5 cm long optical scale was used to measure the distance between the reference elevation of the level and each pole face at points over the entire flat area of the pole. The points selected lay on lines across the gap and parallel to the X axis. There were three points on each line, one in the center of the pole and two at about ± 6.3 cm. There were five of these lines along the axis of the gap, one in each of the five blocks of laminations which were in the core assembly.

The readings on each of the lines across the gap and on each pole had standard deviations from the average values that were less than $12 \mu\text{m}$ (0.0005 in); therefore, the average values were considered in the analysis that follows. The measured distances to the pole tips are shown in Table E.1.

Table E.1

Distances of the Reference Level Elevation to the Pole Tips

Y (cm)	Distances to Pole Tips		Sum (cm)
	Bottom (cm)	Top (cm)	
-48.26	3.698	2.002	5.700
-25.4	3.696	2.004	5.700
0.0	3.693	2.009	5.702
25.4	3.696	2.009	5.705
48.26	3.696	2.009	5.705

Straight lines were fit to the values for each pole by a least squares method. The resulting slopes of the bottom and top poles were -1.6×10^{-5} cm/cm and $+7.8 \times 10^{-5}$ cm/cm. The bottom pole was flat to well within the graduations of the bubble level used to level the magnet. The top pole, however, did have a slope that was

measurably different from that of top surface of the magnet; the value, however, corresponded to only about 78 μm over the length of the magnet.

E.1.b. Gap Height and Geometrical Midplane

The sums of the readings for bottom and top poles in Table E.1 give the gap heights. These sums are also listed in Table E.1 and show that the gap height at the magnet center was 5.702 cm (2.245 in). The total variation of the gap height was 50 μm (0.002 in) with the minimum at the left end.

The geometrical midplane is located at one half the gap height above the bottom poleface. The slope of the half gap points was found to be 3.1×10^{-5} cm/cm. Adding this value to the slope of bottom pole gives a slope of the geometrical midplane of 1.5×10^{-5} cm/cm. This slope corresponds to about 15 μm (0.0006 in) variation over the length of the magnet.

E.2. Gap Height vs Current

Because this dipole is a C-magnet, the gap height does decrease as the excitation current is increased. To measure the size of this change, five optical scales were placed on the top surface of the magnet core. One was placed in each lamination block, and viewed with a Wild N3 optical level setup at L2 (Fig. C.1). The scales were placed directly above the centerline of the gap and readings were taken from 0 A to 1200 A.

There were total variations of about 80 μm between the five scales at any given current setting. The readings for all five scales were fit with a simple polynomial of degree 2 by a least squares method resulting in a standard deviation of 28 μm for the fit. This technique was judged to be appropriate since the stand error of the fit was comparable to the resolution of the measurements. The resulting coefficients of the fit are listed in Table E.2.

Table E.2

Coefficients of Top Pole Deflection vs Current

<u>i</u>	<u>Value</u>
0	0.0 μm
1	-24.2 $\mu\text{m}/\text{kA}$
2	-123.4 $\mu\text{m}/\text{kA}^2$

At 600 A, the calculated deflection was 59 μm .

The deflections of the bottom pole were also measured using a nonmagnetic target, spring loaded against the bottom pole face at (0,0). These

measurements showed no measurable deflections; therefore, the top pole measurements are equivalent to gap height changes as a function of current. This change was $153\text{ }\mu\text{m}$ (0.3%) at 1000 MeV. The slope of the pole was not measured in this process but an estimate was made by using a simple geometrical model, which assumed pivoting at the inside edge of the back yoke at the midplane. This estimate gave a total variation of the gap height of $108\text{ }\mu\text{m}$ (0.2%) at the 1000 MeV excitation.

The elevation of the geometrical midplane also changes as a function of the excitation current. This was $76\text{ }\mu\text{m}$ over the range of 0 A to 1018 A (1000 MeV). When the center of the Hall probe was set to the geometrical midplane by the procedure described in section D.2.d., the current was about 600 A. This meant that the Hall probe was not at the geometrical midplane when the 1000 MeV measurements were made but the error was only about $50\text{ }\mu\text{m}$.

F. Vertical Field Measurements

F.1. Turn-On, Turn-Off, and Warm-Up Procedures

The gross changes in the excitation current of the magnet were always done in a current loop of 0A \rightarrow 1200 A \rightarrow 0A at a rate of about 25 A/sec. The final settings were always reached on the increasing side of the loop. If the magnet supply was tripped off unexpectedly, then the current was run two times through the entire loop. Bidirectional adjustments were made for changes of around 0.1% or less to set the desired current for a particular run. Whenever the magnet was turned-off, the current was always run up to 1200 A and then down to 0A at a rate of about 25 A/sec.

The magnet supply current and all the electrical components in the measuring system were turned on at least two hours before any measurements were taken. It was found, however, that times of about eight hours were actually required to reach the maximum temperature stability for all of the components. As a result, most of the measurements were taken during two periods of four to five days each, during which times none of the elements of the measuring system was turned-off.

The supply currents associated with the three energies of interest for these measurements are listed in Table F.1.

Table F.1

<u>Supply Current vs Energy</u>	
<u>Energy</u> <u>(MeV)</u>	<u>Current</u> <u>(A)</u>
100.7	87.36
800	730.09
1000	1018.41

These currents were those used in the Aladdin accelerator ring and were based on the original measurements.

F.2. Data Taking Details

F.2.a. Geometries

F.2.a.1. Universe

The term "universe" is used to describe the rectangular space inside of which all movements of the Hall probe were made. Two such regions were used, one for the measurements at each end of the magnet. The parameters of interest are with respect to the absolute coordinate system and are listed in Table F.2.

Table F.2

Universe Parameters

	Left Side	Right Side
Minimum X coordinate (cm)	-24.64	-24.64
Minimum Y coordinate (cm)	-97.79	- 2.54
Length of X side (cm)	49.53	49.53
Length of Y side (cm)	100.33	100.33

F.2.b. Scan Lines

The points at which the vertical field values were measured were chosen to allow the axial field integrals to be found without requiring any interpolation of the measured data. The locations of the points were chosen to make each axial integral equivalent to a measurement of the field integral with a long, curved search coil. If a search coil were actually used, it probably would be constructed to have a uniform radius of curvature over the entire length. A modified search coil which is curved only over the 30° arc of the magnet bend and has straight ends which are tangent to the arc, however, is much more representative of the actual beam path through the magnet. This modified search coil model was, therefore, the one chosen to select the path for the axial points.

The field measurements across the gap were obtained by moving the "search coil" only in the X direction. The path along the axial center line of the scan is shown in Fig. F.1 relative to the absolute coordinate system for the left side of the magnet. The arc part of the path had a length of 15° and a radius of curvature of 208.3 cm (82 in). The tangent, end line was 43.18 cm long. The measured points were distributed in five sections along this line to provide more concentrated measurements in the gap center and at the gap edges. The parameters for these axial line sections are listed in Table F.3.

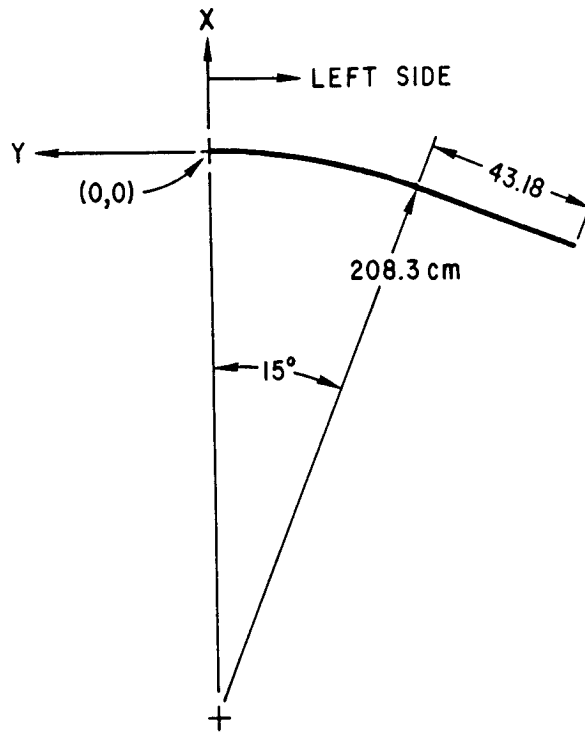


Figure F.1. Central path through the left side of the scan geometry.

Table F.3

Parameters for the Axial Line Sections

Section No.	Section Type	Starting Value	End Value	Step Size
1	Arc	0.0°	0.75°	0.375°
2	Arc	0.375°	11.25°	0.75°
3	Arc	11.25°	15.00°	0.375°
4	Straight	0.0 cm	12.70 cm	1.27 cm
5	Straight	12.70 cm	43.18 cm	2.54 cm

The lines across the gap are called "radial" scan lines even though they run parallel to the X-axis and are not truly radial except for the line at $Y = 0$. Measurements were taken over ± 7.62 cm relative to the center path in three sections of each radial line. The parameters for these radial line sections are listed in Table F.4.

Table F.4

Parameters for the Radial Line Sections

Section No	Starting Value (cm)	End Value (cm)	Step Size (cm)
1	-7.62	-5.08	1.27
2	-5.08	5.08	0.635
3	5.08	7.62	1.27

F.2.b. Multiple Readings

Whenever the Hall probe or any of the auxiliary probes was read, three readings were actually taken; these readings were taken with random delays between successive attempts. This process was used to minimize the errors caused by periodic electrical noise that may exist in a measuring environment; one, for example, that contains an operating accelerator. It will also minimize the effects of the probe vibrations that may occur after the probe, mounted on the end of a long, flexible boom, reaches the desired location.

The three values are averaged and the deviation from this average is found for each of the measured numbers. If the deviation for any reading is larger than 1 gauss or 0.01%, whichever is larger, then three new readings are taken. This process continues until the test is satisfied.

F.2.c. Readings Taken During a Scan

F.2.c.1. Parameters Measured

Of course, the vertical field value is measured at every point in the scan geometry. These values were measured with the Hall probe which was held in a small aluminum fixture at the end of a laminated fiberglass and epoxy tube. This put the probe at about 0.92 m from the center of the manipulator support platform. An entire scan required about 100 minutes to complete. Besides the vertical field values, the values from the auxiliary probes were read before and after each radial scan. The following are the auxiliary probes that were utilized. The NMR was used to measure the central field at a fixed point during all scans taken at 800 and 1000 MeV. It was positioned approximately at $X = 0$ and $Y = +5$ cm for the runs at the left side of the magnet and $Y = -5$ cm for the runs at the right

side. The exact location of the NMR probe was adjusted to allow the magnetometer to find a stable tune. Once located for the measurements on a given side of the magnet, however, it was not moved again until all measurements on that side had been completed. The resulting values were then used to normalize the vertical field values measured by the Hall probe.

For the 100 MeV case, the NMR could not be used, but the ADC was used to measure the output of the precision transducer monitoring the supply current. These readings were used for normalizing the 100 MeV data.

The final parameter measured was the temperature of the Hall probe. The temperature sensor described in section B.3.b. was mounted directly beneath the Hall element with thermally conductive grease between them. This sensor was also carried inside the aluminum fixture holding the Hall probe.

F.2.c.2. Repeatability of the Vertical Field Measurements

To get some idea of how well the measuring system could reproducably measure the vertical field values, one of the scans was redone immediately upon completion. Whenever a scan was completed, the probe was returned to the primary reference point. For the repeat run no adjustments in this starting point were made. The vertical field values in the two runs were normalized internally first to the associated NMR readings. The two runs were then normalized to each other by using the first NMR reading in each run. After these normalizing steps had been completed, the deviations of the measured values from the average value for each point were found. The RMS deviation for the entire scan geometry was 1.0 gauss and for the points with values greater than 1.53 T, i.e., on the central field plateau, the RMS deviation was 0.9 gauss ($< 0.006\%$).

F.2.d. Reference Checks

Before every scan was begun, the current was set to the desired value and the Hall probe calibration constant was adjusted to

the value determined in the procedures described in section B.2.a. After each run was completed, the Hall probe calibration constant was recorded. These values had a standard deviation of about 0.01%.

The location of the Hall probe with respect to the primary reference points was also checked from time to time and found to be shifted by $\leq 50 \mu\text{m}$.

F.2.e. Storage Media and Data Files

The vertical fields were measured for excitations of 1000 MeV, 800 MeV, and 100 MeV. At each excitation, data was taken at various vertical positions relative to the geometrical midplane selected from the values 0, ± 0.635 , ± 1.27 , and ± 1.7272 cm. The combinations of excitation, plane elevation and magnet end (L or R) for which measurements were taken are summarized in Table F.5 along with the names of the raw data files and the names of the unified (processed) data files. The raw data files are stored and backed-up on magnetic tapes read by the Hewlett Packard 9845 computer used to take the data. These data were used for all the analysis steps described here. These files were also stored on media, disks and tapes, accessible to the HEP/VAX computer at Argonne. These files are then also accessible to other users through node named ANLHEP on the BITNET network.

The raw data files are stored as card images in the VAX. There are some descriptive entries at the top of each file with the scan data following. Each scan data card contains values for a single point in the scan geometry in a 6F10.4 format. The values include the vertical field (gauss), the X, Y, and Z coordinates (cm), the normalizing probe value (gauss or volts), and the Hall probe temperature ($^{\circ}\text{C}$).

The unified (processed) data files contain data that has been normalized and merged with the data from the corresponding scan at the same excitation and vertical plane location from the other end of the magnet if one exists. For planes other than the geometrical midplane, the values are also normalized to the data in the midplane scan. These unified files are assembled with card images like the raw data files except that the point data includes only the vertical field value (gauss) and X, Y, and Z coordinates (cm).

The file names in the VAX have the following form:

ajjYbkkc.Enn

where

a = B for Bending magnet
 jj = 03 is magnet number
 Y = the Y coordinate of plane follows
 b = P for Plus (above geometrical midplane)
 = M for Minus (below geometrical midplane)
 kk = Integer part of the Y value (mm)
 c = L for raw data at left end of magnet
 = R for raw data at right end of magnet
 = U for unified data
 E = the Energy of excitation follows
 nn = energy of excitation divided by 100 MeV

Table F.5

Summary of Data Files

		RAW DATA FILES				UNIFIED DATA FILES
		Left End		Right End		
E (MeV)	Y (mm)	HP	VAX	HP	VAX	VAX
1000	17.27	AL.P13	B03YP17L.E10	AL.P33	B03YP17R.E10	B03YP17U.E10
	12.70	AL.P10	B03YP12L.E10	AL.P32	B03YP12R.E10	B03YP12U.E10
	6.35	AL.P9	B03YP06L.E10	AL.P29	B03YP06R.E10	B03YP06U.E10
	0.00	AL.P15	B03YP00L.E10	AL.P28	B03YP00R.E10	B03YP00U.E10
	- 6.35	AL.P14	B03YM06L.E10	AL.P30	B03YM06R.E10	B03YM06U.E10
	-12.70	AL.P11	B03YM12L.E10	AL.P31	B03YM12R.E10	B03YM12U.E10
	-17.27	AL.P12	B03YM17L.E10	AL.P34	B03YM17R.E10	B03YM17U.E10
	800	6.35	AL.P24	B03YP06L.E08	AL.P26	B03YPOOR.E08
0.00		AL.P23	B03YP00L.E08	BP3YP00U.E08		
-6.35		AL.P25	B03YM06L.E08	BP3YM06U.E08		
100	17.27	AL.P20	B03YP17L.E01	AL.P27	B03YP00R.E01	B03YP17U.E01
	12.70	AL.P19	B03YP12L.E01			B03YP12U.E01
	6.35	AL.P16	B03YP06L.E01			B03YP06U.E01
	0.00	AL.P22	B03YP00L.E01			B03YP00U.E01
	- 6.35	AL.017	B03YM06L.E01			B03YM06U.E01
	-12.70	AL.P18	B03YM12L.E01			B03YM12U.E01
	-17.27	AL.P21	B03YM17L.E01			B03YM17U.E01

F.2.f. Estimated Measurement Error

An estimate of the RMS error in the measured vertical field values involves contributions from a number of sources. The constituents of the error in the Hall probe portion are listed in Table F.6. The values listed are the RMS errors as measured or estimated. The total was found by adding the constituents in quadrature.

Table F.6

Hall Probe Center Position Error (μm)

	Axis			Reference Section
	X	Y	Z	
Setting optics to reference targets	18	18	-	*
Setting magnet to optics	18	18	8	*
Manipulator errors	38	64	190	B.1.a.
Setting probe to absolute system:				
Set to primary reference point	18	18	-	*
Manipulator errors at primary ref.	38	64	-	B.1.a.
Probe center	8	18	13	B.2.b.2.
Total	63	97	191	

* Estimated

The errors in the position of the Hall probe contribute to the errors in the vertical field values most significantly in regions where there are large field gradients; the field errors were calculated for one representative scan line in both the axial and radial directions. The chosen axial and radial lines were the paths through the left side of the reference data listed in Appendix G which had the largest gradients. The effective errors for the axial and radial directions were calculated separately by finding the square root of the corresponding sum of the errors at the points, weighted by the corresponding step size relative to the entire length of the line. The final error corresponding to the axial line was reduced slightly to compensate for the fact that the other axial scan lines have smaller gradients. The errors on the radial line were similarly summed only over ± 5.08 cm since the end points were not used in any of the analyses steps to obtain the harmonic coefficients. The resulting errors are listed in Table F.7.

There are also errors related to the temperature fluctuations of the Hall probe. In general, the probe temperature was a little higher when it was inside the magnet gap. Total variations were less than 4.6°C in any given scan and less than 5°C over all the measurements. This corresponds to a total field variation of 0.015% (see section B.2.c.) or 3.2 gauss at 1.6 T. This was assumed to be three standard deviations, probably an over estimate.

The constituents of the estimated measurement error of the vertical field at any given point are listed in Table F.7. The effective total was found by adding the individual components in quadrature.

Table F.7

Constituents of the Estimated Measurement
Error (G) in the Vertical Field Values

<u>Central field</u>	<u>0.15 T</u>	<u>1.55 T</u>	<u>Reference</u> <u>Section</u>
Due to manipulator position errors	0.5	3.4	F.2.f.
NMR errors	0.1	0.1	B.3.a.
Hall probe calibration	2.0*	2.9	B.2.c.
Repeatability	0.5*	1.0	F.2.c.2.
Temperature stability	1.1	1.1	B.2.c.
Total	2.4	4.7	

* Estimated values

The 1.55 T value was applied to both the 1000 MeV and 800 MeV data.

G. Data Analysis Programs

This section contains brief descriptions of the various programs used to process the measured data. Some are required to extract effective lengths and harmonic coefficients of the fields while others are useful in making tabular listings and plots of the data. These tables and plots are not actually needed to extract the ultimately required harmonic coefficients. They can, however, be useful in doing manual calculations used to validate other program sections and to qualitatively inspect the measured data.

Example tables and plots produced by the various programs are contained in the Appendices. The same set of raw data was used as the ultimate source for all of these examples. This data was for a magnet excitation of 1000 MeV with the probe on the geometrical midplane and is called the reference data.

G.1 Data Presentation

These programs are used only to provide listings of the measured and processed data and to provide 3D plots.

G.1.a. Tabular Listings

G.1.a.1. Field and X, Y, Z coordinates.

Field values and the X, Y, and Z coordinates can be separately listed in tables organized by successive radial and axial scan lines. The rows are labeled with the corresponding x position relative to the central path and the columns are labeled with the axial position. The axial scans are divided into separate sections, each containing a part of the path along either an arc or a tangent line region of the path. The arc section columns are labeled by the angular distance from the center of the magnet. The tangent line section columns are labeled by the linear distance from the end of the arc section to which it is tangent. An example of a table for the raw field data for the left side scan of the reference data is contained in Appendix I. The tables for the X and Y coordinates for the measured points in the left side scan of the reference data set are contained in Appendices II and III. The right side values for X are identical to those shown; the right side Y values are opposite in sign. The Z coordinate values for all data points are contained in Appendix IV. Note that the Z coordinates

vary from point to point. The value at (0,0) is exactly the value quoted as the vertical position of the plane for the data with respect to the geometric midplane. The variations correspond to the calculated Z-coordinate shifts; these are not corrected during a run for this manually adjusted axis.

G.1.b.2. Logged Readings of Auxiliary Probes

Each auxiliary probe is read periodically during a run. The values and the associated dates and times for each reading can be listed separately for each auxiliary probe. The average value, the standard deviation, and the total range of variation during the run are also listed. Representative tables are shown in Appendix V for the NMR and Hall probe temperature readings for the left side data of the reference set.

G.1.b. 3D Plots of Field Values

An isometric plot can be made for each individual scan data set. This does not have hidden line removal but allows the quick identification of runs that contain obviously questionable values. A sample plot is shown in Appendix VI for the left side scan of the reference data.

G.2. Normalize, Match, and Merge

A table containing the field values at all points in the scan geometry after the values from the two associated runs have been normalized, matched, and merged is contained in Appendix VII.

G.2.a. Normalizing

The 21 field values in each radial scan line of each data taking run were first normalized by multiplying by the appropriate factor. The reference value used for normalizing was selected as the first reading taken in the run with the NMR probe. The normalizing factor that was used for each radial scan line was the average value of the NMR readings taken at each end of the corresponding scan line divided by the reference reading.

G.2.b. Matching

Much of the analysis involved data constructed by merging the normalized data taken during two separate runs, one from the left side of the magnet and one from the right side at the corresponding vertical position and magnet excitation, into a single data set. The

NMR could not be used to match these two data sets since the NMR probe location was different for the data taken at each side of the magnet. The left side data was used as the primary data set and the normalized values were not changed. The right side data, however, was changed by multiplying all values by a factor that made the value at (0,0) equal to that in the left side data set. This produced values for the three overlapping scan lines which gave an RMS difference of about 0.01%.

The matching of the data from corresponding runs taken on the left and right sides of the magnet was done automatically when merging was specified. Data taken at the same excitation but at different elevations, however, had to be matched to the midplane data. This matching was accomplished by manually specifying the multiplication factor for the primary, left side, data. The factor was the ratio of the corresponding reference NMR readings that were used to normalize the two left side data sets being matched. These reference NMR values are displayed during the regular normalizing procedures.

G.2.c. Merging

The data in the two corresponding runs at the left and right ends of the magnet for a given vertical plane and excitation were merged into one unified data set containing the normalized and matched values of the vertical field for the entire magnet geometry. Only one of the radial scan lines from the three overlapping pairs of lines taken in the two runs was included in the merged data set. The center line was always taken from the left side data.

G.3 Field Integration

The measured field values, as was described in section F.2.a.2., are located on an arc with a radius of 2.083 m and a length of 30° centered in the gap and on two straight line sections each 43.18 cm long, and tangent to the arc at each end. The center ($X = 0$) axial scan line passes through the (0,0) point. Other axial scans were taken by moving this center scan line in only the X direction (i.e., parallel to the nominal end planes of the magnet).

The field integration was done for each axial scan line by finding the field value at each point and the value equal to one half the distance between the points on each side of the point of interest. The product of these values was summed over the entire length of each scan line specified

to find the integral. The end points of the line to be integrated could be manually specified.

The effective length was determined for each axial scan line by dividing the field integral by the field value on the same scan line but at the axial center location ($Y = 0$). When the data from only one side was analyzed, the effective length was translated into a location, (X, Y) , of the intersection of the path of interest and the effective edge. Using these coordinates for scans across the gap the effective edge angle of the magnetic field can be determined. In Appendix VIII, there are two tables of field integrals and effective lengths associated with the reference data set. One table is for only the left side data; the second table is for the entire reference data set, for both sides.

In addition to integrating the values over the axial paths through the entire magnet and for all paths across the gap, any subsection of the data could also be handled. This allowed, for example, the decoupling of the central field errors from the error contributions at the two ends of the gap.

G.4 Least Squares Fitting

Polynomials in X , the radial position with respect to the gap center, are fit to field values or field integrals by a least squares fitting method. The polynomials used were primarily of the following form:

$$V = \sum_{i=0}^D b_i X^i / i! \quad G1$$

In some special cases coefficients of the form $A_i = b_i / i!$ are used.

The coefficients, b_i , for the polynomials in X and the associated standard errors which resulted from the fits were determined by a matrix method.^{3,4} The complete solution process does include an iterative loop which involves doing successive fits and testing the resulting standard deviations, σ . The process was continued until σ increased. This type of solution greatly reduces the possibility of getting a bad fit as a result of round off errors occurring during the matrix inversion step. It has been found that only two or three iterations are generally required to converge on a solution. The χ^2 , and the χ^2 per degree of freedom as well as the standard deviation of the fit are printed out for each attempt.

G.5 Harmonic Field Coefficients

The primary goal of the field measurements of this magnet was to determine the integrated strengths of the vertical field harmonics up to at least the sextupole component, $i = 2$. The standard errors of the calculated strengths were also required. Two methods were used to find these values. A primary method was used for all the results tabulated in this report. The secondary method was used to verify the primary results and to provide plots of the strengths of each harmonic component calculated along the path through the magnet.

G.5.a. Primary method

The primary method used to determine the harmonic coefficients for the magnet was to first integrate the vertical field values along the specified paths through the magnet and then to perform a least squares fit to the integrals found for a polynomial in X , the radial position of the path with respect to the center path. Examples of the results of this calculation are shown in the tables in Appendix VIII.

G.5.b. Secondary method

The secondary method used to determine the harmonic coefficients for the magnet was to first perform a least squares fit of a polynomial in X to the measured values for each radial scan line and then to integrate the resulting coefficients. The fitting program was the same as that used for the primary method and is described above in section G.4. The measured field values were fit in this case and the measurement error used was only a field value and not multiplied by the effective length and not divided by $N^{1/2}$ (See H.4.a). The integrating program was the same as described in section G.3 except that the calculated coefficients were integrated rather than the measured field values. The squares of the errors were integrated rather than the error values and the final coefficient error was the square root of the above integral divided by the total path length.

The coefficients and standard deviations of the fits were listed for each radial scan line and the coefficients were plotted as a function of the position along the center path (Z). The list and plots were useful in making subjective evaluations of the quality of the measured data and to locate isolated peculiarities in the field shapes through the magnet.

Examples of the lists and plots for this procedure are shown in Appendix IX and section H.4.d.7. These results correspond to the same problem as contained in the tables in Appendix VIII for the total reference data set. Plots of the coefficients at 100 MeV and $Y = 0$ are shown in Appendix IX.C for comparison.

G.6. Vertical Midplane

The process described here to locate the magnetic midplane was the most involved and time consuming operation in the analysis of the data for this magnet. The errors associated with the calculated values at each point are expected to be large because of two facts. First, there is a large number of calculation steps required to find the value at each point (X,Y) in the scan geometry. Second, the spread in the field values that had to be fit was often comparable or even smaller than the estimated measurement errors of the field. The final numbers, however, that were used to define the location and orientation of the midplane involve averages over 663 to 1649 points in the scan geometry.

This process was begun by reading the data for each elevation that was measured and normalizing it. The left side field values were also normalized to the midplane NMR probe reading. For data that included scans from both sides of the magnet (1000 MeV), the two halves were matched to each other and then merged into combined data arrays. The normalizing, matching, and merging steps were the same as those used to define the data that was used to find the field integrals and subsequent harmonic coefficients. The field value and Z-coordinate (vertical) for all points in each plane are placed in two large arrays.

The location of the magnetic midplane at each point in the scan geometry was found by fitting a polynomial to the field values vs the actual Z-coordinate corresponding to the value in each plane. The polynomial was of the form $V = \sum_{i=0}^D A_i Z^i$. The location of the position at which the slope of the polynomial was zero was defined as the location of the magnetic midplane. This location was found for every point in the scan geometry and stored in the arrays that normally contain the field values and the Z-coordinates; this allowed postprocessing to be done with the same programs that were used to display and analyze the regular data.

H. Results

H.1 Field vs Current

The magnet was energized with the turn-on procedure described in section F.1. The current was measured with the precision transducer in the supply.

The Hall probe was placed approximately at (0,0,0) and the NMR at about (0,0,-1.7 cm). The current was changed from about 50 A to 1200 A in steps of about 50 A or 100 A and at time intervals of 4 to 16 minutes. The field readings were taken with both probes wherever possible. Care was taken to only increase the current for all steps up to 1200 A. The measured values of current and magnetic field are contained in Table H.1 and the associated plot for the Hall probe readings of vertical field are contained in Fig. H.1. The two field readings agreed to around 0.5%, but the Hall probe had not been calibrated for these measurements.

Table H.1

Field at (0,0,0) versus Supply Current

Current (A)	Hall (Gauss)	NMR (Gauss)	Comments
50.2	867		
102.9	1781		
150.2	2613		
205.8	3594	3602.6	NMR #4 probe
249.9	4360		
299.9	5230		
350.0	6133		
400.0	7029	7011.4	
450.1	7877		
500.0	8750	8720.9	
550.6	9616		
600.3	10472	10417.4	
650.2	11297		
700.4	12105	12043.0	NMR #5 probe
750.9	12823		
805.2	13588	13518.0	
850.7	14044	14009.3	
900.0	14586	14512.3	
950.1	15025	14985.6	
1000.0	15503	15427.4	NMR noisy from here on up.
1100.0	16314	16236.7	
1150.0	16688	16610	
1200.0	17044	16966	
0	≈ 50		

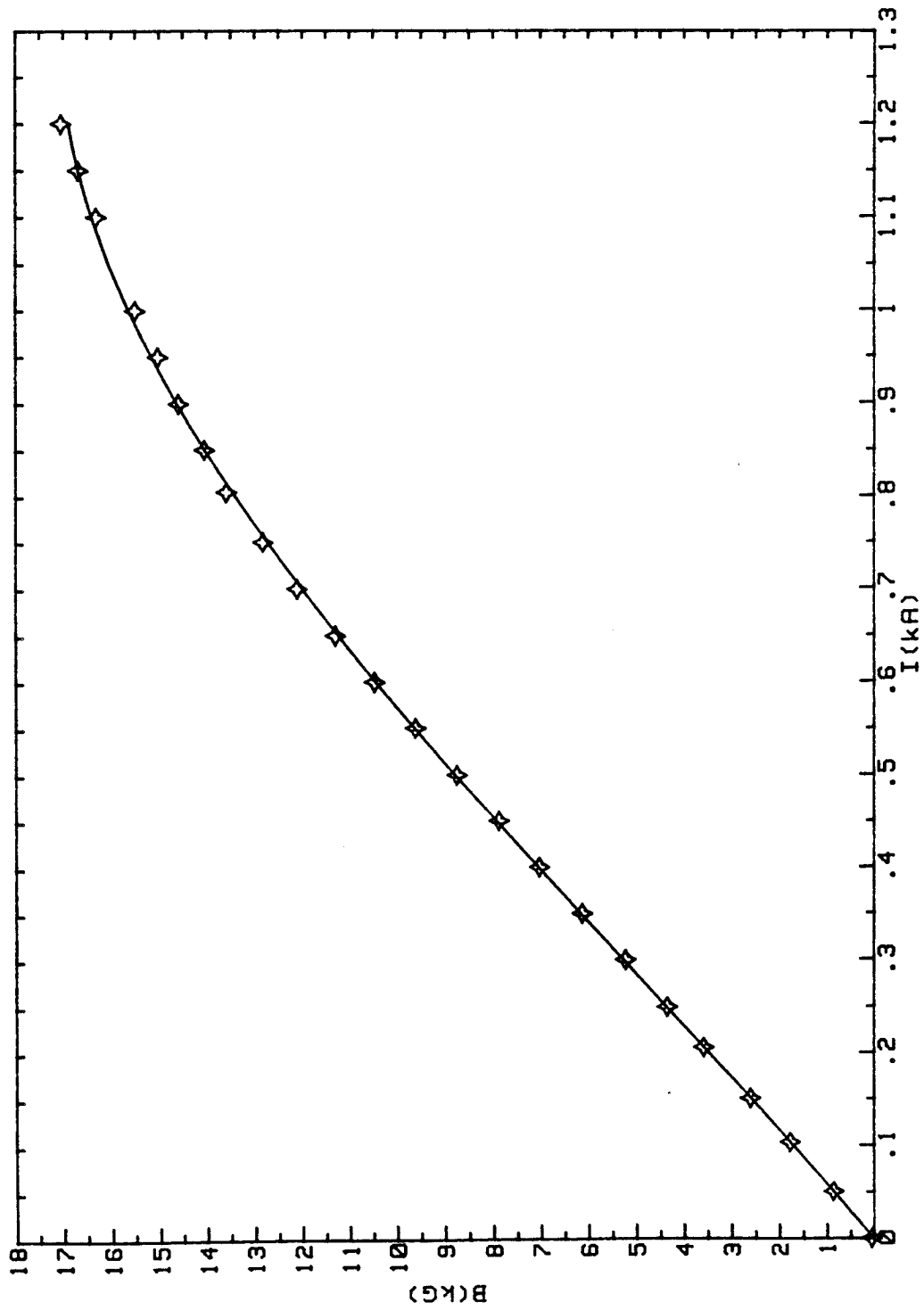


Figure H.1 Vertical magnetic field at (0,0) vs supply current.

H.2 Field Integrals

The measured values of the vertical fields in each run were normalized and the runs for the corresponding excitations and elevations were merged. This processed data is called the unified data. The field integrals were calculated from the unified data and the results are listed in Tables H.2.1, H.2.2, and H.2.3. These contain all of the integrals at each excitation, for all applicable elevations and at all scan positions across the gap between ± 5.08 cm (± 2.0 inches). Each column contains a U or L which designates the data file size. The U type files contain data from BOTH sides of the magnet while the L type files contain only LEFT side data but the integrals listed are the calculated values multiplied by 2 so they can be more easily compared to the U type values. These comparisons are only made here for 800 MeV and 100 MeV excitations at an elevation of $Y = 0$. The differences that result from finding the integrals in the two ways are around 0.15%.

Table H.2.1

1000 MeV Field Integrals (T-m)

Type Y(mm)	U 17.27	U 12.70	U 6.35	U 0.00	U -6.35	U -12.70	U -17.27
X (cm)							
5.08	1.7540	1.7508	1.7471	1.7459	1.7471	1.7525	1.7546
4.44	1.7550	1.7531	1.7509	1.7503	1.7510	1.7548	1.7555
3.81	1.7559	1.7548	1.7534	1.7531	1.7534	1.7564	1.7564
3.18	1.7566	1.7559	1.7549	1.7548	1.7550	1.7575	1.7570
2.54	1.7571	1.7566	1.7559	1.7559	1.7559	1.7581	1.7574
1.90	1.7573	1.7570	1.7564	1.7565	1.7565	1.7585	1.7577
1.27	1.7574	1.7572	1.7567	1.7567	1.7567	1.7587	1.7577
0.64	1.7573	1.7571	1.7566	1.7566	1.7566	1.7585	1.7577
0.00	1.7570	1.7567	1.7562	1.7562	1.7562	1.7582	1.7574
-0.64	1.7564	1.7562	1.7557	1.7556	1.7556	1.7577	1.7569
-1.27	1.7557	1.7553	1.7547	1.7546	1.7547	1.7569	1.7562
-1.90	1.7547	1.7542	1.7534	1.7532	1.7534	1.7558	1.7553
-2.54	1.7535	1.7527	1.7516	1.7513	1.7516	1.7543	1.7540
-3.18	1.7519	1.7506	1.7490	1.7486	1.7490	1.7523	1.7525
-3.81	1.7500	1.7480	1.7455	1.7447	1.7455	1.7495	1.7506
-4.44	1.7477	1.7444	1.7405	1.7391	1.7403	1.7459	1.7482
-5.08	1.7451	1.7395	1.7331	1.7306	1.7327	1.7408	1.7455

Table H.2.2

800 MeV Field Integrals (T-m)

Type	L	U	L	L
Y(mm)	6.35	0.00	0.00	-6.35
X				
(cm)				
5.08	1.4145	1.4155	1.4138	1.4138
4.44	1.4158	1.4171	1.4154	1.4152
3.81	1.4166	1.4180	1.4163	1.4160
3.18	1.4169	1.4185	1.4168	1.4165
2.54	1.4172	1.4187	1.4171	1.4167
1.90	1.4173	1.4188	1.4172	1.4168
1.27	1.4172	1.4188	1.4172	1.4168
0.64	1.4171	1.4187	1.4170	1.4166
0.00	1.4168	1.4184	1.4168	1.4164
-0.64	1.4165	1.4180	1.4164	1.4161
-1.27	1.4160	1.4175	1.4159	1.4156
-1.90	1.4153	1.4169	1.4152	1.4150
-2.54	1.4145	1.4160	1.4143	1.4141
-3.18	1.4133	1.4147	1.4131	1.4129
-3.81	1.4117	1.4130	1.4113	1.4113
-4.44	1.4095	1.4105	1.4088	1.4090
-5.08	1.4062	1.4065	1.4048	1.4055

Table H.2.3

100 MeV Field Integrals (T-m)

Type	L	L	L	U	L	L	L	L
Y(mm)	17.27	12.70	6.35	0.00	0.00	-6.35	-12.70	-17.27
X								
(cm)								
5.08	0.17433	0.17398	0.17406	0.17432	0.17409	0.17372	0.17380	0.17420
4.44	0.17435	0.17399	0.17416	0.17441	0.17417	0.17382	0.17384	0.17421
3.81	0.17436	0.17404	0.17420	0.17447	0.17425	0.17384	0.17386	0.17425
3.18	0.17437	0.17406	0.17424	0.17450	0.17427	0.17389	0.17389	0.17427
2.54	0.17436	0.17408	0.17423	0.17452	0.17430	0.17391	0.17391	0.17427
1.90	0.17440	0.17406	0.17426	0.17453	0.17431	0.17392	0.17393	0.17429
1.27	0.17438	0.17406	0.17425	0.17453	0.17431	0.17392	0.17391	0.17430
0.64	0.17438	0.17407	0.17425	0.17451	0.17430	0.17391	0.17391	0.17427
0.00	0.17436	0.17403	0.17423	0.17449	0.17428	0.17391	0.17388	0.17427
-0.64	0.17434	0.17402	0.17420	0.17446	0.17425	0.17388	0.17388	0.17425
-1.27	0.17428	0.17398	0.17414	0.17442	0.17420	0.17382	0.17383	0.17423
-1.90	0.17426	0.17393	0.17410	0.17436	0.17414	0.17378	0.17378	0.17418
-2.54	0.17419	0.17387	0.17401	0.17426	0.17408	0.17369	0.17373	0.17412
-3.18	0.17416	0.17378	0.17393	0.17419	0.17396	0.17360	0.17362	0.17404
-3.81	0.17404	0.17368	0.17379	0.17404	0.17383	0.17347	0.17354	0.17395
-4.44	0.17397	0.17357	0.17365	0.17386	0.17365	0.17330	0.17340	0.17385
-5.08	0.17388	0.17343	0.17341	0.17357	0.17335	0.17306	0.17325	0.17376

The field integrals over the total scan lengths are plotted for $Y = 0$ at 1000 MeV in Fig. H.2 and for 100 MeV in Fig. H.3. The lines through the points are calculated with the corresponding coefficients listed in Table H.4.9.

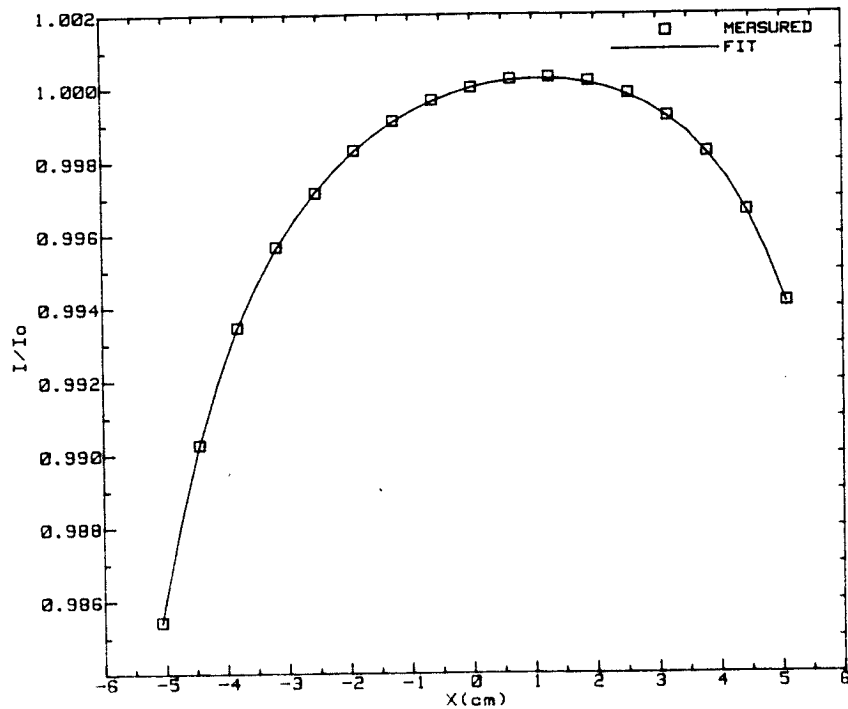


Figure H.2. Field integrals and fit curves at $Y = 0$ and 1000 MeV vs X .

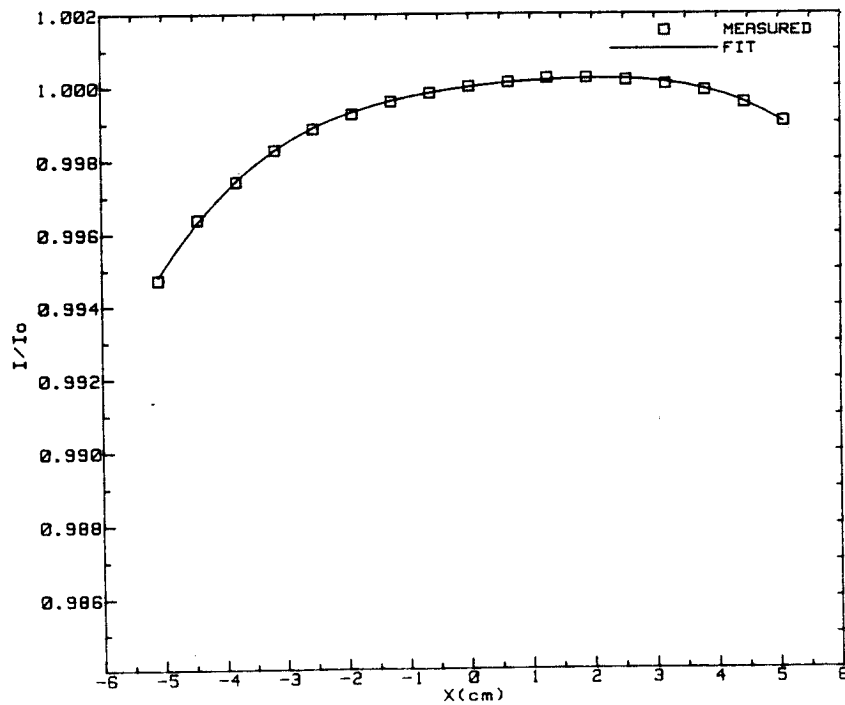


Figure H.3. Field integrals and fit curves at $Y = 0$ and 100 MeV vs X .

H.3 Effective Lengths

The effective lengths were calculated from the field integrals listed in section H.2 by dividing each integral by the vertical field value at the corresponding X value on the radial scan at $Z = 0$, at the magnet center, and at the corresponding elevation. The resulting effective lengths are listed in Tables H.3.1, H.3.2, and H.3.3. The results are listed here in a similar fashion as was done for the field integrals above. The two types of data are also included here, as was done for the integrals, for the $Y = 0$ cases for the 800 MeV and 100 MeV excitations. The differences here are around 0.13%.

Table H.3.1

1000 MeV Effective Lengths (m)

Type Y(mm)	U 17.27	U 12.70	U 6.35	U 0.00	U -6.35	U -12.70	U -17.27
X (cm)							
5.08	1.1273	1.1274	1.1277	1.1280	1.1278	1.1283	1.1273
4.44	1.1277	1.1275	1.1277	1.1279	1.1278	1.1284	1.1276
3.81	1.1278	1.1276	1.1278	1.1280	1.1278	1.1285	1.1277
3.18	1.1279	1.1277	1.1278	1.1280	1.1279	1.1286	1.1279
2.54	1.1279	1.1277	1.1278	1.1279	1.1278	1.1286	1.1279
1.90	1.1280	1.1277	1.1277	1.1279	1.1278	1.1286	1.1279
1.27	1.1278	1.1276	1.1276	1.1278	1.1277	1.1285	1.1278
0.64	1.1278	1.1275	1.1275	1.1277	1.1276	1.1284	1.1278
0.00	1.1276	1.1272	1.1272	1.1274	1.1274	1.1282	1.1275
-0.64	1.1273	1.1270	1.1270	1.1271	1.1271	1.1279	1.1273
-1.27	1.1270	1.1266	1.1265	1.1267	1.1267	1.1275	1.1271
-1.90	1.1266	1.1262	1.1261	1.1262	1.1262	1.1271	1.1266
-2.54	1.1261	1.1257	1.1254	1.1255	1.1255	1.1265	1.1260
-3.18	1.1255	1.1249	1.1246	1.1247	1.1247	1.1258	1.1254
-3.81	1.1248	1.1241	1.1235	1.1236	1.1236	1.1249	1.1246
-4.44	1.1238	1.1229	1.1222	1.1221	1.1223	1.1237	1.1235
-5.08	1.1227	1.1215	1.1205	1.1203	1.1204	1.1221	1.1222

Table H.3.2

800 MeV Effective Lengths (m)

Type	L	U	L	L
Y(mm)	6.35	0.00	0.00	-6.35
X				
(cm)				
5.08	1.1337	1.1349	1.1336	1.1332
4.44	1.1339	1.1350	1.1337	1.1333
3.81	1.1340	1.1351	1.1338	1.1336
3.18	1.1341	1.1354	1.1340	1.1336
2.54	1.1342	1.1353	1.1340	1.1337
1.90	1.1342	1.1353	1.1340	1.1338
1.27	1.1341	1.1352	1.1339	1.1337
0.64	1.1340	1.1352	1.1339	1.1336
0.00	1.1338	1.1350	1.1337	1.1334
-0.64	1.1336	1.1347	1.1334	1.1332
-1.27	1.1333	1.1344	1.1331	1.1329
-1.90	1.1328	1.1339	1.1326	1.1324
-2.54	1.1323	1.1334	1.1321	1.1318
-3.18	1.1316	1.1327	1.1314	1.1311
-3.81	1.1306	1.1316	1.1303	1.1302
-4.44	1.1295	1.1304	1.1291	1.1289
-5.08	1.1278	1.1286	1.1273	1.1273

Table H.3.3

100 MeV Effective Lengths (m)

Type	L	L	L	U	L	L	L	L
Y(mm)	17.27	12.70	6.35	0.00	0.00	-6.35	-12.70	-17.27
X								
(cm)								
5.08	1.1387	1.1384	1.1379	1.1406	1.1391	1.1367	1.1377	1.1380
4.44	1.1388	1.1387	1.1380	1.1407	1.1391	1.1370	1.1377	1.1381
3.81	1.1394	1.1391	1.1388	1.1411	1.1397	1.1370	1.1381	1.1383
3.18	1.1389	1.1389	1.1388	1.1411	1.1396	1.1373	1.1380	1.1385
2.54	1.1396	1.1298	1.1390	1.1415	1.1400	1.1374	1.1382	1.1385
1.90	1.1391	1.1389	1.1387	1.1412	1.1398	1.1375	1.1383	1.1386
1.27	1.1390	1.1392	1.1391	1.1415	1.1400	1.1475	1.1382	1.1392
0.64	1.1395	1.1390	1.1384	1.1411	1.1397	1.1374	1.1382	1.1385
0.00	1.1390	1.1387	1.1384	1.1410	1.1396	1.1374	1.1380	1.1385
-0.64	1.1387	1.1386	1.1380	1.1410	1.1397	1.1372	1.1377	1.1383
-1.27	1.1383	1.1384	1.1379	1.1403	1.1388	1.1368	1.1376	1.1382
-1.90	1.1382	1.1381	1.1378	1.1401	1.1387	1.1363	1.1373	1.1379
-2.54	1.1378	1.1377	1.1375	1.1397	1.1383	1.1355	1.1362	1.1370
-3.18	1.1376	1.1371	1.1370	1.1390	1.1375	1.1349	1.1363	1.1370
-3.81	1.1368	1.1364	1.1361	1.1381	1.1366	1.1340	1.1350	1.1357
-4.44	1.1361	1.1357	1.1352	1.1371	1.1357	1.1334	1.1346	1.1358
-5.08	1.1352	1.1346	1.1336	1.1355	1.1340	1.1318	1.1331	1.1342

H.4 Harmonic Field Coefficients

H.4.a. Estimated Measurement Errors

In order to find the χ^2 for a fit and the errors for each harmonic coefficient, an estimate was needed for the standard measurement error for the values being fit. The estimated error, 4.7 gauss, derived in section F.2.f was used for fits to the field values at 1000 MeV and 800 MeV and 2.4 gauss was used for 100 MeV. For fits of the field integrals, however, the error value above was multiplied by the effective length of the integrated data and divided by $N^{1/2}$, where N is the number of points used in the integral.

H.4.b. Radial Scan Length Used

The field values were measured across the gap in lines parallel the nominal ends of the magnet. These lines are actually scans in the X direction but are referred to here as "radial" lines. The X coordinates of the points along these lines are relative to the center path through the magnet gap. Data was taken from -5.08 cm (-2.00 in) to +5.08 cm in 0.635 cm (0.25 in) steps and from ± 5.08 cm to ± 7.62 cm (± 3.00 in) respectively in 1.27 cm (0.5 in) steps.

The points used in determining the harmonic coefficients throughout this report were those between ± 5.08 cm. There were several reasons for eliminating the two points on each end. First, the region of real interest is only the center 11.16 cm. Secondly, the points on the ends are in fields with gradients that are about 10 times larger than those in the central span. As a result, the measurement errors corresponding to the probe positioning errors for these end points are much larger. Also they have an effect on the coefficient values that may be disproportionately large compared to the useability of the region containing the points. Thirdly, fits were performed for both ranges of data, full versus central, and the coefficients found for the center fits were not significantly different from those found for the total-fits while requiring a lower degree. The criteria described in section H.4.c. was used to determine the degree of the polynomial to best fit the two data sets. Lastly, there were four data points at each end of the two axial scans at the inside radius edge of the gap that could not be reached by the measuring system. This resulted in zeros in the data. If these axial scans

were included in the fits, the unmeasured points should have been given field values. This procedure, however, was not attempted.

H.4.c. Degree of Polynomial Used

The degree of the polynomial used for the fits to all the measured data at 1000 MeV and 800 MeV in this report was 7. This value was determined by performing fits for various degrees to the integrated field values for the entire set of reference data contained in the Appendices. The standard error of the fit, the average χ^2 , and the maximum index of the coefficient which had a value more than two times the corresponding error for each case were examined. The results are listed in Table H.4.1.a. for a measurement error of 4.7 gauss.

Table H.4.1.a.

Goodness of Fit vs Degree for the Central Span in Radius at 1000 MeV

D	Fit Error (gauss)	$\chi^2/(n-D-1)$	Max Index	Time to Solve (sec)
4	16.3 (11.4)	12.0 (5.9)	4 (4)	35
5	13.6 (9.6)	8.4 (4.2)	5 (5)	50
6	1.9 (1.6)	0.16 (0.12)	6 (6)	53
7	1.7 (1.5)	0.13 (0.10)	7 (4)	66
8	1.1 (0.9)	0.06 (0.04)	8 (4)	89
10	1.3 (0.9)	0.07 (0.04)	4 (3)	123

() for the left side data only.

The appropriate choice of degree clearly lies between 6 and 8 as indicated by the average χ^2 values and the maximum index numbers; the value of $D = 7$ was selected.

A similar process was used to determine the degree of fit appropriate for the 100 MeV data. Because the estimated measurement error is proportionately larger for this data, the proper choice was expected to be smaller than 7. The results of the fits to the 100 MeV data for BOTH sides of the magnet at $Y = 0$ are listed in Table H.4.1.b.

Table H.4.1.b.

Goodness of Fit vs Degree for 100 MeV

D	Fit Error (gauss)	$\chi^2/(n-D-1)$	Max Index
1	16.6 (12.0)	48.1 (24.9)	1 (1)
2	4.1 (2.8)	2.9 (1.3)	2 (2)
3	2.8 (1.8)	1.4 (0.6)	3 (3)
4	0.8 (0.7)	0.12 (0.08)	4 (4)
5	0.6 (0.5)	0.06 (0.05)	5 (5)
6	0.5 (0.46)	0.045 (0.037)	6 (3)
7	0.53 (0.45)	0.048 (0.035)	6 (2)
8	0.54 (0.48)	0.051 (0.040)	2 (2)

() left side only.

The appropriate choice here lies between 3 and 5; the degree used for the 100 MeV was $D = 4$. For the 100 MeV data, the left side only type of data forms a majority of the cases analyzed; therefore, these results were considered too.

H.4.d. Harmonic Coefficient Values

H.4.d.1. Representative Coefficient Errors

The coefficients actually calculated were b_0 through b_7 , but all were not significantly different from zero. For integrals involving only the left side data, there were cases (see Table H.4.1., for example,) where b_4 was the highest useable coefficient. This is also high enough to evaluate all the components that may be corrected in the Aladdin ring. The b_4 coefficient, therefore, is the highest one listed in the following tables. The coefficient and associated errors for the reference data are shown in Appendix VIII and are listed below in Table H.4.2 for $i = 0$ through $i = 4$. A similar list is shown in Table H.4.3. for 100 MeV data at $Y = 0$.

Table H.4.2

Harmonic Coefficients and Errors for the
Reference Data (1000 MeV at $Y = 0$)

i	b_i	
0	$1.7563 \pm 5 \times 10^{-6}$	T-m
1	0.0783 ± 0.0005	T-m/m
2	-7.53 ± 0.05	T-m/m ²
3	$100. \pm 8.$	T-m/m ³
4	$-10701. \pm 550.$	T-m/m ⁴

Table H.4.3

Harmonic Coefficients and Errors for
Both Sides at 100 MeV at $Y = 0$

i	b_i	
0	$0.17449 \pm 2 \times 10^{-6}$	T-m
1	0.0036 ± 0.0001	T-m/m
2	-0.19 ± 0.01	T-m/m ²
3	8.4 ± 0.3	T-m/m ³
4	$-1068. \pm 44.$	T-m/m ⁴

H.4.d.2 Representative Relative Strengths of Harmonics

An alternative way to express the harmonic field strengths is to determine the associated field strength $B_i = b_i r^i / i!$, at a given radius, $r(m)$, from the center path through the magnet. The coefficients above were used with a sample radius of 0.05 m, the assumed radius of the useable magnet aperture. The field values, B_i , for $i = 0$ through $i = 4$ are shown in Table H.4.4.

Table H.4.4

Harmonic Strengths at 0.05 m for
1000 MeV and 100 MeV

i	1000 MeV		100 MeV	
	B_i (Gauss-m)	B_i/B_0 (%)	B_i (Gauss-m)	B_i/B_0 (%)
0	$17563. \pm 0.000005$	100.0	1744.9 ± 0.000002	100.0
1	$39. \pm 0.25$	0.22 ± 0.001	1.8 ± 0.05	0.10 ± 0.003
2	$-94. \pm 0.62$	-0.54 ± 0.004	-2.4 ± 0.12	-0.14 ± 0.007
3	$21. \pm 1.7$	0.12 ± 0.009	1.8 ± 0.06	0.10 ± 0.004
4	$-28. \pm 1.4$	-0.16 ± 0.008	-2.8 ± 0.11	-0.16 ± 0.007

H.4.d.3. Central Gap vs Gap Ends

There are at least two reasons to try to separate the central part of the scan data from that at the two ends of the magnet. One, it is useful to know the harmonic strengths for the central region relative to those at the ends. Two, there appears to be a displacement of the peak value in the field integrals listed in H.2 with respect to the center scan line through the magnet. Also, the integrals vs X curves do not have symmetric shapes (See Figs. H.2 and H.3). In order to shed more light on these areas, the integrals were found over the central regions of the scans and separate integrals were found for the points at each end. The definition of the "central" region was somewhat arbitrary. Plots of the coefficients for $i > 0$ found for each radial scan line (see Section H.4.d.7. and Appendix IX) show sharp peaks at the two edges of the magnet. The center was chosen to be as large as possible but not to include any of the edge peaks for any of the coefficients. The reference data set shown in the Appendices was used and the center was selected to include the radial scan numbers 30 through 68 which includes points within $\pm 12.375^\circ$ with respect to the axial center of the magnet. The two ends were then chosen to include scan numbers 1 through 30 and 68 through 97. The resulting coefficients, the sum of the three regions, and the coefficients for all scan numbers, 1 through 97, for reference, are contained in Table H.4.5 for 1000 MeV and Table H.4.6 for 100 MeV.

Table H.4.5

Harmonic Coefficients, b_i , for Center vs Ends at 1000 MeV

Region Type	ER	C	EL	ER+C+EL	TOTAL
Scan #'s	1-30	30-68	68-97	Σ	1-97
1					
0	0.1818	1.3949	0.1796	1.7563	1.7563
1	0.0312	0.0150	0.0315	0.0777	0.0783
2	-1.925	-3.640	-1.972	-7.537	-7.534
3	44.7	27.9	36.7	109.3	99.8
4	-2435.	-5374.	-2742.	-10551.	-10701.

Table H.4.6
Harmonic Coefficients, b_i for Center vs Ends at 100 MeV

Region Type	ER	C	EL	ER+C+EL	TOTAL
Scan #'s	1-30	30-68	68-97	Σ	1-97
i					
0	0.01861	0.13756	0.01832	0.17449	0.17449
1	0.0023	-0.0010	0.0023	0.0036	0.0036
2	-0.11	+0.04	-0.12	-0.19	-0.19
3	3.4	1.8	3.2	8.4	8.4
4	-287.	-530.	-242.	-1059.	-1068.

Relative comparisons of the columns in Tables H.4.5 and H.4.6 may be of interest to some persons so these comparisons were done and the results are contained in Table H.4.7.

Table H.4.7
Relative Strength Differences (%) for the Axial Scan Regions
1000 MeV

i	Σ : Total	C: Σ	(ER+EL): Σ	ER:EL
0	0.0	79.4	20.6	+1.2
1	-0.8	19.3	80.7	-1.0
2	+0.04	48.3	51.7	-2.4
3	+9.5	25.5	74.5	+22
4	-1.4	50.9	49.1	-11

100 MeV

0	0.0	78.8	21.2	+1.6
1	0.0	-27.8	127.8	0.0
2	0.0	-21.1	121.1	-8.3
3	0.0	21.4	78.6	+6.2
4	-0.8	-50.0	50.0	+18.6

H.4.d.4. Left Side vs Both Sides

Because of limitations in the time available to make the measurements, every run taken at the left side of the magnet does NOT have a corresponding run at the same excitation and elevation at the right side. In those cases which do not, the results are multiplied by two to provide an estimate of the

values for the whole magnet. It is necessary to estimate what errors are added to the figures when this is done.

In order to estimate the errors, the reference data and the 100 MeV data at $Y = 0$ were analyzed both ways. Already in sections H.2 and H.3, it was shown that the field integrals and effective lengths obtained from only the left data are within about 0.15% of the corresponding values for the two sided data for 800 MeV and 100 MeV. The resulting field coefficients and relative errors are shown in Table H.4.8.

Table H.4.8

Harmonic Coefficients, b_i , and Standard Errors
for Two-Side and Left-Side Data

Energy (MeV)	i	Both		Left *2		Magnitude Difference
1000	0	1.7563 ±	0.000005	1.7538 ±	0.00001	-0.0025
	1	0.0783 ±	0.0005	0.0774 ±	0.001	-0.0009
	2	-7.53 ±	0.05	-7.66 ±	0.11	+0.13
	3	100. ±	8.	112. ±	15.	+12.
	4	-10701. ±	555.	-10980. ±	968.	+279.
100	0	0.17449 ±	0.000002	0.17427 ±	0.000004	-0.0002
	1	0.0036 ±	0.0001	0.0036 ±	0.0001	0.0
	2	-0.19 ±	0.01	-0.22 ±	0.01	+0.03
	3	8.4 ±	0.3	8.2 ±	0.5	-0.2
	4	-1068. ±	44.	-961. ±	74.	-107.

H.4.d.5. Coefficient Lists

The harmonic coefficients for all combinations of excitation and elevation for which measurements were taken are listed in Table H.4.9. Each set of coefficients is associated with either a combined data set, U, containing values taken from both sides of the magnet or a data set, L, containing values taken only on the left side. The data type, U or L, is shown for each set of coefficients.

The coefficients for the L type of data are multiplied by two so the results are comparable to the U type values. It should be remembered, however, that there are some added errors associated with these L type values, as described in section H.4.d.4.

Table H.4.9

Harmonic Coefficients

1000 MeV

Y (mm)	Type	b_0 (T-m)	b_1 (T-m/m)	b_2 (T-m/m ²)	b_3 (T-m/m ³)	b_4 (T-m/m ⁴)
17.27	U	1.7570	0.0672	-4.87	10.7	- 6825.
12.70	U	1.7567	0.0712	-5.94	45.3	- 9119.
6.35	U	1.7563	0.0747	-7.13	94.6	-10042.
0.00	U	1.7563	0.0783	-7.53	99.8	-10701.
-6.35	U	1.7563	0.0742	-7.07	103.5	-10371.
-12.70	U	1.7582	0.0651	-5.56	110.2	-10935.
-17.27	U	1.7574	0.0594	-4.80	62.0	- 5108.

800 MeV

Y (mm)	Type	b_0 (T-m)	b_1 (T-m/m)	b_2 (T-m/m ²)	b_3 (T-m/m ³)	b_4 (T-m/m ⁴)
6.35	L	1.4168	0.0469	-2.82	56.3	-336.
0.00	L	1.4168	0.0475	-3.20	68.7	-782.
0.00	U	1.4184	0.0483	-3.15	60.2	-1221.
-6.35	L	1.4164	0.0453	-2.97	53.6	-231.

100 MeV

Y (mm)	Type	b_0 (T-m)	b_1 (T-m/m)	b_2 (T-m/m ²)	b_3 (T-m/m ³)	b_4 (T-m/m ⁴)
17.27	L	0.17436	0.0032	-0.21	3.2	-138.
12.70	L	0.17404	0.0035	-0.23	4.2	-1133.
6.35	L	0.17422	0.0039	-0.21	5.9	-717.
0.00	L	0.17427	0.0036	-0.22	8.2	-961.
0.00	U	0.17449	0.0036	-0.19	8.4	-1068.
-6.35	L	0.17390	0.0033	-0.24	7.3	-691.
-12.70	L	0.17389	0.0032	-0.24	5.1	-215.
-17.27	L	0.17428	0.0028	-0.25	3.6	-860.

H.4.d.6 Coefficients vs Y (vertical)

The coefficient values expressed in terms of the differences in the magnitudes with respect to the midplane values are listed in Table H.4.10. The midplane values used were for

the same data type (U or L) as the off midplane data. For this reason, the L type data at $Y = 0$ is also contained in the 800 MeV and 100 MeV sections of Table H.4.9 even though the U type results are more accurate.

Table H.4.10

Variations of Harmonic Coefficients
With Respect to the $Y = 0$ Results

1000 MeV

Y (mm)	Type	b_0 (%)	b_1 (%)	b_2 (%)	b_3 (%)	b_4 (%)
17.27	U	+0.04	-14.	-35.	-89.	-36.
12.70	U	+0.02	-9.1	-21.	-54.	-15.
6.35	U	0.0	- 4.6	- 5.3	- 5.2	- 6.2
0.00	U	0.0	0.0	0.0	0.0	0.0
-6.35	U	0.0	- 5.2	- 6.1	+ 3.7	- 3.
-12.70	U	+0.1	-17.	-26.	+10.	+ 2.
-17.27	U	+0.06	-24.	-36.	-38.	-52.

800 MeV

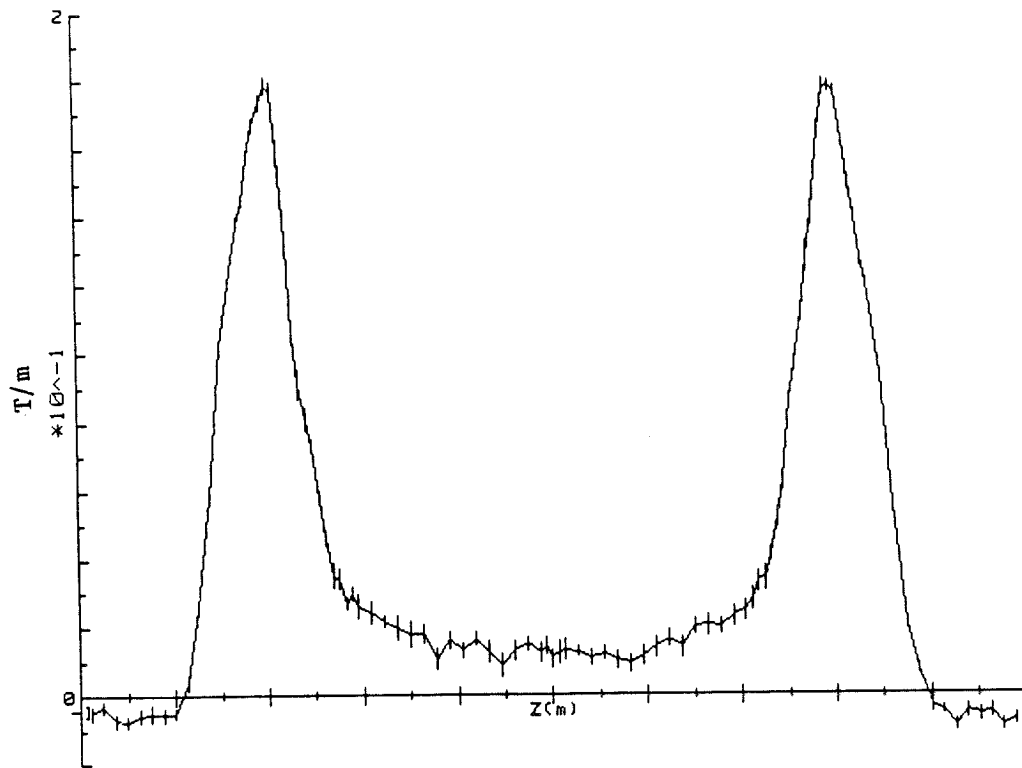
Y (mm)	Type	b_0 (%)	b_1 (%)	b_2 (%)	b_3 (%)	b_4 (%)
6.35	L	0.0	-1.3	-12.	-18.	-57.
0.0	L	0.0	0.0	0.0	0.0	0.0
-6.35	L	-0.03	-4.6	-7.2	-22.	-70.

100 MeV

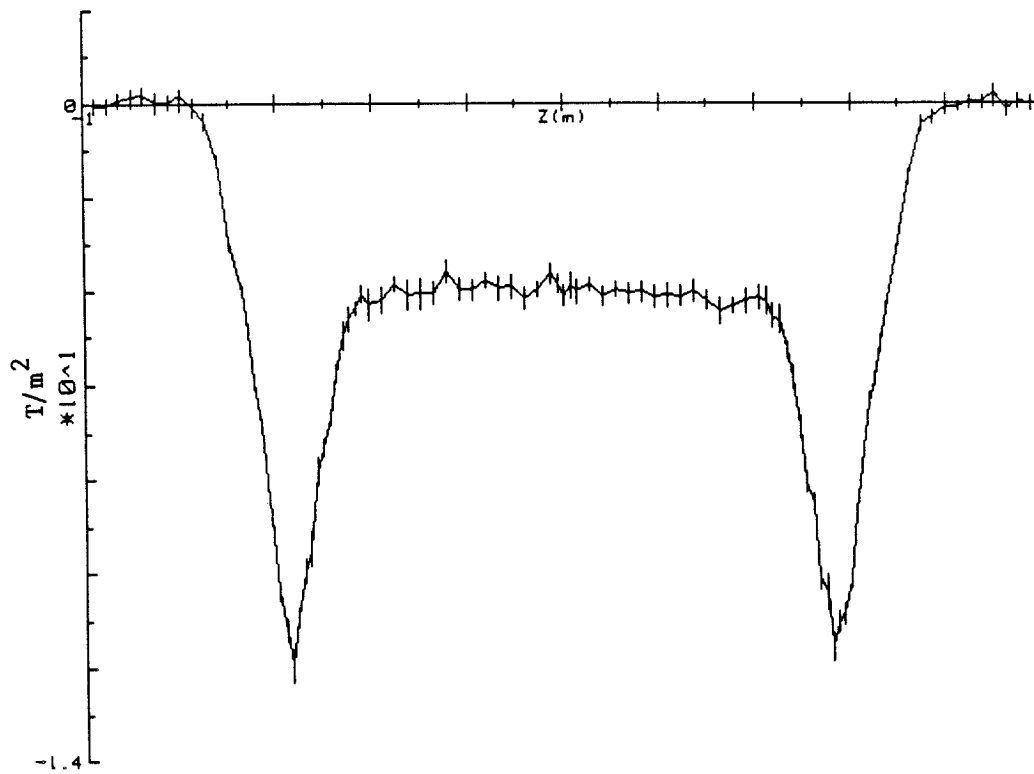
Y (mm)	Type	b_0 (%)	b_1 (%)	b_2 (%)	b_3 (%)	b_4 (%)
17.27	L	+0.5	-11.	- 4.5	-61.	---
12.70	L	-0.13	- 2.8	- 4.5	-49.	---
6.35	L	-0.03	+83.	- 4.5	-28.	-25.
0.00	L	0.0	0.0	0.0	0.	0.
-6.35	L	-0.21	- 8.3	+ 9.1	-11.	-28.
-12.70	L	-0.22	-11.	+ 9.1	-38.	-78.
-17.27	L	-0.01	-22.	+14.	-56.	---

H.4.d.7. Coefficients vs Z(axial)

The harmonic coefficients were calculated for the field values on each radial scan line through the scan geometry at $Y = 0$ for 1000 MeV. The lists of the resulting coefficients are located in Appendix IX-A. The values were plotted for each coefficient from $i = 0$ through $i = 7$. Figure H.4.1. contains plots for the quadrupole and sextupole coefficients ($i = 1$ and $i = 2$) for $Y = 0$ at 1000 MeV. Figure H.4.2. contains the same for 100 MeV.

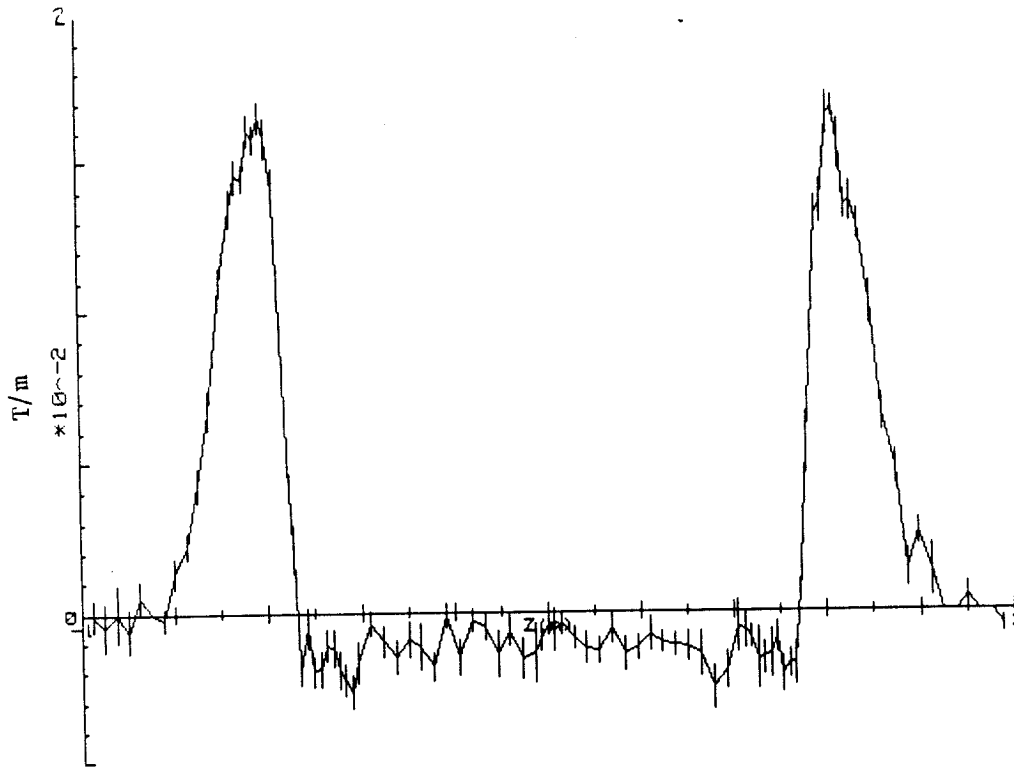


a. Quadrupole (i = 1) Coefficient

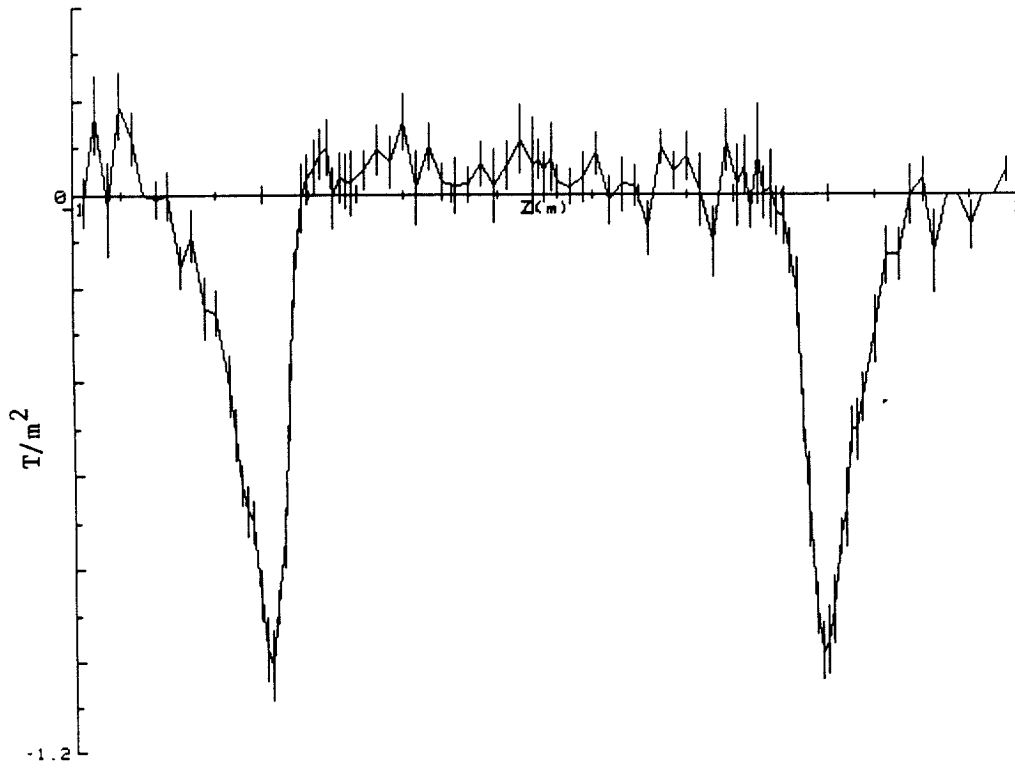


b. Sextupole (i = 2) Coefficient

Figure H.4.1 Field harmonic coefficients vs Z for Y = 0 and 1000 MeV.



a. Quadrupole (i = 1) Coefficient



b. Sextupole (i = 2) Coefficient

Fig. H.4.2. Field Harmonic Coefficients vs Z for Y = 0 and 100 MeV

The plots for the other coefficients are contained in Appendix IX-B and C. The integrals of the coefficients were also found and Table H.4.11 lists the results obtained by both methods.

Table H.4.11

Field Harmonic Coefficients vs Method of Calculation
at Y = 0

1000 MeV

i	Primary (See Table H.4.2.)	Secondary (See Appendix IX-A)	Magnitude Difference
0	1.7563 ± 0.000005	1.7538	-0.0
1	0.0783 ± 0.0005	0.0778	-0.0005
2	-7.53 ± 0.05	-7.55	+0.02
3	100. ± 8.	107.	+7.
4	-10701. + 555.	-10500.	-201.

100 MeV

i	Primary (See Table H.4.3.)	Secondary (See Appendix IX-A)	Magnitude Difference
0	1.7449 ± 0.000002	1.7449	0.0
1	0.0036 ± 0.0001	0.0036	0.0
2	-0.19 ± 0.01	-0.19	0.0
3	8.4 ± 0.3	8.4	0.0
4	-1068. + 44.	-1059.	9.

H.5. Vertical Midplane

The program described in section G.6 was used to define the elevation of the magnetic midplane at all points in the scan geometry. The results for 1000 MeV are contained in Appendix X for a fit degree of 2 to the vertical distribution. The integration and fitting programs described in sections G.3, G.4, and G.5 were then used to obtain the parameters that were used to define the magnetic midplane. The method of fitting the data and then integrating the polynomial coefficients described in section G.5.b was used to find the average elevation, the A_0 coefficient, and slope, A_1 , of the magnetic midplane in the X direction for each radial scan line. A tabular listing and plots of these coefficients for linear fits to the reference data are contained in Appendix X.

Integrals of the coefficients divided by the total length, L, over which they were integrated were used to give the average values for the entire magnet scan geometry. This process was equivalent to finding the

weighted averages of the coefficients but used the same programs as the field data. The plots for the 1000 MeV data, however, show that there are large errors in the coefficient values and some abrupt peaks for the radial scans at the far ends of the scan geometry. Because of this, an integrate-then-fit (see Section G.5.a) process was performed using the calculated offset values rather than the field values. The integrals were also performed over the central region of the axial scans and over the center plus the edges but excluding the tails. The central region was defined as in section H.4.d.3 to include radial scans 30 through 68. The edges include just the peak for the b_1 coefficient for the reference data shown in Fig. H.4.1.a. This region, then, covered scan numbers 9 through 89.

The total length of the integrals and the average magnetic midplane parameters are contained in Table H.5.1 for the 1000 MeV. Table H.5.2 contains the results for 100 MeV; for this case, the plots show no reasons to neglect the tails.

Table H.5.1

Average Magnetic Midplane Locations at 1000 MeV

Axial Scan Numbers	L (m)	Y (mm) [in.]	X-Slope (mm/mm)*10 ⁻³	Description
1-97	1.954	+1.4 [0.055]	-2.0	Total
30-68	0.900	+1.8 [0.071]	-2.3	Central
30-49	0.450	+3.5 [0.135]	+4.5	Right-Central
49-68	0.450	+0.05 [0.002]	-9.0	Left-Central
9-89	1.548	+0.9 [0.036]	-1.0	Center & Edges
9-49	0.774	+1.9 [0.074]	+1.6	Right - C+E
49-89	0.774	-0.03 [0.001]	-3.6	Left - C+E

Average Y over entire scan geometry = +0.97 mm [+0.038 in.].

Table H.5.2

Average Magnetic Midplane Locations at 100 MeV

Axial Scan Numbers	L (m)	Y (mm) [in.]	X-Slope (mm/mm)*10 ⁻³	Description
3-51	0.977	-0.084 [0.003]	+6.8	Total
Average Y over entire scan geometry = -0.09 mm [-0.0004 in.].				

I. Magnetostatic Field Calculation

The program PE2D⁵ was used by R. Lari to calculate the magnetic fields in this magnet. A BH table for SAE 1010 steel was used and the center field was about 1.25 T. A sketch of the as-built magnet geometry is shown in Fig. A.1. and a plot of the flux lines is shown in Fig. I.1.

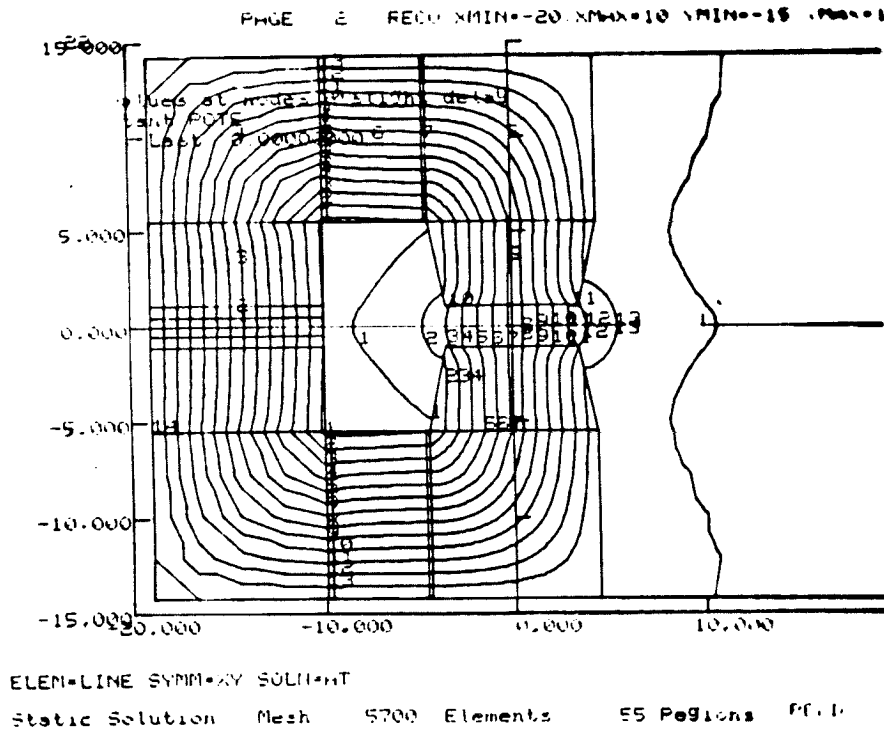


Fig. I.1 Plot of flux lines determined by PE2D calculation.

The primary purpose of this calculation was to determine how the asymmetric placement of the coils in the vertical direction affects the location of the magnetic midplane. Little time was spent in optimizing this calculation, but it is felt that the results are relatively true to life. To get some idea of how realistic the results were, the vertical field components were compared to the measured values at several points. A plot of these values is shown in Fig. I.2 along with a curve connecting the measured values at $Z = 0$. The fact that there were a couple of sets of adjacent points which had the same field values indicated affects of the finite element geometry.

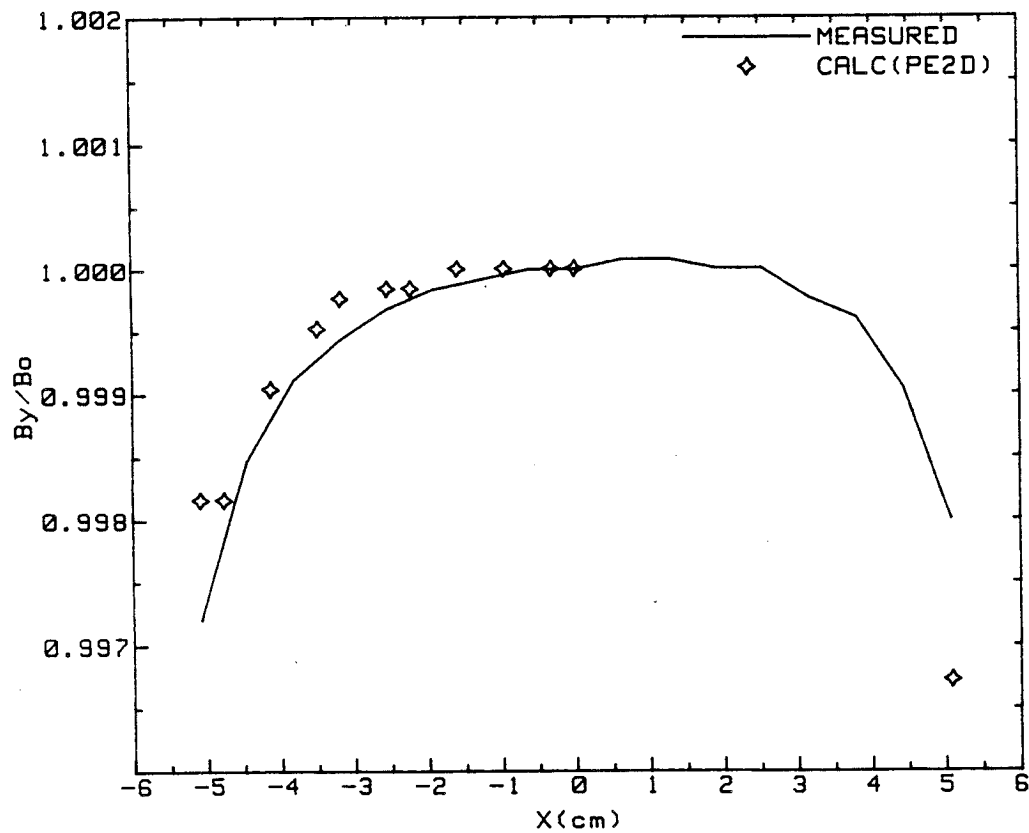


Fig. I.2 Comparison of measured and calculated vertical field component across the gap at $Z = 0$ cm.

The position of the magnetic midplane was estimated by plotting the radial component of the fields, B_x , and finding the location of the point at which the curve crossed through zero. A representative plot for such a curve at $X = -4.1$ cm is shown in Fig. I.3. It can be seen that this curve is not smooth, which was interpreted as indicating residual effects of the finite element geometry used in the calculation; no attempts were made, however, to remove these effects. The locations of the calculated zero-crossing points, the magnetic midplane, are listed in Table I.1. These values have an estimated error of about ± 0.5 mm. There is also listed, in Table I.1, the average location of the magnetic midplane as determined from the measured data at a central field of 1.5 T for the points between $Z = +2.727$ and 37.966 cm. The points listed are close to the calculated points.

Table I.1

The Magnetic Midplane Relative to the Geometrical Midplane

Calculated		Measured	
X (cm)	Y (mm)	X (cm)	Y (mm)
-5.08	$1.3 \pm 0.5^*$	-5.08	$0.6 \pm 0.5^*$
-4.76	1.3	-4.44	1.1
-4.13	1.3	-3.81	1.7
-3.49	2.5		
-2.86	3.7	-3.18	2.6
-2.50	3.8	-2.54	3.8
-2.22	5.1	-1.90	4.9
+5.08	-1.3	+5.08	1.0

*Estimated error

A second calculation was done with the coils located symmetrically in the vertical direction, and the locations of the magnetic midplane were all found to be at $Y = 0$.

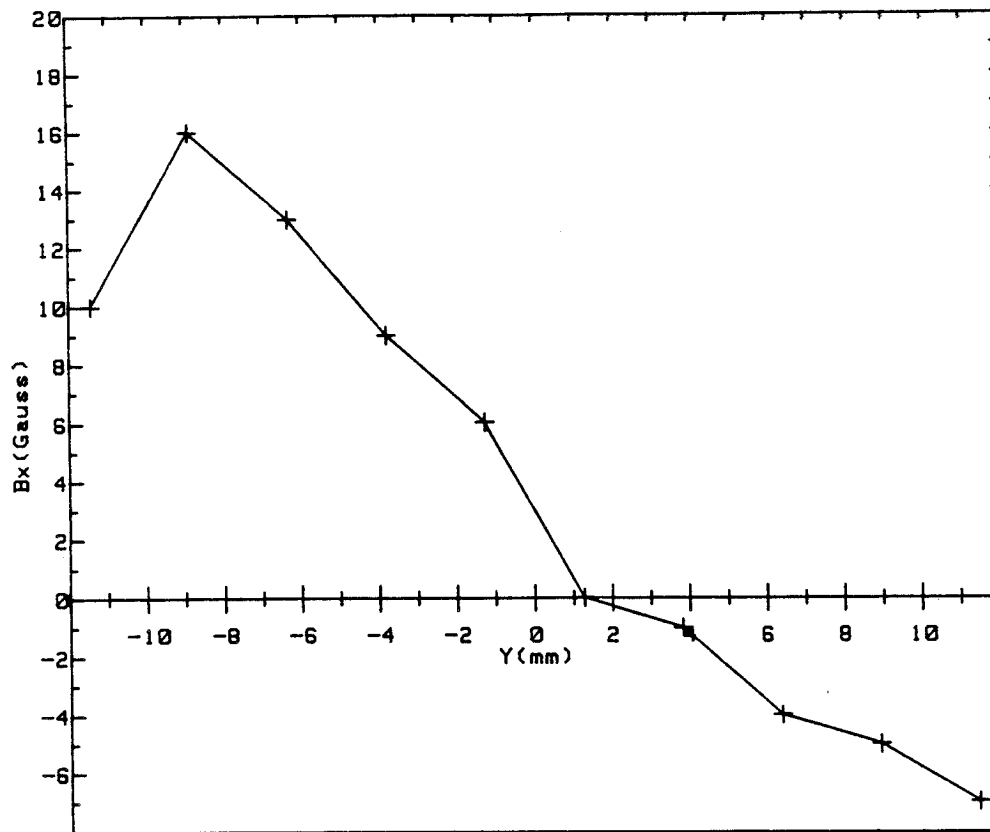


Fig. I.3 Plot of B_x vs Y at $X = -4.1$ cm as calculated by PE2D.

J. Discussions

There was no attempt in the following discussions to cover all of the areas that might be addressed with these measurements and analyses, but a few of the more obvious ones are covered. The absolute accuracy of the results described in this report is of interest. A number of tests were conducted and described here that verify the accuracy of these measurements. The estimated error in the measurement of the vertical field at a given point (Sections H.2 and H.3), for example, was derived in section F.2.f. to be about 0.03% at 1.55 T. Other data repeatabilities for measurements taken several days apart provided more evidence to support this conclusion. Looking at the field integrals and effective lengths (Sections H.2 and H.3), for example, shows that the results at 1000 MeV have nearly identical values for the three cases at $Y = 0$, and ± 0.635 cm. This was expected and shows that the measuring system was repeatable over a several day time period.

The representative plots of the field integrals over the entire scan geometry shown in Figs. H.2 and H.3 show an obvious asymmetry. The peak value is also displaced from the geometrical center of the gap ($X = 0$) by between 1 and 2 cm. These effects are primarily due to the field asymmetries at the ends of the magnet. To demonstrate this a plot of the integrals over the entire axial scan geometry and over only the central portion are shown in Fig. J.1 for 1000 MeV and $Y = 0$; the values plotted are relative to the value at the $X = 0$. This clearly shows that the integrals for the central part of the scan are much more symmetric and centered than those for the entire scan. Similar plots for 100 MeV are shown in Fig. J.2 using the same scales as those in Fig. J.1. This shows that at 100 MeV, the integrals are much more symmetric and centered than at 1000 MeV. The center integrals at 100 MeV actually have a slope of opposite sign.

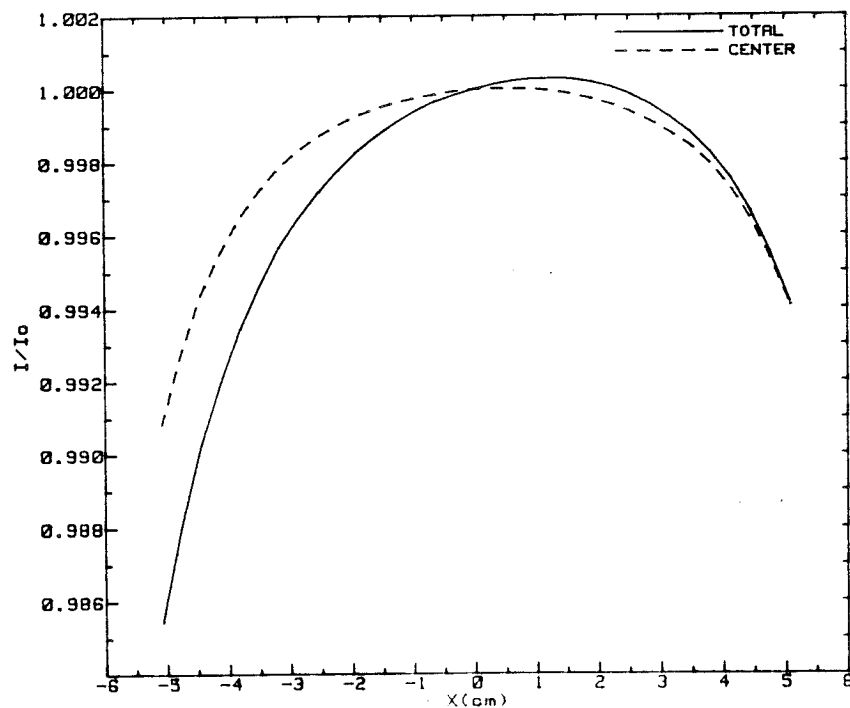


Fig. J.1 Integrals vs X for 1000 MeV and Y = 0 for total and center sections of axial scans. Values shown are relative to the value at X = 0.

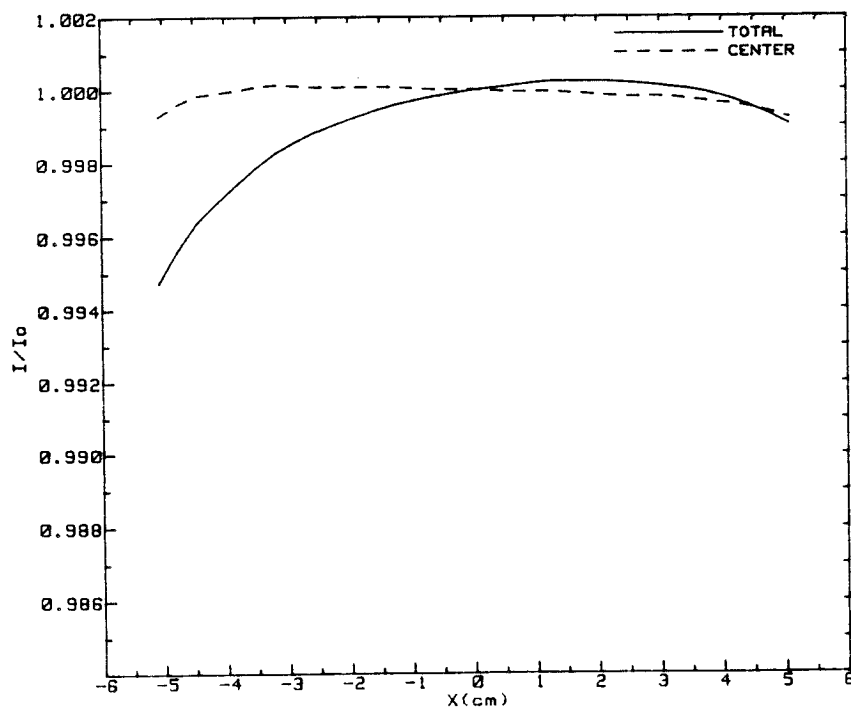


Figure J.2 Integrals vs X for 100 MeV and Y = 0 for total and center sections of axial scans. Values shown are relative to the value at X = 0.

The plot of the dipole field strength vs Z at 1000 MeV and $Y = 0$ in Appendix IX.B shows that the field has a significant hump throughout the central region of the gap. This indicated that the core is well saturated at 1000 MeV. The corresponding plot for 100 MeV is in Appendix IX.C and shows no such problem.

The plots of the harmonic coefficients for $i > 0$ shown in Appendix IX.B and IX.C clearly indicate which ones are not significantly different from zero; see IX.B.6 for example. They also clearly show the relative sizes of the errors at every axial scan and the locations of isolated features; see IX.B.4, for an example of an isolated peak in an otherwise nondescript plot. It is also easy to subjectively compare the ends of the magnet by examining the shapes of the peaks which usually appear at each end and for each harmonic for $i > 0$.

The representative relative harmonic strengths in Table H.4.4. show that the quadrupole and sextupole errors are proportionately larger for 1000 MeV by two to three times. The higher harmonics, however, are proportionately the same. Also Table H.4.6. shows that the center region of the 100 MeV data has quadrupole and sextupole harmonic coefficients that are opposite in sign to those of the end regions. This is desirable but would be even better if the magnitudes in the center were larger by around five times. The higher harmonics, on the other hand, have the same signs for all regions. The 1000 MeV results in Table H.4.5. show no sign reversals.

The vertical distribution of the harmonic coefficients is shown in the list in Table H.4.10 for the variations from the $Y = 0$ values. This shows that the dipole fields are constant to $\leq 0.2\%$ for all the planes and excitations and are $\leq 0.1\%$ for 15 out of 17 cases. All coefficients at 1000 MeV for $i > 0$ are $\leq 5\%$ at $Y = \pm 0.635$ cm. Generally, the magnitudes of coefficients for $i > 0$ decrease towards the poles; i.e., the worst case is at the midplane. The trends for the 100 MeV data are not totally monotonic but they do seem to follow this same pattern.

The need to fully measure both sides of the magnet was addressed. There is no question that the second side does need to be measured at least once to verify that there are no localized problems in the core or coil, like a void in the core, a large slip in a block of laminations, or a misplaced conductor. Furthermore, to get the most accurate results, it is mandatory that both sides be measured. Looking at Table H.3.2, which contains the effective lengths for 800 MeV, it can be seen that the effective lengths

derived from the left side data are only 1.3 mm shorter at all values of X than the results for the two-sided data. This corresponds to 0.11% or less than the thickness of one lamination. This source of error could be minimized by appropriately normalizing the integrals for the single side data. The factor used could be found by finding the appropriate field integrals for the one set of two sided data. This process is even appropriate for the other required excitations; Table H.3.3 shows that for the 100 MeV results the difference is about 1.4 mm at 100 MeV. The values in Table H.4.8, however, show that the harmonic coefficients for $i > 0$ for the whole magnet can be estimated to within the calculated errors of the values at 1000 MeV and to within two times the calculated errors for 100 MeV. These differences correspond to field strengths at a radius of 5 cm that are $\leq 0.03\%$ of the value at $X = 0$. If the above corrections are made, the agreement would be even better.

The angles of the effective edge at the ends of the gap were also found. These edges should be parallel to the X -axis for an ideal magnet. The coordinates of the left edge are shown in Table A in Appendix VIII. The effective edges are not straight but were fit with a straight line so an angle could be easily defined. A plot of the effective edge is shown in Fig. J.3 for the left end at 1000 MeV; the location of the core end is at $Z = 0.0$. The 100 MeV data provides a very similar plot except that it is displaced in Z . The angle of the calculated straight lines for the left and right ends with respect to the X -axis were 1.761° and 1.752° respectively, and the RMS deviations of the edge points from the fit lines were both about 0.6 mm which corresponds to an angle of $\pm 0.03^\circ$. For 100 MeV, the angles were both $1.1^\circ \pm 0.03^\circ$.

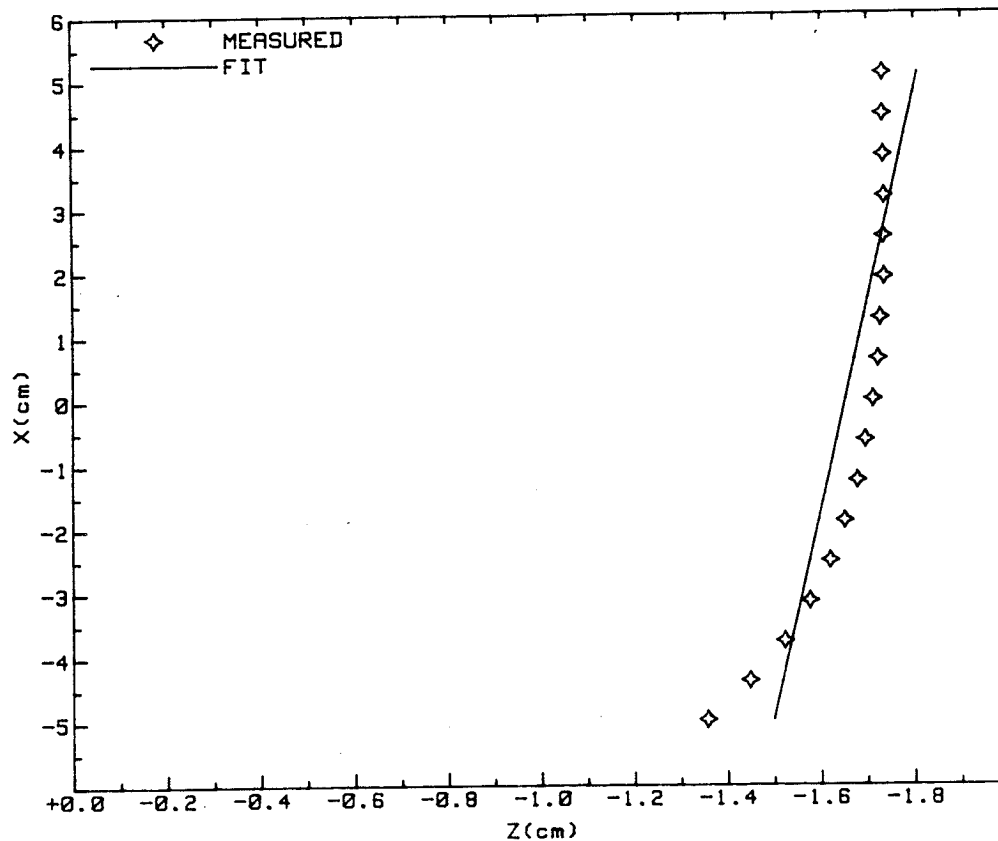


Figure J.3 The core left end and the effective edge at 1000 MeV.

The final area that will be discussed here is the magnetic midplane. The process used to find its location at each point in the measured scan geometry was described in sections G.6. and H.5., and the reasons for expecting large errors in these values was described. The results listed in Table H.5.2 for the average locations of the midplane at 100 MeV indicate that it is not appreciably shifted from the geometrical midplane for this energy. The 1000 MeV results, however, show that it is shifted to about $Y = +1.4$ mm on the average. The error in this value was estimated to be large, at least 0.5 mm. The radial distributions of the calculated shifts at the individual scan points listed and plotted in Appendix X show some general trends in the values. First the distributions in the central part of the axial scan show that the shift is small at the inside radius edge of the gap and the values tend to increase towards $X = 0$ and then decrease towards the outside radius. Also, since there is considerable curvature in these values, fitting with straight lines did result in rather poor fits. This was chosen, however, because only linear errors are correctable by simple elevation adjustments in the magnet.

A plot of the calculated, magnetic midplane average locations vs X for the central portion of the 1000 MeV data is shown in Fig. J.4. This was felt to be the best case to use from those listed in Table H.5.1 to represent the magnetic midplane at 1000 MeV. The relatively smooth shape of the curve supports this choice as reasonably good. The straight line fit to this data is also shown here.

The plot of the average elevation vs Z in Appendix X.C also shows a definite step occurring at the center of the magnet. The size of the step was about 3 mm. This might be a real shift in the magnet geometry. The field calculations described in Section I seems to agree with the high side of the step not the low side. The fact that the step occurs right at the magnet center also indicates that it may be related to the movement of the measuring system between the ends of the magnet. Because of time limitations, no attempts were made to validate these results any further.

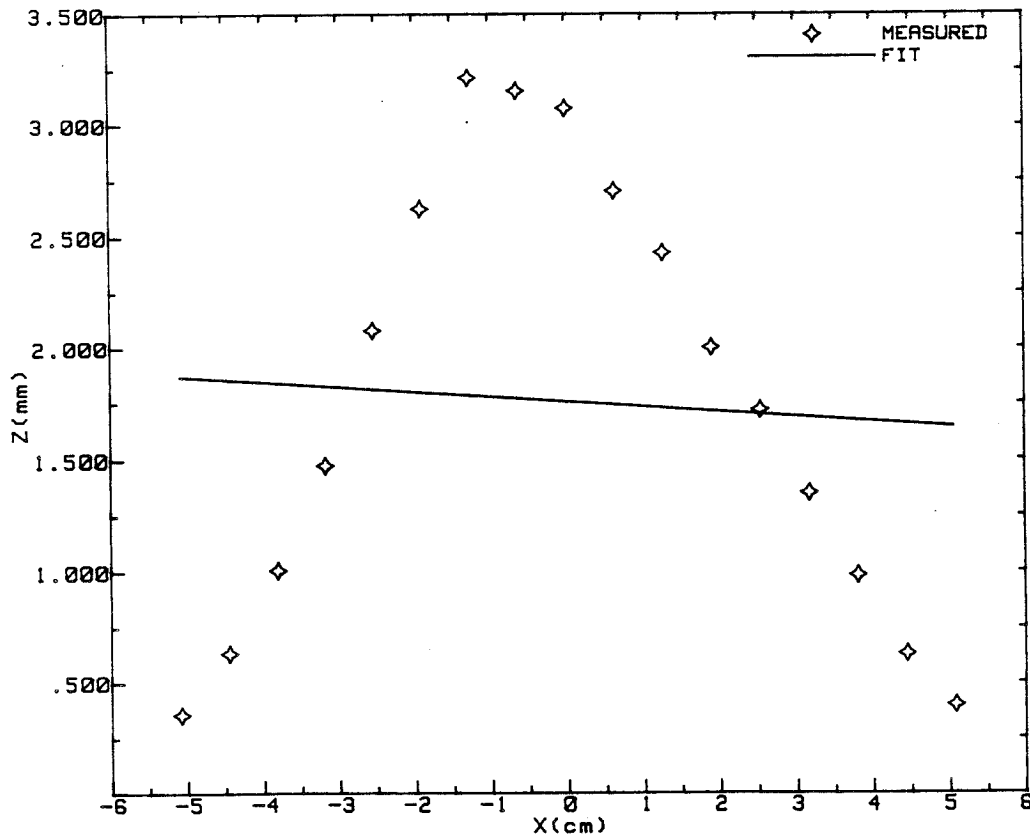


Figure J.4 The average location of the magnetic midplane found for the center portion of the scan from measured data vs X and the fit line used to define the average parameters for the entire magnet.

As a final note to this report, some suggestions will be made here that might help to improve the existing magnets at Aladdin and help to expedite future measurements if any are required. The most obvious source of problems seems to be the vertical asymmetries in the locations of the coils. This would be reduced by adding the appropriate spacers between the lower coil, the thinner one, and the bottom yoke. The stainless mounting bars that hold the coils to the cores also show evidence of being bent. It would not be difficult to install larger bars and prevent possible coil movements at the high excitation currents.

The measurements were taken on a one shift per day schedule over about a two week, ten working day, period. The measuring system operated flawlessly during this time and was energized for 96 to 120 hours at a time. The power supply also worked reliably, but there was one cooling water trip probably caused by a pressure bump. This experience showed that the measuring system could be operated, unattended, for long periods of time. It is proposed, therefore, that the system be modified to be able to automatically initiate scans at different elevations and even at different excitations. To change the elevation of the scanning plane would require that the Z-axis be motorized. The control hardware is already installed in the system interface and the motor hardware is on hand. This would, however, require modifications in the control program and some new motor mounting components. To change the magnet current would require both new hardware and program changes. With these changes, one magnet could easily be measured in one week.

Some more effort could be spent in optimizing the magnetic field calculations with particular attention spent in finding the magnetic midplane.

In summary, it is felt that the original goals for these measurements were met. The vertical magnetic fields were measured for excitations of 1000 MeV, 800 MeV, and 100 MeV. The harmonic coefficients corresponding to the integrated field values were found, and the errors in the coefficients were determined. And finally, the magnetic midplane was found and some of the associated parameters and trends were presented.

Acknowledgments

The following persons provided much appreciated assistance in obtaining the measurements, analyzing the data, and preparing this report:

P. Bertucci	D. McGhee	R. Swanstrom
F. Brumwell	W. Mehler	D. Voss
Y. Cho	W. Praeg	D. Wallace (U of Wisc.)
R. Kliss	E. Rizzo	E. Wallace
M. Knott	J. Sendera	R. Wehrle
R. Lari	G. Sprau	W. Winter (U of Wisc.)

References

1. K. Thompson, "Precision Magnet Measuring System," ANL-GEM-14-81, Oct. 1981.
2. K. M. Thompson, et al., "Field Properties of a Three Orbit Prototype Sector Magnet for the 4 GeV CW Electron Microtron," J. Physique 45 (1984) C1-229.
3. J. Orear, "Notes on Statistics for Physicists," UCRL-8417, August 13, 1965.
4. R. Cziffna and M. J. Moravscik, "A Practical Guide for the Method of Least Squares," UCRL-8522.
5. C. S. Biddlecombe, N. S. Diserens, C. P. Riley, J. Simkin, "PE2D User Guide," RL-81-089 (Version 6.3) Sept. 1983, Available from Vector Fields.

APPENDICES

The data contained in the tables and plots contained in the following sections are all based on the measurements of the vertical magnetic fields at $Y = 0$ for an excitation corresponding to 1000 Mev except where noted.

I.	Raw field values for left side only	I-1
II.	The X-coordinates for left side only	II-1
III.	The Y-coordinates left side only	III-1
IV.	The Z-coordinates for all the points	IV-1
V.	Auxiliary probe data for left side only	V-1
	A. NMR	V-2
	B. Temperature of Hall probe	V-2
VI.	3D plot of left side data only	VI-1
VII.	Normalized, matched, and merged field values for all points	VII-1
VIII.	Field integrals, effective lengths, harmonic coefficients	VIII-1
	A. Left side only	VIII-1
	B. Both sides	VIII-1
IX.	Secondary method for defining harmonic coefficients for all points	IX-1
	A. Table of coefficients for each radial scan	IX-1
	1. Integrated coefficients for 1000 MeV	IX-2
	2. Integrated coefficients for 100 MeV and $Y = 0$	IX-2
	B. Plots of coefficients vs Z at 1000 MeV ($i = 0,3,4,5,6,7$)	IX-3
	C. Plots of coefficients vs Z at 100 MeV ($i = 0,3,4$)	IX-6
X.	Vertical midplane	X-1
	A. Calculated locations at all scan points	X-1
	B. Fit coefficients on each radial scan	X-5
	C. Plot of coefficients vs Z	X-6

I. Raw field values for left side only.

The following data is derived from the data file(AL.PI5) described here:

TITLE:ALADDIN Dipole-Polar Grid Left End (Z=0.00) Offset arc scan R=2.08m

Run number (15) was started at 9:48:5AM on 7/3/85.

The scan area is defined for this run by the parameters for region #1 in the geometry file named ALPIE.

The following is a list of the data in the ARC section of the scan:

Page 2

X		Field(Gauss)									
(in)	T(deg)	T(deg)	T(deg)	T(deg)	T(deg)	T(deg)	T(deg)	T(deg)	T(deg)	T(deg)	T(deg)
-3.000	0.0	14489.3	14493.7	14497.7	14473.7	14421.3	14340.0	14272.3	14131.0	14160.0	14171.0
-2.500	0.0	15215.7	15213.3	15207.7	15189.7	15161.0	15135.7	15109.0	14989.0	14976.0	14949.3
-2.000	0.0	15447.7	15448.3	15447.3	15445.3	15437.7	15425.3	15415.0	15240.0	15246.3	15210.3
-1.750	0.0	15499.0	15499.0	15497.3	15495.3	15489.0	15472.0	15457.0	15335.0	15304.0	15266.3
-1.500	0.0	15527.3	15528.0	15527.3	15521.0	15514.0	15507.0	15497.0	15320.0	15339.3	15302.0
-1.250	0.0	15547.3	15547.3	15547.3	15546.0	15540.7	15535.0	15528.0	15339.3	15361.7	15323.0
-1.000	0.0	15560.0	15559.7	15558.7	15558.0	15554.0	15548.0	15541.7	15360.0	15376.3	15339.0
-0.750	0.0	15567.7	15567.0	15567.0	15566.0	15562.3	15557.3	15550.0	15423.7	15391.7	15355.0
-0.500	0.0	15573.0	15573.0	15572.7	15572.0	15568.0	15563.0	15556.0	15427.7	15396.7	15358.7
-0.250	0.0	15576.0	15576.0	15575.0	15575.0	15570.7	15566.3	15559.0	15430.3	15398.7	15361.7
0.000	0.0	15577.0	15577.7	15577.0	15576.7	15572.7	15568.3	15561.0	15430.0	15398.0	15361.7
0.250	0.0	15577.0	15577.0	15576.0	15576.0	15571.0	15566.3	15559.0	15426.3	15396.0	15358.7
0.500	0.0	15576.3	15576.3	15576.0	15574.3	15571.0	15566.3	15559.0	15426.3	15396.0	15358.7
0.750	0.0	15572.3	15572.3	15572.0	15571.7	15568.3	15562.3	15556.0	15421.3	15390.0	15354.0
1.000	0.0	15567.0	15567.0	15567.3	15565.0	15562.0	15557.0	15550.0	15413.0	15382.7	15345.0
1.250	0.0	15557.3	15557.3	15557.0	15556.3	15553.0	15547.7	15540.0	15399.3	15368.0	15332.0
1.500	0.0	15541.7	15542.0	15541.7	15540.0	15536.0	15533.0	15526.0	15378.0	15347.0	15310.0
1.750	0.0	15518.0	15518.0	15517.0	15517.0	15514.0	15509.3	15502.0	15378.0	15347.0	15310.0
2.000	0.0	15473.0	15473.0	15472.0	15475.7	15475.0	15472.0	15465.0	15343.0	15311.7	15274.0
2.500	0.0	15289.0	15289.0	15287.7	15289.0	15294.7	15299.7	15296.0	15184.7	15147.7	15106.0
3.000	0.0	14707.0	14703.7	14705.7	14714.0	14742.3	14781.0	14795.0	14705.7	14644.0	14567.0

X		Field(Gauss)									
(in)	T(deg)	T(deg)	T(deg)	T(deg)	T(deg)	T(deg)	T(deg)	T(deg)	T(deg)	T(deg)	T(deg)
-3.000	14300.0	14366.0	14400.0	14403.3	14371.7	14305.7	14210.0	14126.0	13424.3	12370.0	11052.3
-2.500	15140.0	15131.3	15156.0	15150.0	15129.3	15098.7	15066.3	15013.3	14327.7	13514.7	11970.3
-2.000	15410.0	15408.0	15403.0	15394.0	15379.0	15358.3	15332.3	15303.0	14671.3	13963.0	12392.3
-1.750	15467.7	15463.3	15457.0	15446.7	15431.7	15413.3	15391.0	15364.7	14755.7	14002.0	12502.3
-1.500	15500.7	15495.3	15488.0	15478.0	15464.0	15447.0	15426.0	15400.0	14807.7	14066.0	12577.0
-1.250	15522.7	15516.7	15508.7	15498.3	15485.0	15467.0	15448.0	15423.0	14844.3	14108.0	12627.0
-1.000	15535.7	15529.7	15521.3	15511.7	15498.0	15481.0	15461.3	15438.0	14869.0	14137.0	12662.0
-0.750	15544.3	15538.3	15532.3	15519.3	15506.3	15490.0	15470.7	15447.3	14886.0	14159.3	12686.0
-0.500	15549.7	15543.0	15535.7	15525.7	15512.0	15496.0	15477.0	15454.0	14899.0	14173.7	12703.0
-0.250	15553.3	15547.3	15538.0	15529.0	15516.0	15499.0	15480.3	15458.0	14907.0	14184.0	12714.3
0.000	15554.0	15548.0	15540.7	15530.0	15517.3	15501.7	15483.0	15459.7	14912.3	14191.0	12722.7
0.250	15555.0	15549.0	15540.0	15530.0	15517.3	15500.3	15482.7	15459.3	14915.7	14195.3	12727.7
0.500	15555.0	15549.3	15540.3	15530.3	15517.3	15500.3	15482.7	15459.3	14915.7	14195.3	12727.7
0.750	15555.0	15549.3	15540.3	15530.3	15517.3	15500.3	15482.7	15459.3	14915.7	14195.3	12727.7
1.000	15549.3	15537.7	15529.7	15519.7	15507.3	15491.0	15473.3	15451.0	14907.7	14177.0	12720.0
1.250	15543.3	15537.7	15529.7	15519.7	15507.3	15491.0	15473.3	15451.0	14897.7	14177.0	12720.0
1.500	15519.7	15520.0	15520.0	15511.0	15497.3	15483.0	15465.7	15443.3	14882.0	14160.0	12692.3
1.750	15496.3	15490.0	15481.3	15473.0	15460.0	15445.7	15430.0	15408.0	14855.7	14134.0	12667.7
2.000	15460.0	15452.3	15443.0	15432.7	15421.0	15408.0	15394.3	15372.3	14816.0	14093.0	12629.7
2.500	15290.7	15278.0	15263.7	15243.0	15215.7	15189.0	15163.0	15137.0	14642.0	13926.0	12476.0
3.000	14784.7	14743.7	14708.0	14689.7	14693.0	14715.0	14746.0	14746.0	14151.0	13475.7	12098.0

The following is a list of the data in the TANGENT line sections of the scan:

X (in)	Field(Gauss)									
	L(in)= -5.000	L(in)= -1.000	L(in)= -1.500	L(in)= -2.000	L(in)= -2.500	L(in)= -3.000	L(in)= -3.500	L(in)= -4.000		
-3.000	5984.3	4905.0	4040.3	3338.0	2745.3	2238.0	1796.0	1401.0	-3.000	-17.000
-2.500	6467.0	5270.3	4321.0	3557.0	2922.0	2384.0	1918.0	1506.0	-2.500	-16.000
-2.000	6791.3	5534.0	4532.0	3727.7	3061.0	2500.0	2017.7	1591.3	-2.000	-15.000
-1.750	6901.0	5630.0	4614.0	3796.0	3117.0	2547.3	2057.7	1626.0	-1.750	-14.000
-1.500	6983.0	5705.0	4680.0	3851.0	3165.3	2588.0	2092.0	1657.0	-1.500	-13.000
-1.250	7044.0	5765.7	4733.0	3897.7	3205.0	2622.0	2123.0	1683.0	-1.250	-12.000
-1.000	7091.0	5811.0	4776.0	3935.0	3238.3	2651.3	2147.7	1705.0	-1.000	-11.000
-750	7125.0	5844.3	4808.0	3965.0	3264.7	2675.0	2169.0	1723.3	-750	-10.000
-500	7148.3	5870.0	4834.3	3989.0	3286.0	2694.0	2185.3	1739.3	-500	-9.000
-250	7165.0	5888.3	4853.0	4007.0	3303.7	2721.0	2199.7	1752.0	-250	-8.000
0.000	7177.7	5901.7	4866.0	4020.0	3316.3	2736.0	2219.0	1769.3	0.000	-7.000
.250	7184.7	5908.7	4876.0	4030.0	3325.0	2739.0	2228.0	1779.7	.250	-6.000
.500	7186.0	5913.0	4881.0	4035.3	3332.0	2740.0	2230.0	1780.0	.500	-5.000
.750	7185.7	5914.7	4883.0	4038.0	3335.7	2743.0	2230.0	1780.3	.750	-4.000
1.000	7180.7	5911.0	4880.7	4037.3	3334.0	2739.0	2228.0	1779.7	1.000	-3.000
1.250	7170.3	5903.0	4876.0	4033.0	3328.3	2736.3	2224.0	1777.0	1.250	-2.000
1.500	7156.7	5891.0	4865.3	4026.0	3321.0	2730.7	2224.0	1773.0	1.500	-1.000
1.750	7136.0	5874.7	4851.0	4015.0	3310.0	2723.0	2207.7	1760.0	1.750	0.000
2.000	7107.0	5850.3	4833.0	4000.7	3297.3	2699.3	2185.0	1741.0	2.000	-1.000
2.500	7014.3	5778.0	4777.0	3957.7	3277.3	2669.3	2175.0	1741.0	2.500	-2.000
3.000	6849.0	5657.0	4687.0	3892.0	3229.0	2663.3	2175.0	1741.0	3.000	-3.000

X (in)	Field(Gauss)									
	L(in)= -4.500	L(in)= -5.000	L(in)= -6.000	L(in)= -7.000	L(in)= -8.000	L(in)= -9.000	L(in)= -10.000	L(in)= -11.000		
-3.000	1049.0	737.7	271.0	44.0	-38.0	-64.0	-69.0	-66.0	-3.000	-17.000
-2.500	1141.0	815.7	318.0	63.0	-32.0	-62.0	-69.7	-67.0	-2.500	-16.000
-2.000	1215.0	880.0	359.7	80.3	-26.0	-61.0	-70.0	-68.0	-2.000	-15.000
-1.750	1246.3	907.0	377.7	89.0	-23.0	-60.0	-70.3	-68.7	-1.750	-14.000
-1.500	1273.0	931.0	394.0	97.0	-20.0	-60.0	-70.0	-69.0	-1.500	-13.000
-1.250	1297.0	952.0	408.0	103.7	-18.0	-59.0	-71.0	-69.3	-1.250	-12.000
-1.000	1316.0	969.3	421.0	110.0	-15.0	-59.0	-70.3	-70.0	-1.000	-11.000
-750	1337.7	983.7	432.0	115.0	-13.0	-58.0	-70.7	-70.3	-750	-10.000
-500	1358.0	997.0	441.3	121.0	-11.0	-58.0	-71.0	-71.0	-500	-9.000
-250	1367.7	1007.0	449.0	125.0	-9.7	-57.0	-71.3	-71.3	-250	-8.000
0.000	1374.7	1016.0	456.0	129.0	-8.3	-56.0	-71.0	-72.0	0.000	-7.000
.250	1374.7	1022.0	461.0	132.0	-7.0	-56.0	-72.0	-72.0	.250	-6.000
.500	1380.0	1027.3	465.3	134.3	-6.0	-56.0	-72.0	-73.0	.500	-5.000
.750	1383.0	1031.0	469.0	137.0	-5.0	-56.0	-73.0	-73.7	.750	-4.000
1.000	1385.0	1033.0	471.0	138.0	-4.0	-56.0	-72.0	-74.0	1.000	-3.000
1.250	1385.0	1034.0	473.0	139.0	-4.0	-56.0	-72.0	-74.0	1.250	-2.000
1.500	1385.0	1034.0	473.0	140.0	-3.0	-56.0	-72.0	-74.0	1.500	-1.000
1.750	1383.7	1033.0	473.3	140.7	-3.0	-56.0	-73.7	-74.3	1.750	0.000
2.000	1381.0	1031.3	473.0	140.7	-3.0	-56.0	-74.0	-75.0	2.000	-1.000
2.500	1371.0	1025.0	469.3	139.3	-4.0	-57.0	-74.0	-75.0	2.500	-2.000
3.000	1357.3	1014.0	463.3	137.0	-6.0	-58.0	-75.0	-75.3	3.000	-3.000

II. The X-coordinates for left side only.

The following data is derived from the data file(OL.P15) described here:
TITLE:ALADDIN Dipole-Polar Grid Left End (Z=0.00) Offset arc scan R=2.08m
Run number (15) was started at 9:48:5AM on 7/3/85.

The scan area is defined for this run by the parameters for region #1
in the geometry file named ALPLE.

The following is a list of the data in the ARC section of the scan:

X (in)	X(in)					X(in)				
	T(deg)= .750	T(deg)= .375	T(deg)= 0.000	T(deg)= -3.75	T(deg)= -7.50	T(deg)= -11.25	T(deg)= -15.00	T(deg)= -18.75	T(deg)= -22.50	T(deg)= -26.25
-3.000	-3.0070	-3.0018	-3.0000	-3.0018	-3.0070	-3.0281	-3.0632	-3.1124	-3.1750	-3.2500
-2.500	-2.5070	-2.5018	-2.5000	-2.5018	-2.5070	-2.5281	-2.5632	-2.6124	-2.6750	-2.7500
-2.000	-2.0070	-2.0018	-2.0000	-2.0018	-2.0070	-2.0281	-2.0632	-2.1124	-2.1750	-2.2500
-1.500	-1.5070	-1.5018	-1.5000	-1.5018	-1.5070	-1.5281	-1.5632	-1.6124	-1.6750	-1.7500
-1.000	-1.0070	-1.0018	-1.0000	-1.0018	-1.0070	-1.0281	-1.0632	-1.1124	-1.1750	-1.2500
-.500	-.5070	-.5018	-.5000	-.5018	-.5070	-.5281	-.5632	-.6124	-.6750	-.7500
0.000	0.0070	0.0018	0.0000	0.0018	0.0070	0.0281	0.0632	0.1124	0.1750	0.2500
.500	.5070	.5018	.5000	.5018	.5070	.5281	.5632	.6124	.6750	.7500
1.000	1.0070	1.0018	1.0000	1.0018	1.0070	1.0281	1.0632	1.1124	1.1750	1.2500
1.500	1.5070	1.5018	1.5000	1.5018	1.5070	1.5281	1.5632	1.6124	1.6750	1.7500
2.000	2.0070	2.0018	2.0000	2.0018	2.0070	2.0281	2.0632	2.1124	2.1750	2.2500
2.500	2.5070	2.5018	2.5000	2.5018	2.5070	2.5281	2.5632	2.6124	2.6750	2.7500
3.000	3.0070	3.0018	3.0000	3.0018	3.0070	3.0281	3.0632	3.1124	3.1750	3.2500

X (in)	X(in)					X(in)				
	T(deg)= -9.750	T(deg)= -10.500	T(deg)= -11.250	T(deg)= -12.000	T(deg)= -12.750	T(deg)= -13.500	T(deg)= -14.250	T(deg)= -15.000	T(deg)= -15.750	T(deg)= -16.500
-3.000	-4.1847	-4.3734	-4.5760	-4.7924	-5.0224	-5.2662	-5.5237	-5.7948	-6.0796	-6.3784
-2.500	-3.6847	-3.8734	-4.0760	-4.2924	-4.5224	-4.7662	-5.0237	-5.2948	-5.5796	-5.8784
-2.000	-3.1847	-3.3734	-3.5760	-3.7924	-4.0224	-4.2662	-4.5237	-4.7948	-5.0796	-5.3784
-1.500	-2.6847	-2.8734	-3.0760	-3.2924	-3.5224	-3.7662	-4.0237	-4.2948	-4.5796	-4.8784
-1.000	-2.1847	-2.3734	-2.5760	-2.7924	-3.0224	-3.2662	-3.5237	-3.7948	-4.0796	-4.3784
-.500	-1.6847	-1.8734	-2.0760	-2.2924	-2.5224	-2.7662	-3.0237	-3.2948	-3.5796	-3.8784
0.000	-1.1847	-1.3734	-1.5760	-1.7924	-2.0224	-2.2662	-2.5237	-2.7948	-3.0796	-3.3784
.500	-.6847	-.8734	-.1.0760	-.1.2924	-.1.5224	-.1.7662	-.2.0237	-.2.2948	-.2.5796	-.2.8784
1.000	-.1847	-.3734	-.5760	-.7924	-.1.0224	-.1.2662	-.1.5237	-.1.7948	-.2.0796	-.2.3784
1.500	-.6847	-.8734	-.1.0760	-.1.2924	-.1.5224	-.1.7662	-.2.0237	-.2.2948	-.2.5796	-.2.8784
2.000	-1.1847	-1.3734	-1.5760	-1.7924	-2.0224	-2.2662	-2.5237	-2.7948	-3.0796	-3.3784
2.500	-1.6847	-1.8734	-2.0760	-2.2924	-2.5224	-2.7662	-3.0237	-3.2948	-3.5796	-3.8784
3.000	-2.1847	-2.3734	-2.5760	-2.7924	-3.0224	-3.2662	-3.5237	-3.7948	-4.0796	-4.3784

X (in)	X(in)					X(in)				
	T(deg)= -13.500	T(deg)= -14.250	T(deg)= -15.000	T(deg)= -15.750	T(deg)= -16.500	T(deg)= -17.250	T(deg)= -18.000	T(deg)= -18.750	T(deg)= -19.500	T(deg)= -20.250
-3.000	-5.2662	-5.5237	-5.7948	-6.0796	-6.3784	-6.6876	-6.9968	-7.3060	-7.6152	-7.9244
-2.500	-4.7662	-5.0237	-5.2948	-5.5796	-5.8784	-6.1876	-6.4968	-6.8060	-7.1152	-7.4244
-2.000	-4.2662	-4.5237	-4.7948	-5.0796	-5.3784	-5.6876	-5.9968	-6.3060	-6.6152	-6.9244
-1.500	-3.7662	-4.0237	-4.2948	-4.5796	-4.8784	-5.1876	-5.4968	-5.8060	-6.1152	-6.4244
-1.000	-3.2662	-3.5237	-3.7948	-4.0796	-4.3784	-4.6876	-4.9968	-5.3060	-5.6152	-5.9244
-.500	-2.7662	-3.0237	-3.2948	-3.5796	-3.8784	-4.1876	-4.4968	-4.8060	-5.1152	-5.4244
0.000	-2.2662	-2.5237	-2.7948	-3.0796	-3.3784	-3.6876	-3.9968	-4.3060	-4.6152	-4.9244
.500	-1.7662	-2.0237	-2.2948	-2.5796	-2.8784	-3.1876	-3.4968	-3.8060	-4.1152	-4.4244
1.000	-1.2662	-1.5237	-1.7948	-2.0796	-2.3784	-2.6876	-2.9968	-3.3060	-3.6152	-3.9244
1.500	-.7662	-1.0237	-1.2948	-1.5796	-1.8784	-2.1876	-2.4968	-2.8060	-3.1152	-3.4244
2.000	-.2662	-.5237	-.7948	-1.0796	-1.3784	-1.6876	-1.9968	-2.3060	-2.6152	-2.9244
2.500	.2338	.5237	.8136	1.1036	1.3936	1.6836	1.9736	2.2636	2.5536	2.8436
3.000	.7338	1.0237	1.3136	1.6036	1.8936	2.1836	2.4736	2.7636	3.0536	3.3436

X (in)	X(in)					X(in)				
	T(deg)= -3.750	T(deg)= -4.500	T(deg)= -5.250	T(deg)= -6.000	T(deg)= -6.750	T(deg)= -7.500	T(deg)= -8.250	T(deg)= -9.000	T(deg)= -9.750	T(deg)= -10.500
-3.000	-3.1756	-3.2528	-3.3441	-3.4493	-3.5685	-3.7017	-3.8488	-4.0098	-4.1856	-4.3764
-2.500	-2.6756	-2.7528	-2.8441	-2.9493	-3.0685	-3.2017	-3.3488	-3.5098	-3.6856	-3.8764
-2.000	-2.1756	-2.2528	-2.3441	-2.4493	-2.5685	-2.7017	-2.8488	-3.0098	-3.1856	-3.3764
-1.500	-1.6756	-1.7528	-1.8441	-1.9493	-2.0685	-2.2017	-2.3488	-2.5098	-2.6856	-2.8764
-1.000	-1.1756	-1.2528	-1.3441	-1.4493	-1.5685	-1.7017	-1.8488	-2.0098	-2.1856	-2.3764
-.500	-.6756	-.7528	-.8441	-.9493	-1.0685	-1.2017	-1.3488	-1.5098	-1.6856	-1.8764
0.000	-.1756	-.2528	-.3441	-.4493	-.5685	-.7017	-.8488	-1.0098	-1.1856	-1.3764
.500	.3244	.4016	.4889	.5841	.6893	.8085	.9317	1.0598	1.1880	1.3264
1.000	.8244	.9016	.9889	1.0841	1.1893	1.3085	1.4317	1.5598	1.6880	1.8264
1.500	1.3244	1.4016	1.4889	1.5841	1.6893	1.8085	1.9317	2.0598	2.1880	2.3264
2.000	1.8244	1.9016	1.9889	2.0841	2.1893	2.3085	2.4317	2.5598	2.6880	2.8264
2.500	2.3244	2.4016	2.4889	2.5841	2.6893	2.8085	2.9317	3.0598	3.1880	3.3264
3.000	2.8244	2.9016	2.9889	3.0841	3.1893	3.3085	3.4317	3.5598	3.6880	3.8264

The following is a list of the data in the TANGENT line sections of the scan:

X (in)	X(in)									
	L(in)= -1.500	L(in)= -1.000	L(in)= -0.500	L(in)= -2.000	L(in)= -2.500	L(in)= -3.000	L(in)= -3.500	L(in)= -4.000		
-3.000	-5.9242	-6.9536	-6.1830	-6.3124	-6.4418	-6.5713	-6.7007	-6.8301		
-2.500	-5.4242	-5.9536	-5.6830	-5.8124	-5.9418	-6.0713	-6.2007	-6.3301		
-2.000	-4.9242	-5.4536	-5.1830	-5.3124	-5.4418	-5.5713	-5.7007	-5.8301		
-1.750	-4.6742	-5.2036	-4.9330	-5.0624	-5.1918	-5.3213	-5.4507	-5.5801		
-1.500	-4.4242	-4.9536	-4.6830	-4.8124	-4.9418	-5.0713	-5.2007	-5.3301		
-1.250	-4.1742	-4.7036	-4.4330	-4.5624	-4.6918	-4.8213	-4.9507	-5.0801		
-1.000	-3.9242	-4.4536	-4.1830	-4.3124	-4.4418	-4.5713	-4.7007	-4.8301		
-0.750	-3.6742	-4.2036	-3.9330	-4.0624	-4.1918	-4.3213	-4.4507	-4.5801		
-0.500	-3.4242	-3.9536	-3.6830	-3.8124	-3.9418	-4.0713	-4.2007	-4.3301		
-0.250	-3.1742	-3.7036	-3.4330	-3.5624	-3.6918	-3.8213	-3.9507	-4.0801		
0.000	-2.9242	-3.4536	-3.1830	-3.3124	-3.4418	-3.5713	-3.7007	-3.8301		
0.250	-2.6742	-3.2036	-2.9330	-3.0624	-3.1918	-3.3213	-3.4507	-3.5801		
0.500	-2.4242	-2.9536	-2.6830	-2.8124	-2.9418	-3.0713	-3.2007	-3.3301		
0.750	-2.1742	-2.7036	-2.4330	-2.5624	-2.6918	-2.8213	-2.9507	-3.0801		
1.000	-1.9242	-2.4536	-2.1830	-2.3124	-2.4418	-2.5713	-2.7007	-2.8301		
1.250	-1.6742	-2.2036	-1.9330	-2.0624	-2.1918	-2.3213	-2.4507	-2.5801		
1.500	-1.4242	-1.9536	-1.6830	-1.8124	-1.9418	-2.0713	-2.2007	-2.3301		
1.750	-1.1742	-1.7036	-1.4330	-1.5624	-1.6918	-1.8213	-1.9507	-2.0801		
2.000	-0.9242	-1.4536	-1.1830	-1.3124	-1.4418	-1.5713	-1.7007	-1.8301		
2.500	-0.4242	-0.9536	-0.6830	-0.8124	-0.9418	-1.0713	-1.2007	-1.3301		
3.000	0.0756	-0.4536	-0.1830	-0.3124	-0.4418	-0.5713	-0.7007	-0.8301		

X (in)	X(in)									
	L(in)= -12.000	L(in)= -13.000	L(in)= -14.000	L(in)= -15.000	L(in)= -16.000	L(in)= -17.000				
-3.000	-8.9006	-9.1594	-9.4183	-9.6771	-9.9359	-10.1947				
-2.500	-8.4006	-8.6594	-8.9183	-9.1771	-9.4359	-9.6947				
-2.000	-7.9006	-8.1594	-8.4183	-8.6771	-8.9359	-9.1947				
-1.750	-7.6506	-7.9094	-8.1683	-8.4271	-8.6859	-8.9447				
-1.500	-7.4006	-7.6594	-7.9183	-8.1771	-8.4359	-8.6947				
-1.250	-7.1506	-7.4094	-7.6683	-7.9271	-8.1859	-8.4447				
-1.000	-6.9006	-7.1594	-7.4183	-7.6771	-7.9359	-8.1947				
-0.750	-6.6506	-6.9094	-7.1683	-7.4271	-7.6859	-7.9447				
-0.500	-6.4006	-6.6594	-6.9183	-7.1771	-7.4359	-7.6947				
-0.250	-6.1506	-6.4094	-6.6683	-6.9271	-7.1859	-7.4447				
0.000	-5.9006	-6.1594	-6.4183	-6.6771	-6.9359	-7.1947				
0.250	-5.6506	-5.9094	-6.1683	-6.4271	-6.6859	-6.9447				
0.500	-5.4006	-5.6594	-5.9183	-6.1771	-6.4359	-6.6947				
0.750	-5.1506	-5.4094	-5.6683	-5.9271	-6.1859	-6.4447				
1.000	-4.9006	-5.1594	-5.4183	-5.6771	-5.9359	-6.1947				
1.250	-4.6506	-4.9094	-5.1683	-5.4271	-5.6859	-5.9447				
1.500	-4.4006	-4.6594	-4.9183	-5.1771	-5.4359	-5.6947				
1.750	-4.1506	-4.4094	-4.6683	-4.9271	-5.1859	-5.4447				
2.000	-3.9006	-4.1594	-4.4183	-4.6771	-4.9359	-5.1947				
2.500	-3.4006	-3.6594	-3.9183	-4.1771	-4.4359	-4.6947				
3.000	-2.9006	-3.1594	-3.4183	-3.6771	-3.9359	-4.1947				

X (in)	X(in)									
	L(in)= -4.500	L(in)= -5.000	L(in)= -6.000	L(in)= -7.000	L(in)= -8.000	L(in)= -9.000	L(in)= -10.000	L(in)= -11.000		
-3.000	-6.9595	-7.0889	-7.3477	-7.6065	-7.8654	-8.1242	-8.3830	-8.6418		
-2.500	-6.4595	-6.5889	-6.8477	-7.1065	-7.3654	-7.6242	-7.8830	-8.1418		
-2.000	-5.9595	-6.0889	-6.3477	-6.6065	-6.8654	-7.1242	-7.3830	-7.6418		
-1.750	-5.7095	-5.8389	-6.0977	-6.3565	-6.6154	-6.8742	-7.1330	-7.3918		
-1.500	-5.4595	-5.5889	-5.8477	-6.1065	-6.3654	-6.6242	-6.8830	-7.1418		
-1.250	-5.2095	-5.3389	-5.5977	-5.8565	-6.1154	-6.3742	-6.6330	-6.8918		
-1.000	-4.9595	-5.0889	-5.3477	-5.6065	-5.8654	-6.1242	-6.3830	-6.6418		
-0.750	-4.7095	-4.8389	-5.0977	-5.3565	-5.6154	-5.8742	-6.1330	-6.3918		
-0.500	-4.4595	-4.5889	-4.8477	-5.1065	-5.3654	-5.6242	-5.8830	-6.1418		
-0.250	-4.2095	-4.3389	-4.5977	-4.8565	-5.1154	-5.3742	-5.6330	-5.8918		
0.000	-3.9595	-4.0889	-4.3477	-4.6065	-4.8654	-5.1242	-5.3830	-5.6418		
0.250	-3.7095	-3.8389	-4.0977	-4.3565	-4.6154	-4.8742	-5.1330	-5.3918		
0.500	-3.4595	-3.5889	-3.8477	-4.1065	-4.3654	-4.6242	-4.8830	-5.1418		
0.750	-3.2095	-3.3389	-3.5977	-3.8565	-4.1154	-4.3742	-4.6330	-4.8918		
1.000	-2.9595	-3.0889	-3.3477	-3.6065	-3.8654	-4.1242	-4.3830	-4.6418		
1.250	-2.7095	-2.8389	-3.0977	-3.3565	-3.6154	-3.8742	-4.1330	-4.3918		
1.500	-2.4595	-2.5889	-2.8477	-3.1065	-3.3654	-3.6242	-3.8830	-4.1418		
1.750	-2.2095	-2.3389	-2.5977	-2.8565	-3.1154	-3.3742	-3.6330	-3.8918		
2.000	-1.9595	-2.0889	-2.3477	-2.6065	-2.8654	-3.1242	-3.3830	-3.6418		
2.500	-1.4595	-1.5889	-1.8477	-2.1065	-2.3654	-2.6242	-2.8830	-3.1418		
3.000	-0.9595	-1.0889	-1.3477	-1.6065	-1.8654	-2.1242	-2.3830	-2.6418		

III. The Y-coordinates for left side only.

The following data is derived from the data file(AL.P15) described here:

TITLE:ALADDIN Dipole-Polar Grid Left End (Z=0.00) Offset arc scan R=2.08m

Run number (15) was started at 9:48:50AM on 7/3/85.

The scan area is defined for this run by the parameters for region #1 in the geometry file named ALPLE.

The following is a list of the data in the ARC section of the scan:

X (in)	T(deg)= -9.750	T(deg)= -3.75	T(deg)= 0.000	T(deg)= -1.500	T(deg)= -2.250	T(deg)= -3.000
-3.000	1.0736	.5368	0.0000	-2.1471	-3.2201	-4.2926
-2.500	1.0736	.5368	0.0000	-2.1471	-3.2201	-4.2926
-2.000	1.0736	.5368	0.0000	-2.1471	-3.2201	-4.2926
-1.750	1.0736	.5368	0.0000	-2.1471	-3.2201	-4.2926
-1.500	1.0736	.5368	0.0000	-2.1471	-3.2201	-4.2926
-1.250	1.0736	.5368	0.0000	-2.1471	-3.2201	-4.2926
-1.000	1.0736	.5368	0.0000	-2.1471	-3.2201	-4.2926
-.750	1.0736	.5368	0.0000	-2.1471	-3.2201	-4.2926
-.500	1.0736	.5368	0.0000	-2.1471	-3.2201	-4.2926
-.250	1.0736	.5368	0.0000	-2.1471	-3.2201	-4.2926
0.000	1.0736	.5368	0.0000	-2.1471	-3.2201	-4.2926
.250	1.0736	.5368	0.0000	-2.1471	-3.2201	-4.2926
.500	1.0736	.5368	0.0000	-2.1471	-3.2201	-4.2926
.750	1.0736	.5368	0.0000	-2.1471	-3.2201	-4.2926
1.000	1.0736	.5368	0.0000	-2.1471	-3.2201	-4.2926
1.250	1.0736	.5368	0.0000	-2.1471	-3.2201	-4.2926
1.500	1.0736	.5368	0.0000	-2.1471	-3.2201	-4.2926
1.750	1.0736	.5368	0.0000	-2.1471	-3.2201	-4.2926
2.000	1.0736	.5368	0.0000	-2.1471	-3.2201	-4.2926
2.500	1.0736	.5368	0.0000	-2.1471	-3.2201	-4.2926
3.000	1.0736	.5368	0.0000	-2.1471	-3.2201	-4.2926

Page 2

X (in)	T(deg)= -9.750	T(deg)= -10.500	T(deg)= -11.250	T(deg)= -11.825	T(deg)= -12.000	T(deg)= -12.375	T(deg)= -12.750	T(deg)= -13.125
-3.000	-13.8902	-14.9471	-16.0015	-16.5277	-17.0531	-17.5779	-18.1018	-18.6250
-2.500	-13.8902	-14.9471	-16.0015	-16.5277	-17.0531	-17.5779	-18.1018	-18.6250
-2.000	-13.8902	-14.9471	-16.0015	-16.5277	-17.0531	-17.5779	-18.1018	-18.6250
-1.750	-13.8902	-14.9471	-16.0015	-16.5277	-17.0531	-17.5779	-18.1018	-18.6250
-1.500	-13.8902	-14.9471	-16.0015	-16.5277	-17.0531	-17.5779	-18.1018	-18.6250
-1.250	-13.8902	-14.9471	-16.0015	-16.5277	-17.0531	-17.5779	-18.1018	-18.6250
-1.000	-13.8902	-14.9471	-16.0015	-16.5277	-17.0531	-17.5779	-18.1018	-18.6250
-.750	-13.8902	-14.9471	-16.0015	-16.5277	-17.0531	-17.5779	-18.1018	-18.6250
-.500	-13.8902	-14.9471	-16.0015	-16.5277	-17.0531	-17.5779	-18.1018	-18.6250
-.250	-13.8902	-14.9471	-16.0015	-16.5277	-17.0531	-17.5779	-18.1018	-18.6250
0.000	-13.8902	-14.9471	-16.0015	-16.5277	-17.0531	-17.5779	-18.1018	-18.6250
.250	-13.8902	-14.9471	-16.0015	-16.5277	-17.0531	-17.5779	-18.1018	-18.6250
.500	-13.8902	-14.9471	-16.0015	-16.5277	-17.0531	-17.5779	-18.1018	-18.6250
.750	-13.8902	-14.9471	-16.0015	-16.5277	-17.0531	-17.5779	-18.1018	-18.6250
1.000	-13.8902	-14.9471	-16.0015	-16.5277	-17.0531	-17.5779	-18.1018	-18.6250
1.250	-13.8902	-14.9471	-16.0015	-16.5277	-17.0531	-17.5779	-18.1018	-18.6250
1.500	-13.8902	-14.9471	-16.0015	-16.5277	-17.0531	-17.5779	-18.1018	-18.6250
1.750	-13.8902	-14.9471	-16.0015	-16.5277	-17.0531	-17.5779	-18.1018	-18.6250
2.000	-13.8902	-14.9471	-16.0015	-16.5277	-17.0531	-17.5779	-18.1018	-18.6250
2.500	-13.8902	-14.9471	-16.0015	-16.5277	-17.0531	-17.5779	-18.1018	-18.6250
3.000	-13.8902	-14.9471	-16.0015	-16.5277	-17.0531	-17.5779	-18.1018	-18.6250

X (in)	T(deg)= -3.750	T(deg)= -6.000	T(deg)= -8.250	T(deg)= -10.500	T(deg)= -12.750	T(deg)= -15.000
-3.000	-5.3644	-6.4353	-7.5051	-8.5735	-9.6405	-10.7059
-2.500	-5.3644	-6.4353	-7.5051	-8.5735	-9.6405	-10.7059
-2.000	-5.3644	-6.4353	-7.5051	-8.5735	-9.6405	-10.7059
-1.750	-5.3644	-6.4353	-7.5051	-8.5735	-9.6405	-10.7059
-1.500	-5.3644	-6.4353	-7.5051	-8.5735	-9.6405	-10.7059
-1.250	-5.3644	-6.4353	-7.5051	-8.5735	-9.6405	-10.7059
-1.000	-5.3644	-6.4353	-7.5051	-8.5735	-9.6405	-10.7059
-.750	-5.3644	-6.4353	-7.5051	-8.5735	-9.6405	-10.7059
-.500	-5.3644	-6.4353	-7.5051	-8.5735	-9.6405	-10.7059
-.250	-5.3644	-6.4353	-7.5051	-8.5735	-9.6405	-10.7059
0.000	-5.3644	-6.4353	-7.5051	-8.5735	-9.6405	-10.7059
.250	-5.3644	-6.4353	-7.5051	-8.5735	-9.6405	-10.7059
.500	-5.3644	-6.4353	-7.5051	-8.5735	-9.6405	-10.7059
.750	-5.3644	-6.4353	-7.5051	-8.5735	-9.6405	-10.7059
1.000	-5.3644	-6.4353	-7.5051	-8.5735	-9.6405	-10.7059
1.250	-5.3644	-6.4353	-7.5051	-8.5735	-9.6405	-10.7059
1.500	-5.3644	-6.4353	-7.5051	-8.5735	-9.6405	-10.7059
1.750	-5.3644	-6.4353	-7.5051	-8.5735	-9.6405	-10.7059
2.000	-5.3644	-6.4353	-7.5051	-8.5735	-9.6405	-10.7059
2.500	-5.3644	-6.4353	-7.5051	-8.5735	-9.6405	-10.7059
3.000	-5.3644	-6.4353	-7.5051	-8.5735	-9.6405	-10.7059

X (in)	T(deg)= -13.500	T(deg)= -13.875	T(deg)= -14.250	T(deg)= -14.625	T(deg)= -15.000
-3.000	-19.1474	-19.6690	-20.1897	-20.7096	-21.2286
-2.500	-19.1474	-19.6690	-20.1897	-20.7096	-21.2286
-2.000	-19.1474	-19.6690	-20.1897	-20.7096	-21.2286
-1.750	-19.1474	-19.6690	-20.1897	-20.7096	-21.2286
-1.500	-19.1474	-19.6690	-20.1897	-20.7096	-21.2286
-1.250	-19.1474	-19.6690	-20.1897	-20.7096	-21.2286
-1.000	-19.1474	-19.6690	-20.1897	-20.7096	-21.2286
-.750	-19.1474	-19.6690	-20.1897	-20.7096	-21.2286
-.500	-19.1474	-19.6690	-20.1897	-20.7096	-21.2286
-.250	-19.1474	-19.6690	-20.1897	-20.7096	-21.2286
0.000	-19.1474	-19.6690	-20.1897	-20.7096	-21.2286
.250	-19.1474	-19.6690	-20.1897	-20.7096	-21.2286
.500	-19.1474	-19.6690	-20.1897	-20.7096	-21.2286
.750	-19.1474	-19.6690	-20.1897	-20.7096	-21.2286
1.000	-19.1474	-19.6690	-20.1897	-20.7096	-21.2286
1.250	-19.1474	-19.6690	-20.1897	-20.7096	-21.2286
1.500	-19.1474	-19.6690	-20.1897	-20.7096	-21.2286
1.750	-19.1474	-19.6690	-20.1897	-20.7096	-21.2286
2.000	-19.1474	-19.6690	-20.1897	-20.7096	-21.2286
2.500	-19.1474	-19.6690	-20.1897	-20.7096	-21.2286
3.000	-19.1474	-19.6690	-20.1897	-20.7096	-21.2286

The following is a list of the data in the TANGENT line sections of the scan:

X (in)	Y(in)					
	L(in)= -3.000	L(in)= -1.000	L(in)= -1.500	L(in)= -2.000	L(in)= -2.500	L(in)= -3.000
-3.000	-21.7116	-22.1945	-22.6775	-23.1604	-23.6434	-24.1264
-2.500	-21.7116	-22.1945	-22.6775	-23.1604	-23.6434	-24.1264
-2.000	-21.7116	-22.1945	-22.6775	-23.1604	-23.6434	-24.1264
-1.750	-21.7116	-22.1945	-22.6775	-23.1604	-23.6434	-24.1264
-1.500	-21.7116	-22.1945	-22.6775	-23.1604	-23.6434	-24.1264
-1.250	-21.7116	-22.1945	-22.6775	-23.1604	-23.6434	-24.1264
-1.000	-21.7116	-22.1945	-22.6775	-23.1604	-23.6434	-24.1264
-0.750	-21.7116	-22.1945	-22.6775	-23.1604	-23.6434	-24.1264
-0.500	-21.7116	-22.1945	-22.6775	-23.1604	-23.6434	-24.1264
-0.250	-21.7116	-22.1945	-22.6775	-23.1604	-23.6434	-24.1264
0.000	-21.7116	-22.1945	-22.6775	-23.1604	-23.6434	-24.1264
0.250	-21.7116	-22.1945	-22.6775	-23.1604	-23.6434	-24.1264
0.500	-21.7116	-22.1945	-22.6775	-23.1604	-23.6434	-24.1264
0.750	-21.7116	-22.1945	-22.6775	-23.1604	-23.6434	-24.1264
1.000	-21.7116	-22.1945	-22.6775	-23.1604	-23.6434	-24.1264
1.250	-21.7116	-22.1945	-22.6775	-23.1604	-23.6434	-24.1264
1.500	-21.7116	-22.1945	-22.6775	-23.1604	-23.6434	-24.1264
1.750	-21.7116	-22.1945	-22.6775	-23.1604	-23.6434	-24.1264
2.000	-21.7116	-22.1945	-22.6775	-23.1604	-23.6434	-24.1264
2.500	-21.7116	-22.1945	-22.6775	-23.1604	-23.6434	-24.1264
3.000	-21.7116	-22.1945	-22.6775	-23.1604	-23.6434	-24.1264

X (in)	Y(in)					
	L(in)= -12.000	L(in)= -13.000	L(in)= -14.000	L(in)= -15.000	L(in)= -16.000	L(in)= -17.000
-3.000	-32.8197	-33.7856	-34.7516	-35.7175	-36.6834	-37.6493
-2.500	-32.8197	-33.7856	-34.7516	-35.7175	-36.6834	-37.6493
-2.000	-32.8197	-33.7856	-34.7516	-35.7175	-36.6834	-37.6493
-1.750	-32.8197	-33.7856	-34.7516	-35.7175	-36.6834	-37.6493
-1.500	-32.8197	-33.7856	-34.7516	-35.7175	-36.6834	-37.6493
-1.250	-32.8197	-33.7856	-34.7516	-35.7175	-36.6834	-37.6493
-1.000	-32.8197	-33.7856	-34.7516	-35.7175	-36.6834	-37.6493
-0.750	-32.8197	-33.7856	-34.7516	-35.7175	-36.6834	-37.6493
-0.500	-32.8197	-33.7856	-34.7516	-35.7175	-36.6834	-37.6493
-0.250	-32.8197	-33.7856	-34.7516	-35.7175	-36.6834	-37.6493
0.000	-32.8197	-33.7856	-34.7516	-35.7175	-36.6834	-37.6493
0.250	-32.8197	-33.7856	-34.7516	-35.7175	-36.6834	-37.6493
0.500	-32.8197	-33.7856	-34.7516	-35.7175	-36.6834	-37.6493
0.750	-32.8197	-33.7856	-34.7516	-35.7175	-36.6834	-37.6493
1.000	-32.8197	-33.7856	-34.7516	-35.7175	-36.6834	-37.6493
1.250	-32.8197	-33.7856	-34.7516	-35.7175	-36.6834	-37.6493
1.500	-32.8197	-33.7856	-34.7516	-35.7175	-36.6834	-37.6493
1.750	-32.8197	-33.7856	-34.7516	-35.7175	-36.6834	-37.6493
2.000	-32.8197	-33.7856	-34.7516	-35.7175	-36.6834	-37.6493
2.500	-32.8197	-33.7856	-34.7516	-35.7175	-36.6834	-37.6493
3.000	-32.8197	-33.7856	-34.7516	-35.7175	-36.6834	-37.6493

X (in)	Y(in)					
	L(in)= -4.500	L(in)= -5.000	L(in)= -6.000	L(in)= -7.000	L(in)= -8.000	L(in)= -9.000
-3.000	-25.5753	-26.0582	-27.0242	-27.9901	-28.9560	-29.9219
-2.500	-25.5753	-26.0582	-27.0242	-27.9901	-28.9560	-29.9219
-2.000	-25.5753	-26.0582	-27.0242	-27.9901	-28.9560	-29.9219
-1.750	-25.5753	-26.0582	-27.0242	-27.9901	-28.9560	-29.9219
-1.500	-25.5753	-26.0582	-27.0242	-27.9901	-28.9560	-29.9219
-1.250	-25.5753	-26.0582	-27.0242	-27.9901	-28.9560	-29.9219
-1.000	-25.5753	-26.0582	-27.0242	-27.9901	-28.9560	-29.9219
-0.750	-25.5753	-26.0582	-27.0242	-27.9901	-28.9560	-29.9219
-0.500	-25.5753	-26.0582	-27.0242	-27.9901	-28.9560	-29.9219
0.000	-25.5753	-26.0582	-27.0242	-27.9901	-28.9560	-29.9219
0.250	-25.5753	-26.0582	-27.0242	-27.9901	-28.9560	-29.9219
0.500	-25.5753	-26.0582	-27.0242	-27.9901	-28.9560	-29.9219
0.750	-25.5753	-26.0582	-27.0242	-27.9901	-28.9560	-29.9219
1.000	-25.5753	-26.0582	-27.0242	-27.9901	-28.9560	-29.9219
1.250	-25.5753	-26.0582	-27.0242	-27.9901	-28.9560	-29.9219
1.500	-25.5753	-26.0582	-27.0242	-27.9901	-28.9560	-29.9219
1.750	-25.5753	-26.0582	-27.0242	-27.9901	-28.9560	-29.9219
2.000	-25.5753	-26.0582	-27.0242	-27.9901	-28.9560	-29.9219
2.500	-25.5753	-26.0582	-27.0242	-27.9901	-28.9560	-29.9219
3.000	-25.5753	-26.0582	-27.0242	-27.9901	-28.9560	-29.9219

IV. The Z-coordinates for all the points.

The following data is derived from the data file(AL-P28/AL-PI5) described here:
 TITLE:ALADDIN Dipole-Polar Grid Right End(Z=0.00)Offset arc scan R=2.08m(E=1000M
 eV)/ALADDIN Dipole-Polar Grid Left End (Z=0.00) Offset arc scan R=2.08m
 Run number (28/15) was started at 9:19:40AM/9:48:5AM on 7/12/85;7/3/85.
 The scan area is defined for this run by the parameters for region #1
 in the geometry file named ALPRE/ALPLE.

The following is a list of the data in a TANGENT line section of the scan:

X (in)	L(in)= 17.000	L(in)= 16.000	L(in)= 15.000	L(in)= 14.000	L(in)= 13.000	L(in)= 12.000	L(in)= 11.000	L(in)= 10.000
-3.000	.0078	.0078	.0074	.0074	.0074	.0070	.0066	.0063
-2.500	.0078	.0078	.0074	.0074	.0069	.0065	.0062	.0059
-2.000	.0082	.0078	.0074	.0069	.0064	.0060	.0057	.0055
-1.750	.0080	.0076	.0071	.0066	.0061	.0057	.0054	.0052
-1.500	.0079	.0074	.0069	.0063	.0058	.0054	.0050	.0048
-1.250	.0078	.0072	.0066	.0060	.0055	.0052	.0049	.0046
-1.000	.0076	.0070	.0063	.0057	.0052	.0049	.0047	.0044
-.750	.0075	.0067	.0060	.0054	.0049	.0046	.0044	.0041
-.500	.0073	.0065	.0057	.0051	.0046	.0043	.0041	.0038
-.250	.0071	.0062	.0055	.0048	.0043	.0040	.0039	.0036
0.000	.0069	.0060	.0052	.0045	.0040	.0037	.0036	.0033
.250	.0067	.0057	.0049	.0042	.0037	.0034	.0031	.0029
.500	.0065	.0055	.0046	.0039	.0034	.0031	.0028	.0026
.750	.0063	.0052	.0043	.0036	.0031	.0028	.0025	.0024
1.000	.0061	.0049	.0039	.0032	.0029	.0026	.0022	.0020
1.250	.0059	.0046	.0036	.0029	.0025	.0022	.0018	.0017
1.500	.0057	.0043	.0033	.0026	.0023	.0020	.0017	.0014
1.750	.0055	.0041	.0030	.0023	.0020	.0018	.0014	.0011
2.000	.0052	.0038	.0027	.0020	.0018	.0015	.0009	.0007
2.500	.0047	.0032	.0021	.0013	.0009	.0008	.0003	
3.000	.0043	.0026	.0014	.0007	.0003	.0002		

Page 2

X (in)	L(in)= 3.000	L(in)= 2.500	L(in)= 2.000	L(in)= 1.500	L(in)= 1.000	L(in)= .500
-3.000	.0059	.0059	.0058	.0058	.0057	.0057
-2.500	.0057	.0057	.0057	.0055	.0056	.0055
-2.000	.0056	.0055	.0055	.0054	.0054	.0053
-1.750	.0055	.0054	.0054	.0053	.0053	.0052
-1.500	.0054	.0053	.0053	.0052	.0052	.0051
-1.250	.0053	.0052	.0052	.0051	.0050	.0049
-1.000	.0052	.0051	.0051	.0050	.0049	.0047
-.750	.0050	.0049	.0049	.0048	.0047	.0046
-.500	.0049	.0048	.0048	.0047	.0046	.0045
-.250	.0048	.0047	.0047	.0046	.0045	.0043
0.000	.0047	.0046	.0046	.0045	.0044	.0042
.250	.0046	.0045	.0045	.0044	.0043	.0041
.500	.0044	.0044	.0043	.0042	.0041	.0039
.750	.0043	.0043	.0041	.0040	.0039	.0038
1.000	.0041	.0040	.0039	.0038	.0037	.0036
1.250	.0040	.0039	.0038	.0037	.0036	.0035
1.500	.0039	.0037	.0036	.0035	.0034	.0033
1.750	.0037	.0035	.0034	.0033	.0032	.0031
2.000	.0035	.0032	.0031	.0030	.0029	.0028
2.500	.0032	.0028	.0028	.0027	.0025	.0024
3.000	.0028					

X (in)	L(in)= 9.000	L(in)= 8.000	L(in)= 7.000	L(in)= 6.000	L(in)= 5.000	L(in)= 4.500	L(in)= 4.000	L(in)= 3.500
-3.000	.0061	.0059	.0059	.0059	.0059	.0059	.0059	.0059
-2.500	.0057	.0056	.0056	.0056	.0057	.0057	.0057	.0057
-2.000	.0054	.0053	.0054	.0054	.0055	.0055	.0055	.0056
-1.750	.0052	.0052	.0053	.0053	.0054	.0054	.0054	.0055
-1.500	.0050	.0050	.0051	.0052	.0053	.0053	.0053	.0054
-1.250	.0048	.0048	.0049	.0050	.0052	.0052	.0052	.0053
-1.000	.0046	.0046	.0048	.0049	.0051	.0051	.0051	.0051
-.750	.0044	.0043	.0046	.0048	.0050	.0050	.0050	.0050
-.500	.0041	.0040	.0044	.0046	.0049	.0049	.0049	.0049
-.250	.0039	.0039	.0043	.0045	.0047	.0047	.0046	.0047
0.000	.0035	.0037	.0040	.0042	.0045	.0045	.0045	.0045
.250	.0033	.0035	.0038	.0040	.0042	.0043	.0044	.0044
.500	.0031	.0033	.0036	.0039	.0041	.0042	.0042	.0043
.750	.0028	.0031	.0034	.0037	.0039	.0040	.0041	.0041
1.000	.0026	.0029	.0033	.0036	.0038	.0039	.0039	.0040
1.250	.0024	.0027	.0031	.0034	.0036	.0037	.0038	.0038
1.500	.0022	.0025	.0029	.0032	.0035	.0036	.0036	.0037
1.750	.0020	.0023	.0027	.0030	.0033	.0034	.0035	.0035
2.000	.0018	.0021	.0025	.0028	.0031	.0032	.0033	.0033
2.500	.0015	.0019	.0023	.0027	.0030	.0031	.0032	.0032
3.000	.0011	.0015	.0019	.0023	.0026	.0027	.0028	.0028

The following is a list of the data in the ARC section of the scan:

X (in)	Z(in)									
	T(deg)= 15.000	T(deg)= 14.625	T(deg)= 14.250	T(deg)= 13.875	T(deg)= 13.500	T(deg)= 13.125	T(deg)= 12.750	T(deg)= 12.375		
-3.000	.0056	.0055	.0053	.0051	.0050	.0048	.0045	.0043		
-2.500	.0054	.0052	.0051	.0049	.0047	.0045	.0043	.0040		
-2.000	.0052	.0050	.0049	.0047	.0045	.0042	.0040	.0038		
-1.750	.0051	.0049	.0047	.0046	.0044	.0041	.0039	.0036		
-1.500	.0050	.0048	.0046	.0044	.0042	.0040	.0037	.0034		
-1.250	.0048	.0047	.0045	.0043	.0041	.0038	.0035	.0033		
-1.000	.0047	.0046	.0044	.0042	.0039	.0037	.0034	.0031		
-.750	.0046	.0044	.0042	.0040	.0038	.0035	.0033	.0030		
-.500	.0045	.0043	.0041	.0039	.0036	.0034	.0031	.0028		
-.250	.0043	.0042	.0040	.0037	.0035	.0032	.0029	.0026		
0.000	.0042	.0040	.0038	.0036	.0033	.0031	.0028	.0025		
.250	.0041	.0039	.0037	.0034	.0032	.0029	.0026	.0023		
.500	.0039	.0037	.0035	.0033	.0030	.0027	.0024	.0021		
.750	.0038	.0036	.0033	.0031	.0028	.0026	.0023	.0020		
1.000	.0036	.0034	.0032	.0029	.0027	.0024	.0021	.0018		
1.250	.0034	.0032	.0030	.0028	.0025	.0022	.0019	.0016		
1.500	.0033	.0031	.0028	.0026	.0023	.0020	.0017	.0014		
1.750	.0031	.0029	.0027	.0024	.0021	.0018	.0015	.0012		
2.000	.0029	.0027	.0025	.0022	.0019	.0017	.0014	.0010		
2.500	.0026	.0024	.0021	.0018	.0016	.0013	.0010	.0007		
3.000	.0022	.0020	.0017	.0015	.0012	.0009	.0006	.0003		

X (in)	Z(in)									
	T(deg)= 6.750	T(deg)= 6.000	T(deg)= 5.250	T(deg)= 4.500	T(deg)= 3.750	T(deg)= 3.000	T(deg)= 2.250	T(deg)= 1.500		
-3.000	.0015	.0015	.0016	.0018	.0021	.0023	.0025	.0025		
-2.500	.0012	.0013	.0014	.0016	.0019	.0022	.0023	.0024		
-2.000	.0009	.0010	.0012	.0014	.0017	.0020	.0022	.0022		
-1.750	.0008	.0009	.0010	.0013	.0016	.0019	.0021	.0021		
-1.500	.0006	.0007	.0009	.0012	.0015	.0018	.0020	.0020		
-1.250	.0005	.0006	.0008	.0011	.0014	.0018	.0020	.0019		
-1.000	.0004	.0005	.0007	.0010	.0013	.0016	.0019	.0018		
-.750	.0002	.0003	.0005	.0008	.0011	.0015	.0017	.0017		
-.500	.0001	.0002	.0003	.0005	.0008	.0011	.0014	.0016		
-.250	.0001	.0001	.0001	.0002	.0003	.0005	.0007	.0008		
0.000	.0000	.0000	.0000	.0000	.0001	.0002	.0003	.0004		
.250	.0000	.0000	.0000	.0000	.0000	.0001	.0002	.0003		
.500	.0000	.0000	.0000	.0000	.0000	.0001	.0002	.0003		
.750	.0000	.0000	.0000	.0000	.0000	.0001	.0002	.0003		
1.000	.0000	.0000	.0000	.0000	.0000	.0001	.0002	.0003		
1.250	.0000	.0000	.0000	.0000	.0000	.0001	.0002	.0003		
1.500	.0000	.0000	.0000	.0000	.0000	.0001	.0002	.0003		
1.750	.0000	.0000	.0000	.0000	.0000	.0001	.0002	.0003		
2.000	.0000	.0000	.0000	.0000	.0000	.0001	.0002	.0003		
2.500	.0000	.0000	.0000	.0000	.0000	.0001	.0002	.0003		
3.000	.0000	.0000	.0000	.0000	.0000	.0001	.0002	.0003		

X (in)	Z(in)									
	T(deg)= 7.50	T(deg)= .375								
-3.000	.0023	.0020								
-2.500	.0021	.0018								
-2.000	.0019	.0016								
-1.750	.0018	.0015								
-1.500	.0017	.0013								
-1.250	.0016	.0012								
-1.000	.0015	.0011								
-.750	.0014	.0010								
-.500	.0013	.0009								
-.250	.0011	.0007								
0.000	.0010	.0006								
.250	.0009	.0005								
.500	.0008	.0004								
.750	.0007	.0003								
1.000	.0005	.0001								
1.250	.0004	.0000								
1.500	.0003	.0000								
1.750	.0001	.0000								
2.000	.0000	.0000								
2.500	.0000	.0000								
3.000	.0000	.0000								

The following is a list of the data in the ARC section of the scan:

X (in)	T(deg)= 0.000	T(deg)= -0.375	T(deg)= -0.750	T(deg)= -1.500	T(deg)= -2.250	T(deg)= -3.000	T(deg)= -3.750	T(deg)= -4.500
-3.000	.0032	.0024	.0017	.0010	.0008	.0010	.0014	.0021
-2.500	.0027	.0018	.0011	.0003	.0001	.0004	.0009	.0016
-2.000	.0021	.0012	.0005	.0003	.0004	.0002	.0004	.0011
-1.750	.0019	.0009	.0003	.0006	.0007	.0005	.0001	.0008
-1.500	.0016	.0008	.0000	.0008	.0010	.0007	.0002	.0006
-1.250	.0013	.0004	.0003	.0011	.0013	.0010	.0004	.0004
-1.000	.0011	.0003	.0006	.0014	.0016	.0013	.0007	.0001
-.750	.0008	.0001	.0009	.0017	.0018	.0015	.0009	.0001
-.500	.0005	.0004	.0011	.0019	.0021	.0018	.0012	.0003
-.250	.0003	.0007	.0014	.0022	.0024	.0020	.0014	.0005
0.000	.0000	.0009	.0016	.0024	.0026	.0023	.0016	.0008
.250	.0002	.0002	.0019	.0027	.0028	.0025	.0019	.0010
.500	.0004	.0014	.0021	.0029	.0031	.0029	.0021	.0014
.750	.0007	.0016	.0023	.0031	.0033	.0031	.0023	.0017
1.000	.0009	.0019	.0026	.0034	.0035	.0032	.0025	.0017
1.250	.0011	.0021	.0028	.0036	.0037	.0034	.0027	.0021
1.500	.0014	.0023	.0030	.0038	.0039	.0035	.0029	.0021
1.750	.0016	.0025	.0032	.0039	.0041	.0037	.0031	.0022
2.000	.0018	.0027	.0034	.0041	.0042	.0039	.0033	.0024
2.500	.0022	.0030	.0037	.0044	.0045	.0042	.0036	.0028
3.000	.0025	.0034	.0040	.0047	.0048	.0045	.0039	.0031

X (in)	T(deg)= -11.250	T(deg)= -11.625	T(deg)= -12.000	T(deg)= -12.375	T(deg)= -12.750	T(deg)= -13.125	T(deg)= -13.500	T(deg)= -13.875
-3.000	.0058	.0057	.0057	.0056	.0055	.0055	.0054	.0053
-2.500	.0055	.0055	.0055	.0054	.0053	.0053	.0052	.0050
-2.000	.0053	.0053	.0053	.0051	.0050	.0049	.0048	.0047
-1.750	.0052	.0051	.0051	.0050	.0049	.0048	.0047	.0046
-1.500	.0050	.0050	.0049	.0049	.0048	.0047	.0046	.0045
-1.250	.0049	.0049	.0048	.0048	.0046	.0045	.0044	.0043
-1.000	.0048	.0047	.0047	.0046	.0045	.0044	.0043	.0042
-.750	.0046	.0046	.0045	.0044	.0043	.0042	.0041	.0040
-.500	.0045	.0044	.0044	.0043	.0042	.0041	.0040	.0038
-.250	.0043	.0043	.0043	.0041	.0040	.0039	.0038	.0037
0.000	.0041	.0041	.0040	.0040	.0039	.0038	.0036	.0035
.250	.0040	.0039	.0038	.0037	.0036	.0035	.0033	.0032
.500	.0038	.0038	.0038	.0036	.0035	.0034	.0031	.0030
.750	.0036	.0036	.0035	.0034	.0033	.0032	.0030	.0028
1.000	.0035	.0034	.0034	.0033	.0032	.0031	.0029	.0027
1.250	.0033	.0033	.0032	.0032	.0030	.0029	.0026	.0025
1.500	.0031	.0031	.0031	.0029	.0028	.0027	.0025	.0023
1.750	.0029	.0029	.0027	.0027	.0026	.0025	.0024	.0021
2.000	.0027	.0027	.0027	.0026	.0025	.0024	.0022	.0020
2.500	.0023	.0023	.0023	.0022	.0021	.0020	.0019	.0017
3.000	.0018	.0018	.0018	.0017	.0016	.0015	.0014	.0014

X (in)	T(deg)= -14.250	T(deg)= -14.625	T(deg)= -15.000
-3.000	.0052	.0051	.0051
-2.500	.0049	.0049	.0048
-2.000	.0046	.0045	.0045
-1.750	.0045	.0044	.0043
-1.500	.0043	.0042	.0041
-1.250	.0042	.0041	.0040
-1.000	.0040	.0039	.0038
-.750	.0039	.0038	.0037
-.500	.0037	.0036	.0035
-.250	.0036	.0034	.0033
0.000	.0034	.0033	.0032
.250	.0032	.0031	.0030
.500	.0031	.0029	.0028
.750	.0029	.0028	.0026
1.000	.0027	.0026	.0025
1.250	.0025	.0024	.0023
1.500	.0024	.0022	.0021
1.750	.0022	.0021	.0019
2.000	.0020	.0019	.0018
2.500	.0016	.0015	.0014
3.000	.0012	.0011	.0010

X (in)	T(deg)= -7.500	T(deg)= -8.250	T(deg)= -9.000	T(deg)= -9.750	T(deg)= -10.500
-3.000	.0047	.0052	.0055	.0057	.0058
-2.500	.0044	.0049	.0052	.0054	.0055
-2.000	.0041	.0046	.0050	.0052	.0053
-1.750	.0039	.0044	.0048	.0051	.0052
-1.500	.0037	.0043	.0047	.0049	.0050
-1.250	.0036	.0041	.0045	.0048	.0049
-1.000	.0034	.0039	.0044	.0046	.0048
-.750	.0032	.0038	.0042	.0045	.0046
-.500	.0030	.0036	.0040	.0043	.0045
-.250	.0028	.0034	.0037	.0040	.0041
0.000	.0026	.0032	.0035	.0038	.0040
.250	.0024	.0031	.0033	.0036	.0038
.500	.0023	.0029	.0032	.0035	.0036
.750	.0021	.0027	.0030	.0033	.0034
1.000	.0019	.0025	.0028	.0031	.0032
1.250	.0017	.0021	.0024	.0027	.0028
1.500	.0015	.0019	.0022	.0025	.0026
1.750	.0013	.0017	.0020	.0023	.0024
2.000	.0011	.0015	.0018	.0021	.0022
2.500	.0008	.0012	.0015	.0018	.0019
3.000	.0006	.0009	.0011	.0014	.0015

The following is a list of the data in the TANGENT line sections of the scan:

X (in)	L(in)= -1.500	L(in)= -1.000	L(in)= -0.500	L(in)= 0.000	L(in)= 0.500	L(in)= 1.000	L(in)= 1.500	L(in)= 2.000	L(in)= 2.500	L(in)= 3.000	L(in)= 3.500	L(in)= 4.000
-3.000	.0050	.0050	.0049	.0049	.0048	.0048	.0048	.0048	.0048	.0048	.0048	.0048
-2.500	.0047	.0046	.0046	.0046	.0045	.0045	.0045	.0045	.0045	.0045	.0045	.0045
-2.000	.0044	.0043	.0043	.0043	.0041	.0041	.0041	.0041	.0041	.0041	.0041	.0041
-1.750	.0042	.0041	.0041	.0041	.0039	.0039	.0039	.0039	.0039	.0039	.0039	.0039
-1.500	.0041	.0040	.0040	.0040	.0038	.0038	.0038	.0038	.0038	.0038	.0038	.0038
-1.250	.0039	.0038	.0038	.0038	.0036	.0036	.0036	.0036	.0036	.0036	.0036	.0036
-1.000	.0037	.0036	.0036	.0036	.0034	.0034	.0034	.0034	.0034	.0034	.0034	.0034
-0.750	.0036	.0035	.0035	.0035	.0033	.0033	.0033	.0033	.0033	.0033	.0033	.0033
-0.500	.0034	.0033	.0033	.0033	.0031	.0031	.0031	.0031	.0031	.0031	.0031	.0031
-0.250	.0032	.0031	.0031	.0031	.0029	.0029	.0029	.0029	.0029	.0029	.0029	.0029
0.000	.0031	.0030	.0030	.0030	.0027	.0027	.0027	.0027	.0027	.0027	.0027	.0027
0.250	.0029	.0028	.0028	.0028	.0026	.0026	.0026	.0026	.0026	.0026	.0026	.0026
0.500	.0027	.0026	.0026	.0026	.0024	.0024	.0024	.0024	.0024	.0024	.0024	.0024
0.750	.0025	.0024	.0024	.0024	.0022	.0022	.0022	.0022	.0022	.0022	.0022	.0022
1.000	.0024	.0023	.0023	.0023	.0021	.0021	.0021	.0021	.0021	.0021	.0021	.0021
1.250	.0022	.0021	.0021	.0021	.0019	.0019	.0019	.0019	.0019	.0019	.0019	.0019
1.500	.0020	.0019	.0019	.0019	.0017	.0017	.0017	.0017	.0017	.0017	.0017	.0017
1.750	.0018	.0017	.0017	.0017	.0015	.0015	.0015	.0015	.0015	.0015	.0015	.0015
2.000	.0016	.0015	.0015	.0015	.0013	.0013	.0013	.0013	.0013	.0013	.0013	.0013
2.250	.0014	.0013	.0013	.0013	.0011	.0011	.0011	.0011	.0011	.0011	.0011	.0011
2.500	.0012	.0011	.0011	.0011	.0009	.0009	.0009	.0009	.0009	.0009	.0009	.0009
3.000	.0009	.0008	.0008	.0008	.0006	.0006	.0006	.0006	.0006	.0006	.0006	.0006

X (in)	L(in)= -12.000	L(in)= -13.000	L(in)= -14.000	L(in)= -15.000	L(in)= -16.000	L(in)= -17.000
-3.000	.0047	.0047	.0047	.0048	.0048	.0052
-2.500	.0045	.0045	.0045	.0046	.0048	.0052
-2.000	.0043	.0043	.0043	.0045	.0047	.0052
-1.750	.0042	.0042	.0042	.0044	.0046	.0054
-1.500	.0041	.0041	.0041	.0043	.0045	.0053
-1.250	.0040	.0040	.0040	.0042	.0044	.0052
-1.000	.0039	.0039	.0039	.0041	.0043	.0050
-0.750	.0038	.0038	.0038	.0040	.0042	.0049
-0.500	.0037	.0037	.0037	.0039	.0041	.0048
-0.250	.0036	.0036	.0036	.0038	.0040	.0046
0.000	.0035	.0035	.0035	.0037	.0039	.0044
0.250	.0034	.0034	.0034	.0036	.0038	.0041
0.500	.0033	.0033	.0033	.0035	.0037	.0040
0.750	.0032	.0032	.0032	.0034	.0036	.0039
1.000	.0031	.0031	.0031	.0033	.0035	.0038
1.250	.0030	.0030	.0030	.0032	.0034	.0037
1.500	.0029	.0029	.0029	.0031	.0033	.0036
1.750	.0028	.0028	.0028	.0030	.0032	.0035
2.000	.0027	.0027	.0027	.0029	.0031	.0034
2.250	.0026	.0026	.0026	.0028	.0030	.0033
2.500	.0025	.0025	.0025	.0027	.0029	.0032
3.000	.0024	.0024	.0024	.0026	.0028	.0031

X (in)	L(in)= -4.500	L(in)= -5.000	L(in)= -6.000	L(in)= -7.000	L(in)= -8.000	L(in)= -9.000	L(in)= -10.000	L(in)= -11.000
-3.000	.0048	.0047	.0047	.0047	.0047	.0047	.0047	.0047
-2.500	.0044	.0044	.0044	.0044	.0044	.0044	.0045	.0045
-2.000	.0040	.0040	.0040	.0041	.0041	.0042	.0042	.0043
-1.750	.0039	.0039	.0039	.0039	.0040	.0040	.0041	.0042
-1.500	.0037	.0037	.0037	.0038	.0038	.0039	.0040	.0041
-1.250	.0035	.0035	.0035	.0036	.0036	.0037	.0038	.0039
-1.000	.0033	.0033	.0033	.0034	.0034	.0035	.0036	.0037
-0.750	.0032	.0032	.0032	.0033	.0033	.0034	.0035	.0036
-0.500	.0030	.0030	.0030	.0031	.0031	.0032	.0033	.0034
-0.250	.0028	.0028	.0028	.0029	.0029	.0030	.0031	.0032
0.000	.0026	.0026	.0026	.0027	.0027	.0028	.0029	.0030
0.250	.0025	.0025	.0025	.0025	.0026	.0026	.0027	.0028
0.500	.0023	.0023	.0023	.0024	.0024	.0024	.0025	.0026
0.750	.0021	.0021	.0021	.0022	.0022	.0022	.0023	.0024
1.000	.0020	.0020	.0020	.0021	.0021	.0021	.0022	.0023
1.250	.0018	.0018	.0018	.0019	.0019	.0019	.0020	.0021
1.500	.0016	.0016	.0016	.0017	.0017	.0017	.0018	.0019
1.750	.0014	.0014	.0014	.0015	.0015	.0015	.0016	.0017
2.000	.0013	.0013	.0013	.0014	.0014	.0014	.0015	.0016
2.250	.0011	.0011	.0011	.0012	.0012	.0012	.0013	.0014
2.500	.0010	.0010	.0010	.0011	.0011	.0011	.0012	.0013
3.000	.0008	.0008	.0008	.0009	.0009	.0009	.0010	.0011

V. Auxiliary probe data for left side only.
A. NMR

The following data is derived from the data file(AL.P15) described here:
TITLE:ALADDIN Dipole-Polar Grid Left End (Z=0.00) Offset arc scan R=2.08m
Run number (15) was started at 9:48:58AM on 7/3/85.
The scan area is defined for this run by the parameters for region #1
in the geometry file named ALPLE.

The following is a list of the LOGGED data for probe #1:

Date Mo/Day Hr:Min	Value (Gauss)	Date Mo/Day Hr:Min	Value (Gauss)
JUL/ 3 10:01AM	15582.300	JUL/ 3 10:52AM	15583.000
JUL/ 3 10:03AM	15582.600	JUL/ 3 10:54AM	15583.100
JUL/ 3 10:05AM	15582.500	JUL/ 3 10:56AM	15583.000
JUL/ 3 10:07AM	15582.300	JUL/ 3 10:58AM	15582.800
JUL/ 3 10:09AM	15582.200	JUL/ 3 11:00AM	15582.800
JUL/ 3 10:11AM	15582.100	JUL/ 3 11:02AM	15582.800
JUL/ 3 10:13AM	15582.200	JUL/ 3 11:04AM	15582.900
JUL/ 3 10:15AM	15582.300	JUL/ 3 11:06AM	15583.100
JUL/ 3 10:17AM	15582.400	JUL/ 3 11:08AM	15583.300
JUL/ 3 10:19AM	15582.300	JUL/ 3 11:10AM	15583.400
JUL/ 3 10:21AM	15582.300	JUL/ 3 11:12AM	15583.300
JUL/ 3 10:23AM	15582.200	JUL/ 3 11:14AM	15583.200
JUL/ 3 10:25AM	15582.100	JUL/ 3 11:16AM	15583.200
JUL/ 3 10:27AM	15582.200	JUL/ 3 11:18AM	15583.500
JUL/ 3 10:29AM	15582.400	JUL/ 3 11:20AM	15583.700
JUL/ 3 10:31AM	15582.400	JUL/ 3 11:22AM	15583.900
JUL/ 3 10:33AM	15582.200	JUL/ 3 11:24AM	15583.800
JUL/ 3 10:35AM	15582.300	JUL/ 3 11:26AM	15583.800
JUL/ 3 10:37AM	15582.300	JUL/ 3 11:28AM	15583.800
JUL/ 3 10:39AM	15582.500	JUL/ 3 11:30AM	15584.000
JUL/ 3 10:41AM	15582.600	JUL/ 3 11:32AM	15584.100
JUL/ 3 10:43AM	15582.900	JUL/ 3 11:34AM	15584.000
JUL/ 3 10:45AM	15582.900	JUL/ 3 11:36AM	15584.300
JUL/ 3 10:47AM	15583.000	JUL/ 3 11:38AM	15584.300
JUL/ 3 10:49AM	15582.800	JUL/ 3 11:40AM	15584.500
JUL/ 3 10:50AM	15582.800	JUL/ 3 11:40AM	15584.500

The average value and the standard deviation are:

Average= 15582.983 Gauss
Sigma= .703 Gauss or .005 %
Total Deviation= 2.400 Gauss

V.B. Temperature of Hall probe.

The following data is derived from the data file(AL.P15) described here:
TITLE:ALADDIN Dipole-Polar Grid Left End (Z=0.00) Offset arc scan R=2.08m
Run number (15) was started at 9:48:58AM on 7/3/85.
The scan area is defined for this run by the parameters for region #1
in the geometry file named ALPLE.

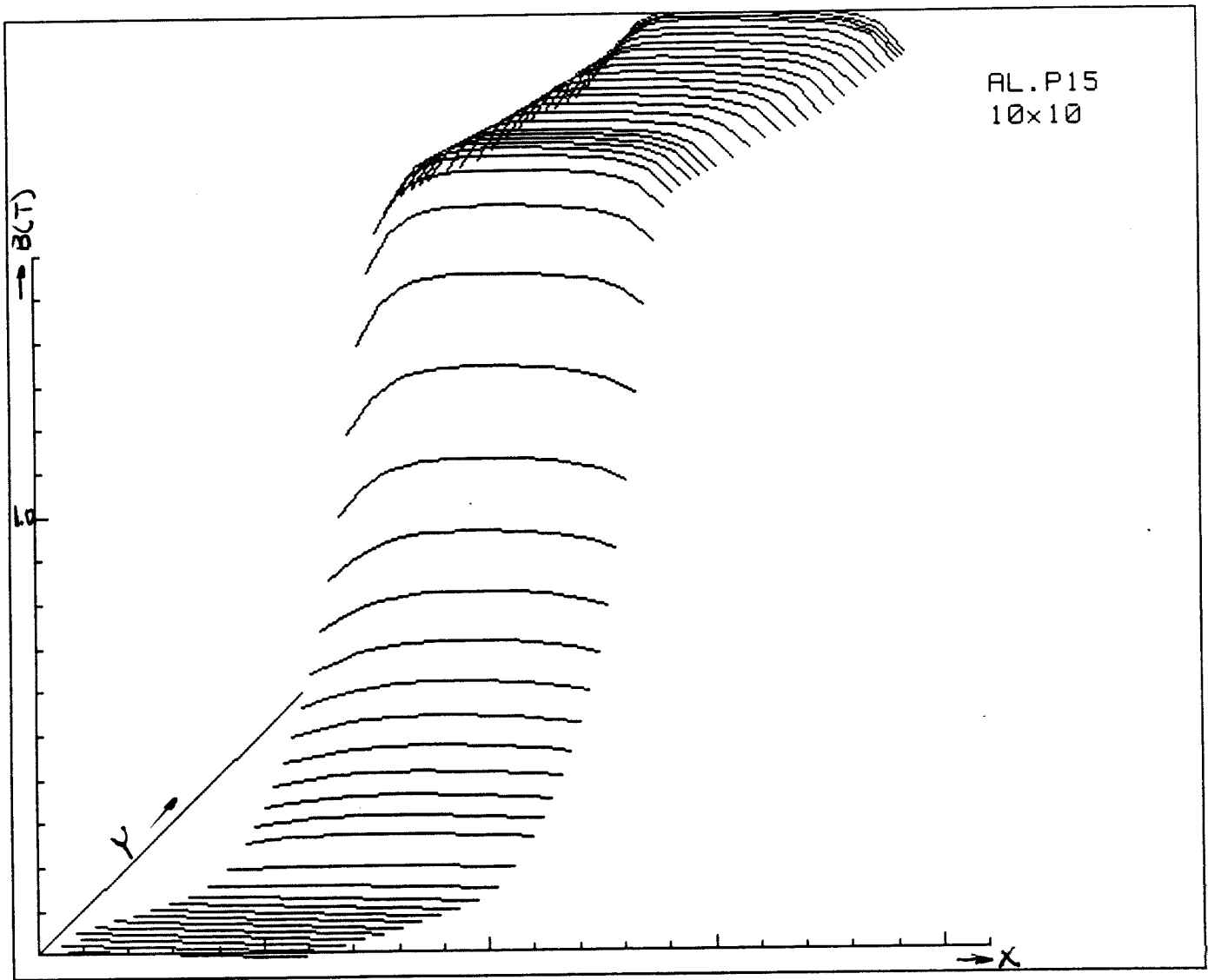
The following is a list of the LOGGED data for probe #2:

Date Mo/Day Hr:Min	Value (°C)	Date Mo/Day Hr:Min	Value (°C)
JUL/ 3 10:01AM	22.669	JUL/ 3 10:52AM	24.794
JUL/ 3 10:03AM	23.172	JUL/ 3 10:54AM	24.674
JUL/ 3 10:05AM	23.636	JUL/ 3 10:56AM	24.308
JUL/ 3 10:07AM	24.071	JUL/ 3 10:58AM	24.601
JUL/ 3 10:09AM	24.283	JUL/ 3 11:00AM	24.716
JUL/ 3 10:11AM	24.542	JUL/ 3 11:02AM	24.850
JUL/ 3 10:13AM	24.598	JUL/ 3 11:04AM	24.803
JUL/ 3 10:15AM	24.803	JUL/ 3 11:06AM	24.813
JUL/ 3 10:17AM	24.886	JUL/ 3 11:08AM	24.537
JUL/ 3 10:19AM	24.796	JUL/ 3 11:10AM	24.330
JUL/ 3 10:21AM	24.745	JUL/ 3 11:12AM	24.205
JUL/ 3 10:23AM	24.818	JUL/ 3 11:14AM	24.303
JUL/ 3 10:25AM	24.645	JUL/ 3 11:16AM	24.259
JUL/ 3 10:27AM	24.584	JUL/ 3 11:18AM	23.850
JUL/ 3 10:29AM	24.452	JUL/ 3 11:19AM	23.678
JUL/ 3 10:31AM	24.264	JUL/ 3 11:21AM	23.531
JUL/ 3 10:33AM	24.293	JUL/ 3 11:23AM	23.407
JUL/ 3 10:35AM	24.440	JUL/ 3 11:25AM	23.282
JUL/ 3 10:37AM	24.425	JUL/ 3 11:27AM	23.231
JUL/ 3 10:39AM	24.413	JUL/ 3 11:29AM	23.158
JUL/ 3 10:41AM	24.483	JUL/ 3 11:32AM	23.072
JUL/ 3 10:43AM	24.171	JUL/ 3 11:34AM	22.962
JUL/ 3 10:45AM	24.374	JUL/ 3 11:36AM	22.874
JUL/ 3 10:47AM	24.532	JUL/ 3 11:38AM	22.813
JUL/ 3 10:49AM	24.613	JUL/ 3 11:40AM	22.823
JUL/ 3 10:50AM	24.718	JUL/ 3 11:40AM	22.835

The average value and the standard deviation are:

Average= 24.117 °C
Sigma= .681 °C or 2.822 %
Total Deviation= 2.217 °C

VI. 3D plot of left side data only.



VII. Normalized, matched, and merged field values for all points.

The following data is derived from the data file (ALP28/RL.P15) described here:

TITLE:ALADDIN Dipole-Polar Grid Right End(2=0.00)Offset arc scan R=2.00m(E=1000M eV)/ALADDIN Dipole-Polar Grid Left End (2=0.00) Offset arc scan R=2.00m

Run number (28/15) was started at 9:40AM/9:48:5AM on 7/12/85:7/3/85.

The scan area is defined for this run by the parameters for region #1 in the geometry file named ALPRE/ALPLE.

The following is a list of the data in a TANGENT line section of the scan:

X (in)	NORMALIZED-Field(Gauss)-MATCHED										L(in)= .500
	L(in)= 17.000	L(in)= 16.000	L(in)= 15.000	L(in)= 14.000	L(in)= 13.000	L(in)= 12.000	L(in)= 11.000	L(in)= 10.000	L(in)= 9.000	L(in)= 8.000	
-3.000	0.0	0.0	0.0	0.0	-49.1	-55.1	-60.1	-62.1	-63.1	-63.1	6114.5
-2.500	0.0	0.0	-39.1	-43.1	-49.1	-56.1	-61.1	-63.1	-64.1	-64.1	5084.0
-2.000	-30.1	-34.1	-39.1	-43.1	-49.1	-56.1	-61.1	-63.1	-64.1	-64.1	5377.7
-1.750	-30.1	-34.1	-39.1	-43.1	-49.1	-56.1	-61.1	-63.1	-64.1	-64.1	6608.1
-1.500	-30.1	-34.1	-39.1	-43.1	-49.1	-56.1	-61.1	-63.1	-64.1	-64.1	5377.7
-1.250	-31.1	-35.1	-40.1	-46.1	-52.1	-59.1	-64.1	-66.1	-67.2	-67.2	6933.7
-1.000	-31.1	-35.1	-40.1	-46.1	-52.1	-59.1	-64.1	-66.1	-67.2	-67.2	5442.9
-0.750	-31.1	-35.1	-40.1	-46.1	-52.1	-59.1	-64.1	-66.1	-67.2	-67.2	7043.3
-0.500	-31.1	-35.1	-40.1	-46.1	-52.1	-59.1	-64.1	-66.1	-67.2	-67.2	5144.8
-0.250	-31.1	-35.1	-40.1	-46.1	-52.1	-59.1	-64.1	-66.1	-67.2	-67.2	5815.2
0.000	-31.1	-35.1	-40.1	-46.1	-52.1	-59.1	-64.1	-66.1	-67.2	-67.2	7186.9
0.250	-31.1	-35.1	-40.1	-46.1	-52.1	-59.1	-64.1	-66.1	-67.2	-67.2	5815.2
0.500	-31.1	-35.1	-40.1	-46.1	-52.1	-59.1	-64.1	-66.1	-67.2	-67.2	7186.9
0.750	-31.1	-35.1	-40.1	-46.1	-52.1	-59.1	-64.1	-66.1	-67.2	-67.2	5815.2
1.000	-31.1	-35.1	-40.1	-46.1	-52.1	-59.1	-64.1	-66.1	-67.2	-67.2	7186.9
1.250	-31.1	-35.1	-40.1	-46.1	-52.1	-59.1	-64.1	-66.1	-67.2	-67.2	5815.2
1.500	-31.1	-35.1	-40.1	-46.1	-52.1	-59.1	-64.1	-66.1	-67.2	-67.2	7186.9
1.750	-31.1	-35.1	-40.1	-46.1	-52.1	-59.1	-64.1	-66.1	-67.2	-67.2	5815.2
2.000	-31.1	-35.1	-40.1	-46.1	-52.1	-59.1	-64.1	-66.1	-67.2	-67.2	7186.9
2.500	-31.1	-35.1	-40.1	-46.1	-52.1	-59.1	-64.1	-66.1	-67.2	-67.2	5815.2
3.000	-31.1	-35.1	-40.1	-46.1	-52.1	-59.1	-64.1	-66.1	-67.2	-67.2	7186.9

X (in)	NORMALIZED-Field(Gauss)-MATCHED										L(in)= 3.500
	L(in)= 9.000	L(in)= 8.000	L(in)= 7.000	L(in)= 6.000	L(in)= 5.000	L(in)= 4.500	L(in)= 4.000	L(in)= 3.500	L(in)= 3.000	L(in)= 2.500	
-3.000	-57.1	-57.1	56.1	291.6	771.0	1086.3	1445.7	1843.8	2292.3	2894.6	6114.5
-2.500	-56.1	-56.1	56.1	291.6	771.0	1086.3	1445.7	1843.8	2292.3	2894.6	5084.0
-2.000	-54.1	-54.1	56.1	291.6	771.0	1086.3	1445.7	1843.8	2292.3	2894.6	5377.7
-1.750	-54.1	-54.1	56.1	291.6	771.0	1086.3	1445.7	1843.8	2292.3	2894.6	6608.1
-1.500	-53.1	-53.1	56.1	291.6	771.0	1086.3	1445.7	1843.8	2292.3	2894.6	5377.7
-1.250	-52.1	-52.1	56.1	291.6	771.0	1086.3	1445.7	1843.8	2292.3	2894.6	6933.7
-1.000	-52.1	-52.1	56.1	291.6	771.0	1086.3	1445.7	1843.8	2292.3	2894.6	5442.9
-0.750	-51.1	-51.1	56.1	291.6	771.0	1086.3	1445.7	1843.8	2292.3	2894.6	7043.3
-0.500	-51.1	-51.1	56.1	291.6	771.0	1086.3	1445.7	1843.8	2292.3	2894.6	5144.8
-0.250	-50.1	-50.1	56.1	291.6	771.0	1086.3	1445.7	1843.8	2292.3	2894.6	5815.2
0.000	-50.1	-50.1	56.1	291.6	771.0	1086.3	1445.7	1843.8	2292.3	2894.6	7186.9
0.250	-49.1	-49.1	56.1	291.6	771.0	1086.3	1445.7	1843.8	2292.3	2894.6	5815.2
0.500	-49.1	-49.1	56.1	291.6	771.0	1086.3	1445.7	1843.8	2292.3	2894.6	7186.9
0.750	-49.1	-49.1	56.1	291.6	771.0	1086.3	1445.7	1843.8	2292.3	2894.6	5815.2
1.000	-49.1	-49.1	56.1	291.6	771.0	1086.3	1445.7	1843.8	2292.3	2894.6	7186.9
1.250	-48.1	-48.1	56.1	291.6	771.0	1086.3	1445.7	1843.8	2292.3	2894.6	5815.2
1.500	-48.1	-48.1	56.1	291.6	771.0	1086.3	1445.7	1843.8	2292.3	2894.6	7186.9
1.750	-48.1	-48.1	56.1	291.6	771.0	1086.3	1445.7	1843.8	2292.3	2894.6	5815.2
2.000	-48.1	-48.1	56.1	291.6	771.0	1086.3	1445.7	1843.8	2292.3	2894.6	7186.9
2.500	-48.1	-48.1	56.1	291.6	771.0	1086.3	1445.7	1843.8	2292.3	2894.6	5815.2
3.000	-48.1	-48.1	56.1	291.6	771.0	1086.3	1445.7	1843.8	2292.3	2894.6	7186.9

The following is a list of the data in the ARC section of the scan:

X (in)	NORMALIZED-Field(Gauss)-MATCHED				
	T(deg)= 15.000	T(deg)= 14.625	T(deg)= 14.250	T(deg)= 13.875	T(deg)= 13.500
-3.000	7523.1	9355.3	11254.5	12712.8	13508.7
-2.500	8159.2	10168.4	12172.8	13647.4	14394.2
-2.000	8550.6	10593.6	12566.6	14024.0	14726.5
-1.750	8658.2	10699.4	12693.4	14119.2	14805.1
-1.500	8752.7	10781.2	12765.9	14180.2	14856.7
-1.250	8811.1	10833.6	12813.9	14221.7	14890.3
-1.000	8844.0	10871.6	12848.3	14248.7	14913.0
-0.750	8884.2	10898.7	12869.4	14268.4	14929.4
-0.500	8905.6	10918.5	12886.7	14282.4	14941.5
-0.250	8918.3	10930.8	12897.1	14291.4	14948.9
0.000	8928.3	10937.5	12904.1	14297.7	14953.5
0.250	8933.3	10941.8	12906.7	14301.4	14956.2
0.500	8934.3	10943.2	12908.4	14301.1	14956.2
0.750	8932.3	10941.2	12906.4	14299.4	14953.2
1.000	8927.3	10935.8	12901.4	14293.4	14947.2
1.250	8919.3	10926.8	12891.4	14283.4	14937.4
1.500	8903.2	10913.1	12876.4	14267.4	14921.0
1.750	8881.2	10890.4	12852.4	14241.4	14896.7
2.000	8850.2	10856.6	12815.3	14202.2	14856.0
2.500	8740.0	10724.1	12661.3	14033.7	14681.3
3.000	8514.5	10419.8	12275.0	13574.9	14179.5

X (in)	NORMALIZED-Field(Gauss)-MATCHED				
	T(deg)= 6.750	T(deg)= 6.000	T(deg)= 5.250	T(deg)= 4.500	T(deg)= 3.750
-3.000	14398.6	14428.5	14424.5	14388.0	14327.8
-2.500	15147.8	15165.2	15170.5	15163.8	15145.9
-2.000	15392.2	15405.3	15413.8	15417.2	15422.0
-1.750	15443.3	15456.5	15465.1	15470.2	15474.4
-1.500	15475.3	15486.9	15497.1	15502.2	15508.8
-1.250	15494.0	15505.6	15515.1	15522.6	15531.1
-1.000	15507.0	15518.7	15528.2	15535.3	15541.9
-0.750	15515.0	15526.4	15536.2	15543.6	15549.5
-0.500	15520.3	15531.0	15541.2	15548.3	15555.5
-0.250	15523.1	15533.7	15544.2	15551.0	15557.9
0.000	15525.4	15536.4	15546.2	15553.3	15559.9
0.250	15524.7	15535.7	15546.2	15554.3	15560.5
0.500	15524.1	15535.7	15546.2	15554.3	15561.1
0.750	15519.7	15532.7	15541.2	15549.3	15558.7
1.000	15516.0	15528.6	15536.7	15538.5	15550.2
1.250	15496.6	15502.6	15511.8	15519.6	15539.9
1.500	15468.3	15479.6	15487.4	15496.9	15508.4
1.750	15431.5	15440.8	15449.1	15458.9	15467.1
2.000	15383.3	15392.8	15401.8	15410.3	15419.3
2.500	15253.3	15259.8	15267.8	15283.0	15298.0
3.000	14701.3	14692.6	14707.9	14742.4	14799.5

X (in)	T(deg)= 3.000	T(deg)= 2.250	T(deg)= 1.500
-3.000	14293.0	14360.4	14434.0
-2.500	15145.9	15171.8	15197.1
-2.000	15422.0	15432.8	15441.0
-1.750	15478.3	15486.8	15493.0
-1.500	15511.3	15519.9	15524.1
-1.250	15533.1	15538.9	15543.0
-1.000	15545.1	15552.9	15556.1
-0.750	15554.4	15560.2	15564.1
-0.500	15559.9	15565.9	15569.1
-0.250	15563.1	15568.9	15572.8
0.000	15563.7	15568.6	15574.1
0.250	15564.4	15569.6	15574.8
0.500	15562.1	15568.5	15570.1
0.750	15558.7	15565.2	15563.4
1.000	15550.2	15558.9	15555.1
1.250	15544.1	15550.2	15550.9
1.500	15539.9	15544.1	15545.9
1.750	15534.6	15539.9	15541.0
2.000	15526.2	15530.4	15531.1
2.500	15508.4	15513.1	15516.7
3.000	15470.3	15478.0	15486.0

NORMALIZED-Field(Gauss)-MATCHED

X (in)	NORMALIZED-Field(Gauss)-MATCHED				
	T(deg)= 9.750	T(deg)= 9.000	T(deg)= 8.250	T(deg)= 7.500	T(deg)= 6.750
-3.000	14175.9	14160.6	14160.6	14160.6	14160.6
-2.500	15014.0	15035.4	15078.6	15118.9	15171.8
-2.000	15291.5	15317.9	15348.2	15373.6	15413.8
-1.750	15348.8	15376.5	15405.8	15427.4	15446.3
-1.500	15368.5	15412.3	15438.8	15459.1	15496.3
-1.250	15372.6	15433.7	15460.1	15479.4	15525.7
-1.000	15388.0	15447.7	15473.4	15492.1	15545.1
-0.750	15396.3	15456.3	15481.4	15500.4	15557.7
-0.500	15403.4	15462.0	15488.1	15506.1	15565.1
-0.250	15406.4	15465.2	15490.4	15509.1	15572.1
0.000	15407.7	15467.3	15492.8	15511.1	15574.1
0.250	15411.7	15471.3	15496.7	15516.1	15576.1
0.500	15417.0	15476.7	15498.4	15518.1	15577.1
0.750	15424.7	15484.7	15501.8	15520.4	15578.4
1.000	15438.7	15498.4	15516.1	15531.1	15587.4
1.250	15454.0	15514.6	15533.0	15541.4	15595.1
1.500	15471.8	15533.3	15547.7	15551.8	15603.4
1.750	15491.9	15558.3	15568.9	15568.9	15616.7
2.000	15513.6	15585.8	15598.9	15598.9	15631.4
2.500	15561.2	15658.8	15681.3	15621.7	15686.0
3.000	15624.1	15746.6	15753.4	15686.0	15748.3

NORMALIZED-Field(Gauss)-MATCHED

The following is a list of the data in the ARC section of the scan:

X (in)	NORMALIZED-Field(Gauss)-MATCHED			
	T(deg)= 0.000	T(deg)= -1.500	T(deg)= -2.250	T(deg)= -3.000
-3.000	14493.6	14421.4	14340.0	14272.3
-2.500	15215.6	15199.8	15135.7	15140.0
-2.000	15448.2	15437.8	15425.3	15415.0
-1.750	15498.9	15493.4	15481.0	15467.7
-1.500	15527.3	15521.1	15514.0	15507.0
-1.250	15547.6	15546.1	15539.0	15522.7
-1.000	15559.6	15558.8	15554.1	15541.7
-0.750	15572.9	15572.1	15568.1	15557.3
-0.500	15572.9	15572.1	15568.1	15557.3
-0.250	15576.6	15575.1	15570.8	15566.3
0.000	15577.6	15576.8	15572.8	15567.3
0.250	15577.6	15576.8	15572.8	15567.3
0.500	15576.6	15574.4	15571.1	15566.3
0.750	15572.2	15571.8	15568.4	15562.3
1.000	15572.2	15567.3	15562.1	15557.7
1.250	15572.2	15564.1	15558.1	15547.7
1.500	15541.9	15538.1	15533.0	15526.0
1.750	15517.9	15517.7	15514.1	15509.3
2.000	15479.9	15475.8	15472.0	15465.0
2.500	15288.2	15287.7	15299.7	15296.0
3.000	14793.6	14785.7	14781.0	14795.0

X (in)	NORMALIZED-Field(Gauss)-MATCHED			
	T(deg)= -5.250	T(deg)= -6.000	T(deg)= -6.750	T(deg)= -7.500
-3.000	14400.0	14403.4	14371.0	14305.7
-2.500	15156.0	15150.1	15129.4	15098.7
-2.000	15403.0	15394.1	15379.1	15358.3
-1.750	15457.0	15446.8	15431.0	15413.3
-1.500	15489.0	15479.0	15464.1	15447.0
-1.250	15508.7	15498.4	15483.1	15467.7
-1.000	15521.3	15511.8	15498.1	15481.0
-0.750	15529.7	15519.4	15506.4	15490.0
-0.500	15535.7	15525.8	15512.1	15496.0
-0.250	15538.0	15529.1	15516.1	15499.0
0.000	15540.7	15530.1	15517.4	15501.7
0.250	15548.0	15538.1	15517.4	15508.3
0.500	15539.0	15529.4	15516.8	15509.3
0.750	15535.0	15526.4	15512.4	15507.3
1.000	15527.0	15519.8	15507.8	15501.0
1.250	15520.0	15511.1	15507.4	15493.0
1.500	15505.7	15496.1	15483.0	15475.0
1.750	15481.3	15473.1	15468.4	15457.7
2.000	15443.0	15432.8	15421.1	15408.0
2.500	15263.7	15251.1	15243.1	15239.3
3.000	14708.0	14689.8	14693.1	14715.0

X (in)	NORMALIZED-Field(Gauss)-MATCHED			
	T(deg)= -11.250	T(deg)= -12.000	T(deg)= -12.375	T(deg)= -13.125
-3.000	14170.9	14156.1	14126.6	13984.4
-2.500	14942.2	14929.4	14900.6	14792.4
-2.000	15210.2	15187.8	15168.6	15072.4
-1.750	15266.2	15243.8	15218.6	15136.4
-1.500	15301.9	15278.8	15253.9	15176.4
-1.250	15322.9	15301.9	15277.6	15202.7
-1.000	15338.9	15315.8	15292.3	15228.4
-0.750	15347.2	15327.1	15302.9	15241.4
-0.500	15354.9	15332.1	15309.3	15247.7
-0.250	15358.6	15338.1	15315.3	15251.1
0.000	15361.2	15339.1	15318.9	15253.1
0.250	15361.2	15341.1	15321.7	15253.1
0.500	15360.9	15340.1	15321.7	15252.4
0.750	15358.6	15337.5	15316.6	15248.4
1.000	15353.9	15333.1	15310.3	15244.4
1.250	15344.9	15323.8	15302.6	15241.4
1.500	15331.9	15310.5	15288.6	15236.1
1.750	15309.9	15288.9	15266.9	15238.4
2.000	15273.9	15251.8	15229.6	15198.1
2.500	15105.9	15093.8	15061.6	15033.1
3.000	14586.9	14562.8	14541.9	14479.4

X (in)	NORMALIZED-Field(Gauss)-MATCHED			
	T(deg)= -14.250	T(deg)= -14.625	T(deg)= -15.000	T(deg)= -15.375
-3.000	11051.0	9143.2	7347.7	13423.9
-2.500	11969.7	9943.5	7981.7	14327.2
-2.000	12391.7	10364.8	8361.0	14670.8
-1.750	12501.7	10483.5	8480.0	14755.2
-1.500	12576.4	10567.5	8565.7	14865.5
-1.250	12626.4	10625.2	8625.7	14867.2
-1.000	12661.4	10665.8	8668.7	14843.8
-0.750	12685.4	10694.5	8699.7	14843.8
-0.500	12702.4	10713.5	8722.7	14843.8
-0.250	12713.7	10728.5	8736.7	14843.8
0.000	12722.1	10737.2	8746.0	14843.8
0.250	12727.1	10741.5	8753.3	14843.8
0.500	12727.4	10743.2	8756.7	14843.8
0.750	12727.4	10743.2	8756.7	14843.8
1.000	12719.4	10741.5	8753.7	14843.8
1.250	12709.4	10734.2	8747.7	14843.8
1.500	12691.7	10723.2	8737.7	14843.8
1.750	12667.1	10707.5	8722.7	14843.8
2.000	12629.1	10684.5	8699.7	14843.8
2.500	12475.4	10514.5	8557.0	14641.5
3.000	12097.4	10217.8	8333.7	14150.5

The following is a list of the data in the TANGENT line sections of the scan:

X (in)	NORMALIZED-Field(Gauss)-MATCHED				
	L(in)=-500	L(in)=-1,000	L(in)=-1,500	L(in)=-2,000	L(in)=-2,500
-3,000	5984.1	4904.8	4040.2	3337.9	2745.2
-2,500	6466.8	5270.2	4320.9	3556.8	2921.6
-2,000	6791.1	5533.8	4531.8	3727.5	3060.8
-1,750	6900.8	5629.8	4613.8	3795.8	3116.8
-1,500	6982.8	5705.8	4679.8	3850.8	3165.2
-1,250	7043.8	5765.5	4732.8	3897.5	3204.8
-1,000	7090.8	5810.8	4775.8	3934.8	3238.1
-750	7124.8	5844.1	4807.8	3964.8	3264.5
-500	7148.1	5869.8	4834.2	3988.8	3285.8
-250	7164.8	5888.1	4852.8	4006.8	3303.5
0,000	7177.4	5900.8	4865.8	4019.8	3316.1
250	7183.8	5908.5	4875.8	4029.8	3325.5
500	7185.4	5912.8	4880.8	4035.2	3331.8
750	7188.4	5914.5	4882.8	4037.2	3334.8
1,000	7180.4	5910.8	4880.5	4032.8	3335.5
1,250	7170.1	5902.8	4875.8	4025.8	3328.1
1,500	7156.4	5890.8	4865.2	4014.8	3320.8
1,750	7135.8	5874.5	4850.8	4000.8	3309.8
2,000	7106.8	5850.1	4832.8	3987.5	3297.1
2,500	7014.1	5777.8	4776.8	3957.5	3277.1
3,000	6848.8	5656.8	4686.8	3891.8	3228.8

X (in)	NORMALIZED-Field(Gauss)-MATCHED									
	L(in)=-12,000	L(in)=-13,000	L(in)=-14,000	L(in)=-15,000	L(in)=-16,000	L(in)=-17,000	L(in)=-18,000	L(in)=-19,000	L(in)=-20,000	L(in)=-21,000
-3,000	-60.0	-55.0	-49.0	-43.0	-37.0	-31.0	-25.0	-19.0	-13.0	-7.0
-2,500	-61.0	-56.0	-50.0	-44.0	-38.0	-32.0	-26.0	-20.0	-14.0	-8.0
-2,000	-63.0	-58.0	-52.0	-46.0	-40.0	-34.0	-28.0	-22.0	-16.0	-10.0
-1,750	-63.0	-58.0	-52.0	-46.0	-40.0	-34.0	-28.0	-22.0	-16.0	-10.0
-1,500	-64.0	-59.0	-53.0	-47.0	-41.0	-35.0	-29.0	-23.0	-17.0	-11.0
-1,250	-64.0	-59.0	-53.0	-47.0	-41.0	-35.0	-29.0	-23.0	-17.0	-11.0
-1,000	-65.0	-60.0	-54.0	-48.0	-42.0	-36.0	-30.0	-24.0	-18.0	-12.0
-750	-65.0	-60.0	-54.0	-48.0	-42.0	-36.0	-30.0	-24.0	-18.0	-12.0
-500	-66.0	-61.0	-55.0	-49.0	-43.0	-37.0	-31.0	-25.0	-19.0	-13.0
-250	-67.0	-62.0	-56.0	-50.0	-44.0	-38.0	-32.0	-26.0	-20.0	-14.0
0,000	-67.0	-62.0	-56.0	-50.0	-44.0	-38.0	-32.0	-26.0	-20.0	-14.0
250	-68.0	-63.0	-57.0	-51.0	-45.0	-39.0	-33.0	-27.0	-21.0	-15.0
500	-68.0	-63.0	-57.0	-51.0	-45.0	-39.0	-33.0	-27.0	-21.0	-15.0
750	-69.0	-64.0	-58.0	-52.0	-46.0	-40.0	-34.0	-28.0	-22.0	-16.0
1,000	-69.0	-64.0	-58.0	-52.0	-46.0	-40.0	-34.0	-28.0	-22.0	-16.0
1,250	-69.0	-64.0	-58.0	-52.0	-46.0	-40.0	-34.0	-28.0	-22.0	-16.0
1,500	-69.0	-64.0	-58.0	-52.0	-46.0	-40.0	-34.0	-28.0	-22.0	-16.0
1,750	-70.0	-65.0	-59.0	-53.0	-47.0	-41.0	-35.0	-29.0	-23.0	-17.0
2,000	-70.0	-65.0	-59.0	-53.0	-47.0	-41.0	-35.0	-29.0	-23.0	-17.0
2,500	-71.0	-66.0	-60.0	-54.0	-48.0	-42.0	-36.0	-30.0	-24.0	-18.0
3,000	-71.7	-66.7	-60.7	-54.7	-48.7	-42.7	-36.7	-30.7	-24.7	-18.7

X (in)	NORMALIZED-Field(Gauss)-MATCHED				
	L(in)=-4,500	L(in)=-5,000	L(in)=-5,500	L(in)=-6,000	L(in)=-6,500
-3,000	1048.9	737.6	44.0	-38.0	-64.0
-2,500	1140.9	815.6	63.0	-32.0	-62.0
-2,000	1214.9	879.9	80.3	-26.0	-61.0
-1,750	1246.3	906.9	89.0	-23.0	-60.0
-1,500	1272.9	930.9	94.0	-20.0	-59.0
-1,250	1296.9	951.9	98.0	-18.0	-58.0
-1,000	1315.9	969.3	103.7	-15.0	-57.0
-750	1332.6	983.5	107.0	-13.0	-56.0
-500	1346.9	996.9	115.0	-11.0	-55.0
-250	1357.9	1006.9	121.0	-9.7	-54.0
0,000	1367.9	1015.9	125.0	-8.3	-53.0
250	1374.6	1021.9	129.0	-7.0	-52.0
500	1379.9	1027.3	134.3	-6.0	-51.0
750	1382.9	1030.9	137.0	-5.0	-50.0
1,000	1384.9	1032.9	138.0	-4.0	-49.0
1,250	1385.9	1033.9	139.0	-4.0	-48.0
1,500	1384.9	1033.9	140.0	-4.0	-47.0
1,750	1383.6	1033.9	140.7	-3.0	-46.0
2,000	1380.9	1031.3	140.7	-3.0	-45.0
2,500	1376.9	1024.9	139.3	-4.0	-44.0
3,000	1357.3	1013.9	137.0	-6.0	-43.0

X (in)	NORMALIZED-Field(Gauss)-MATCHED				
	L(in)=-7,000	L(in)=-7,500	L(in)=-8,000	L(in)=-8,500	L(in)=-9,000
-3,000	-69.0	-69.0	-69.0	-69.0	-69.0
-2,500	-69.0	-69.0	-69.0	-69.0	-69.0
-2,000	-69.0	-69.0	-69.0	-69.0	-69.0
-1,750	-69.0	-69.0	-69.0	-69.0	-69.0
-1,500	-69.0	-69.0	-69.0	-69.0	-69.0
-1,250	-69.0	-69.0	-69.0	-69.0	-69.0
-1,000	-69.0	-69.0	-69.0	-69.0	-69.0
-750	-69.0	-69.0	-69.0	-69.0	-69.0
-500	-69.0	-69.0	-69.0	-69.0	-69.0
-250	-69.0	-69.0	-69.0	-69.0	-69.0
0,000	-69.0	-69.0	-69.0	-69.0	-69.0
250	-69.0	-69.0	-69.0	-69.0	-69.0
500	-69.0	-69.0	-69.0	-69.0	-69.0
750	-69.0	-69.0	-69.0	-69.0	-69.0
1,000	-69.0	-69.0	-69.0	-69.0	-69.0
1,250	-69.0	-69.0	-69.0	-69.0	-69.0
1,500	-69.0	-69.0	-69.0	-69.0	-69.0
1,750	-69.0	-69.0	-69.0	-69.0	-69.0
2,000	-69.0	-69.0	-69.0	-69.0	-69.0
2,500	-69.0	-69.0	-69.0	-69.0	-69.0
3,000	-69.0	-69.0	-69.0	-69.0	-69.0

VIII. Field integrals, effective lengths, harmonic coefficients. A. Left side only.

The following data is derived from the data file(ALP28/AL.P15) described here:
TITLE:ALADDIN Dipole-Polar Grid Left End (2=0.00) Offset arc scan R=2.08m
ev)/ALADDIN Dipole-Polar Grid Left End (2=0.00) Offset arc scan R=2.08m
Run number (15) was started at 9:48:5AM on 7/3/85.

The scan area is defined for this run by the parameters for region #1
in the geometry file named ALPLE.
The following field integrals are listed for paths at the SAME radii as
to the central beam path at R=208.3cm inside the gap for scan #s 3 through 51.

X (cm)	Field Integral (T-m)	Effective Edge X(cm)	Y(cm)	Effective Length (cm)
-5.080	0.863956	-12.5371	-55.2579	55.9260
-4.445	0.868236	-11.9262	-55.3479	56.0192
-3.810	0.871855	-11.3111	-55.4222	56.0961
-3.175	0.873018	-10.6904	-55.4756	56.1513
-2.540	0.874390	-10.0670	-55.5189	56.1962
-1.905	0.875365	-9.4405	-55.5585	56.2289
-1.270	0.876089	-8.8129	-55.5779	56.2573
-0.635	0.876569	-8.1824	-55.5948	56.2747
0.000	0.876894	-7.5518	-55.6115	56.2920
0.635	0.877075	-6.9198	-55.6226	56.3036
1.270	0.877095	-6.2861	-55.6274	56.3085
1.905	0.876986	-5.6534	-55.6360	56.3174
2.540	0.876681	-5.0180	-55.6345	56.3159
3.175	0.876143	-4.3834	-55.6361	56.3175
3.810	0.875261	-3.7481	-55.6348	56.3162
4.445	0.873879	-3.1126	-55.6330	56.3143
5.080	0.871637	-2.4778	-55.6336	56.3149

The above data was fit with a polynomial of DEGREE=7 giving:
The coefficients*1 and RMS errors for the field INTEGRALS, using an
estimated RMS error at each measured point of 4.7 Gauss, are:

b(0)= +8.7690E-01+/- 6.5741E-06 T-m
b(1)= +3.8722E-02+/- 6.6381E-04 T-m/m
b(2)= -3.8284E+00+/- 5.7869E-02 T-m/m^2
b(3)= +5.5788E+01+/- 1.0620E+01 T-m/m^3
b(4)= -5.4903E+03+/- 6.8432E+02 T-m/m^4
b(5)= +8.2291E+04+/- 1.6125E+05 T-m/m^5
b(6)= -1.1056E+08+/- 5.2822E+06 T-m/m^6
b(7)= +2.4383E+09+/- 1.4996E+09 T-m/m^7

The coefficients*1 and RMS errors for the CENTRAL field equal to the
above coefficients divided by the effective length of .5629 m are:

b(0)=+1.5578E+00+/- 1.1679E-05 T
b(1)=+6.8789E-02+/- 1.1792E-03 T/m
b(2)=-6.8011E+00+/- 1.0280E-01 T/m^2
b(3)=+9.9106E+01+/- 1.8866E+01 T/m^3
b(4)=-9.7533E+03+/- 1.2157E+03 T/m^4
b(5)=+1.4619E+05+/- 2.8646E+05 T/m^5
b(6)=-1.9641E+08+/- 9.3837E+06 T/m^6
b(7)=+4.3316E+09+/- 2.6641E+09 T/m^7

Signal= 1.51286 Gauss
Q= .935483
Q/(N-D-1)= .10394259

The PEAK value is at R= 1.0627 cm.

VIII.B. Both sides.

The following data is derived from the data file(ALP28/AL.P15) described here:
TITLE:ALADDIN Dipole-Polar Grid Right End(2=0.00)Offset arc scan R=2.08m(E=1000M
ev)/ALADDIN Dipole-Polar Grid Left End (2=0.00) Offset arc scan R=2.08m
Run number (28/15) was started at 9:9:40AM/9:48:5AM on 7/12/85:7/3/85.
The scan area is defined for this run by the parameters for region #1
in the geometry file named ALPRE/ALPLE.

The following field integrals are listed for paths at the SAME radii as
to the central beam path at R=208.3cm inside the gap for scan #s 1 through 97.

X (cm)	Field Integral (T-m)	Effective Length (cm)
-5.080	1.730619	112.0272
-4.445	1.739105	112.2083
-3.810	1.744700	112.3596
-3.175	1.748572	112.4657
-2.540	1.751279	112.5530
-1.905	1.753210	112.6170
-1.270	1.754632	112.6721
-0.635	1.755602	112.7077
0.000	1.756245	112.7417
0.635	1.756616	112.7655
1.270	1.756656	112.7753
1.905	1.756458	112.7945
2.540	1.755854	112.7919
3.175	1.754812	112.7974
3.810	1.753070	112.7964
4.445	1.750394	112.7945
5.080	1.745887	112.7987

The above data was fit with a polynomial of DEGREE=7 giving:
The coefficients*1 and RMS errors for the field INTEGRALS, using an
estimated RMS error at each measured point of 4.7 Gauss, are:

b(0)= +1.7563E+00+/- 5.2581E-06 T-m
b(1)= +7.8285E-02+/- 5.3893E-04 T-m/m
b(2)= -7.5337E+00+/- 4.6285E-02 T-m/m^2
b(3)= +9.9781E+01+/- 8.4939E+00 T-m/m^3
b(4)= -1.0701E+04+/- 5.4734E+02 T-m/m^4
b(5)= +2.7692E+05+/- 1.2897E+05 T-m/m^5
b(6)= -2.2258E+08+/- 4.2249E+06 T-m/m^6
b(7)= +4.0255E+09+/- 1.1995E+09 T-m/m^7

The coefficients*1 and RMS errors for the CENTRAL field equal to the
above coefficients divided by the effective length of 1.127 m are:

b(0)=+1.5578E+00+/- 4.6639E-06 T
b(1)=+6.9438E-02+/- 4.7093E-04 T/m
b(2)=-6.6823E+00+/- 4.1054E-02 T/m^2
b(3)=+8.8505E+01+/- 7.5340E+00 T/m^3
b(4)=-9.4918E+03+/- 4.8549E+02 T/m^4
b(5)=+2.4563E+05+/- 1.1440E+05 T/m^5
b(6)=-1.9736E+08+/- 3.7474E+06 T/m^6
b(7)=+3.5706E+09+/- 1.0639E+09 T/m^7

Signal= 1.705218 Gauss
Q= 1.184695
Q/(N-D-1)= .13163281

The PEAK value is at R= 1.1176 cm.

IX. Secondary method for defining harmonic coefficients for all points.

A. Table of coefficients for each radial scan.

The following data is derived from the data file (ALP20/ALP15) described here:

TITLE:ALADDIN Dipole-Polar Grid Right End(Z=0.00)Offset arc scan R=2.08m(E=1000M eV)/ALADDIN Dipole-Polar Grid Left End (Z=0.00) Offset arc scan R=2.08m

Run number (20/15) was started at 9:19:40AM/9:48:50AM on 7/12/85:7/3/85.

The scan area is defined for this run by the parameters for region #1 in the geometry file named ALPRE/ALPLE.

The following results are for the fits of a polynomial of DEGREE=7 to the field measurements at each radial scan #:

Scan #	b(0) (T)	b(1) (T/m) $\times 10^{-1}$	b(2) (T/m ²) $\times 10^{-2}$	b(3) (T/m ³) $\times 10^{-2}$	b(4) (T/m ⁴) $\times 10^{-4}$	b(5) (T/m ⁵) $\times 10^{-6}$	b(6) (T/m ⁶) $\times 10^{-8}$	b(7) (T/m ⁷) $\times 10^{-9}$	Sigma (Gauss)
1	-0.0032	-0.050	-0.050	+0.238	+0.084	-0.400	-0.078	+3.024	.3470
2	-0.0037	-0.031	-0.054	-0.291	+0.194	-0.420	-0.192	-3.712	.3100
3	-0.0042	-0.070	+0.065	+0.292	-0.020	-0.475	+0.021	-4.667	.3401
4	-0.0048	-0.074	+0.135	+0.130	-0.061	-0.219	+0.007	+2.366	.3302
5	-0.0055	-0.056	+0.179	-0.116	+0.081	-0.080	-0.080	-1.228	.3427
6	-0.0061	-0.052	+0.108	-0.200	+0.110	-0.246	-0.120	-1.977	.4654
7	-0.0066	-0.055	+0.023	+0.044	+0.042	-0.161	-0.046	+1.929	.3457
8	-0.0065	-0.051	+0.192	+0.463	-0.681	+0.209	+6.173	.2248	.2248
9	-0.0050	+0.041	-0.085	+0.273	-0.086	-0.310	+0.064	+1.963	.4037
10	+0.0001	+0.257	-0.379	-0.121	-0.120	+0.158	+0.076	-1.328	.3645
11	+0.0142	+0.592	-1.230	+0.081	-1.175	+0.152	-2.150	.2658	.2912
12	+0.0477	+1.053	-2.954	+0.507	-1.148	-0.135	+0.066	.2129	.2912
13	+0.1050	+1.283	-4.004	+0.876	-0.409	+0.104	+0.184	.2129	.2912
14	+0.1407	+1.381	-4.869	+0.916	-1.332	-0.025	+0.654	.3494	.3494
15	+0.1611	+1.451	-5.923	+1.322	+0.058	-0.546	-0.181	+0.334	.2920
16	+0.2264	+1.578	-6.069	+1.172	-1.082	-0.142	-0.103	+1.231	.2686
17	+0.2783	+1.668	-8.069	+1.752	-1.254	-0.657	-0.170	+5.990	.3369
18	+0.3384	+1.785	-10.377	+2.382	-1.531	-1.478	+0.013	+3.698	.3864
19	+0.4058	+1.786	-10.377	+2.382	-1.437	+0.164	+0.021	-0.584	.4224
20	+0.4959	+1.765	-11.207	+2.682	-1.437	+0.360	+0.106	+3.472	.4683
21	+0.6018	+1.588	-11.560	+3.159	-1.508	+0.453	-0.517	-2.146	.4683
22	+0.7316	+1.323	-10.940	+3.632	-2.632	+0.241	-0.340	+3.217	.3994
23	+0.8928	+1.056	-9.950	+3.416	-2.725	+0.329	-0.992	+7.057	.5326
24	+1.0938	+0.910	-9.469	+3.122	-1.592	+0.069	-2.171	+11.677	.8096
25	+1.2904	+0.810	-7.829	+2.059	-2.052	+0.631	-1.879	+9.415	.6100
26	+1.4298	+0.729	-7.316	+1.197	-1.252	+0.339	-2.329	+9.415	.3606
27	+1.4934	+0.578	-6.661	+0.572	-0.773	+0.734	-2.315	+1.280	.3600
28	+1.5178	+0.464	-5.761	+0.491	-0.722	+0.327	-2.001	+3.602	.3691
29	+1.5256	+0.353	-4.608	+0.833	-0.635	+0.748	-1.972	-3.136	.6139
30	+1.5295	+0.272	-4.368	+0.655	-0.581	+0.246	-1.891	+3.610	.5184
31	+1.5323	+0.298	-4.071	-0.832	-0.750	+0.764	-1.841	-3.610	.3540
32	+1.5348	+0.261	-2.266	+0.346	-0.381	+0.025	-2.161	+4.651	.6729
33	+1.5371	+0.261	-0.362	+0.362	-0.432	+0.079	-2.194	+4.695	.5645
34	+1.5410	+0.216	-0.840	+0.196	-0.892	+0.455	-1.945	+1.967	.3301
35	+1.5441	+0.197	-4.082	+0.148	-0.310	+0.480	-2.390	+2.753	.6035
36	+1.5468	+0.177	-4.086	+0.212	-0.359	+0.255	-2.244	+4.620	.7035
37	+1.5493	+0.179	-4.045	+0.009	-0.239	+0.611	-2.310	-1.588	.4829
38	+1.5511	+0.165	-3.569	+0.822	-0.921	-0.819	-1.738	+11.267	.5722
39	+1.5525	+0.160	-3.959	-0.003	-0.519	+0.201	-2.018	+2.252	.4781
40	+1.5537	+0.160	-3.979	+0.049	-0.525	+0.218	-2.044	+2.212	.4307
41	+1.5546	+0.165	-3.779	+0.227	-0.820	+0.749	-1.847	+2.129	.3155
42	+1.5554	+0.126	-3.896	+0.789	-0.690	+0.234	-1.970	+10.809	.5323
43	+1.5560	+0.087	-3.896	+0.789	-0.731	-0.576	-1.987	+0.061	.5323
44	+1.5564	+0.129	-4.148	-0.038	-0.381	+0.571	-2.213	-0.466	.4326
45	+1.5571	+0.150	-3.962	-0.106	-0.534	+0.464	-2.050	+0.850	.3608
46	+1.5574	+0.125	-3.623	-0.224	-0.915	+0.634	-1.783	-4.987	.4562
47	+1.5576	+0.143	-3.845	-0.027	-1.670	-1.921	+0.231	.4266	.4266
48	+1.5575	+0.143	-3.845	-0.027	-1.670	-1.921	+0.231	.4266	.4266

Scan #	b(0) (T)	b(1) (T/m) $\times 10^{-1}$	b(2) (T/m ²) $\times 10^{-2}$	b(3) (T/m ³) $\times 10^{-2}$	b(4) (T/m ⁴) $\times 10^{-4}$	b(5) (T/m ⁵) $\times 10^{-6}$	b(6) (T/m ⁶) $\times 10^{-8}$	b(7) (T/m ⁷) $\times 10^{-9}$	Sigma (Gauss)
49	+1.5578	+1.106	-4.107	+0.445	-0.445	-0.450	-2.071	+7.156	.4816
50	+1.5577	+1.126	-3.896	+0.156	-0.683	+0.916	-1.923	+1.421	.5896
51	+1.5577	+1.132	-4.021	-0.237	-0.553	+0.816	-2.042	-5.338	.5224
52	+1.5573	+1.127	-3.864	+0.337	-0.858	-0.750	-1.785	+2.782	.2631
53	+1.5568	+1.109	-4.132	+0.085	-0.663	-0.750	-1.990	+12.322	.4100
54	+1.5561	+1.121	-3.977	+0.348	-0.846	+0.832	-1.925	+5.369	.3301
55	+1.5555	+1.102	-4.054	+0.613	-0.695	-0.430	-2.012	+10.677	.4580
56	+1.5548	+1.091	-4.016	+0.717	-0.644	-0.489	-2.028	+9.083	.4519
57	+1.5540	+1.114	-4.134	+0.589	-0.493	-0.529	-2.106	+9.352	.4825
58	+1.5531	+1.140	-4.096	+0.223	-0.488	-0.322	-2.120	+9.553	.4825
59	+1.5518	+1.164	-4.109	-0.072	-0.620	-0.694	-1.978	-3.862	.4571
60	+1.5501	+1.139	-4.086	+0.639	-0.646	-0.309	-2.021	+7.533	.5192
61	+1.5483	+1.201	-4.182	+0.276	-0.470	-0.199	-2.196	+5.288	.4087
62	+1.5460	+1.204	-4.439	+0.439	-0.367	-0.254	-2.304	+9.941	.5642
63	+1.5430	+1.200	-4.310	+0.608	-0.446	-0.171	-2.241	+9.157	.5624
64	+1.5399	+1.230	-4.210	+0.332	-0.607	+0.350	-2.028	+2.265	.5255
65	+1.5361	+1.246	-4.122	+0.487	-0.735	+0.844	-1.905	+4.091	.5350
66	+1.5340	+1.281	-4.233	+0.168	-0.726	+0.580	-1.902	-1.366	.6141
67	+1.5318	+1.332	-4.541	+0.087	-0.463	+0.581	-1.945	-0.383	.5272
68	+1.5291	+1.344	-4.613	+0.493	-0.766	+0.020	-1.902	+5.193	.6462
69	+1.5251	+1.412	-5.261	+0.542	-0.606	+0.056	-2.109	+5.489	.3694
70	+1.5166	+1.516	-5.834	+0.652	-0.920	+0.246	-2.002	+4.114	.5011
71	+1.4912	+1.625	-6.905	+1.436	-0.856	-0.536	-2.352	+15.003	.5234
72	+1.4191	+1.856	-8.068	+0.918	-1.028	+0.632	-2.546	+7.865	.4564
73	+1.2722	+1.963	-8.492	+1.209	-2.098	+1.490	-1.838	-7.795	.4053
74	+1.0737	+1.115	-10.099	+2.297	-2.225	+2.784	-1.607	-12.479	.4903
75	+0.8747	+1.277	-10.404	+2.074	-2.708	+1.671	-0.984	-2.305	.7518
76	+0.7177	+1.403	-11.569	+1.381	-2.444	+0.577	-0.453	+4.434	.6045
77	+0.5901	+1.643	-11.844	+2.727	-2.630	+0.972	-0.289	-7.078	.4556
78	+0.4866	+1.769	-10.874	+3.121	-2.630	-0.833	+0.294	+9.176	.4335
79	+0.4020	+1.771	-10.148	+2.408	-0.923	-0.569	+0.116	+5.728	.3083
80	+0.3316	+1.757	-8.696	+1.446	-0.770	-0.349	+0.117	+3.549	.3140
81	+0.2721	+1.609	-7.707	+1.262	-0.361	+0.278	-0.087	-3.286	.2594
82	+0.2210	+1.492	-6.350	+1.111	-0.544	+0.209	+0.193	-3.384	.3666
83	+0.1762	+1.392	-5.067	+0.683	-0.099	+0.450	-0.850	+4.313	.3162
84	+0.1367	+1.271	-5.112	+0.680	-0.145	+0.262	-0.020	-2.205	.3612
85	+0.1016	+1.196	-4.110	+0.421	-0.182	+0.416	+0.067	-3.487	.2922
86	+0.0456	+0.933	-2.922	+0.625	-0.176	-0.347	+0.133	+3.116	.2361
87	+0.0129	+0.551	-1.567	+0.067	+0.076	-0.076	-0.066	+1.665	.3134
88	-0.0008	+0.204	-0.440	+0.111	-0.106	-0.114	+0.099	+1.121	.2961
89	-0.0057	-0.033	-0.235	-0.208	+0.157	+0.179	-0.099	-0.986	.2634
90	-0.0071	-0.073	-0.083	-0.835	+0.065	-0.017	-0.060	-0.253	.3663
91	-0.0071	-0.049	-0.072	-0.263	+0.077	+0.391	-0.039	-3.432	.1989
92	-0.0067	-0.092	+0.024	+0.242	+0.014	-0.391	-0.016	+3.464	.2813
93	-0.0051	-0.050	+0.013	+0.346	+0.022	+0.565	-0.005	-5.690	.3214
94	-0.0054	-0.060	+0.214	+0.050	-0.085	+0.238	+0.469	-3.318	.3181
95	-0.0048	-0.051	-0.136	-0.027	+0.212	+0.023	-0.173	-0.275	.3437
96	-0.0043	-0.090	+0.042	+0.598	+0.022	-0.813	-0.036	+6.870	.3600
97	-0.0038	-0.075	-0.013	+0.562	+0.074	-0.820	-0.080	+7.290	.3051

IX.A.1. Integrated coefficients for 1000 MeV.

The INTEGRALS of the field coefficients*i!* and RMS errors, using an estimated RMS error at each measured point of 4.7 Gauss, are:

```
b(0)= +1.7563E+00+/- 5.3474E-07 T-m  
b(1)= +7.7836E-02+/- 5.3995E-05 T-m/m  
b(2)= -7.5497E+00+/- 4.7070E-03 T-m/m^2  
b(3)= +1.0715E+02+/- 8.6381E-01 T-m/m^3  
b(4)= -1.0501E+04+/- 5.5664E+01 T-m/m^4  
b(5)= +1.6579E+05+/- 1.3116E+04 T-m/m^5  
b(6)= -2.2388E+08+/- 4.2966E+05 T-m/m^6  
b(7)= +5.0496E+09+/- 1.2198E+08 T-m/m^7
```

The coefficients*i!* and RMS errors for the CENTRAL field equal to the above coefficients divided by the effective length of 1.127 m are:

```
b0(0)=+1.5578E+00+/- 4.7431E-07 T  
b0(1)=+6.9039E-02+/- 4.7893E-05 T/m  
b0(2)=-6.6965E+00+/- 4.1751E-03 T/m^2  
b0(3)=+9.5042E+01+/- 7.6619E-01 T/m^3  
b0(4)=-9.3142E+03+/- 4.9373E+01 T/m^4  
b0(5)=+1.4705E+05+/- 1.1634E+04 T/m^5  
b0(6)=-1.9858E+08+/- 3.8110E+05 T/m^6  
b0(7)=+4.4790E+09+/- 1.0820E+08 T/m^7
```

Sigma= .4370 Gauss

IX.A.2. Integrated coefficients for 100 MeV and Y = 0.

The INTEGRALS of the field coefficients*i!* and RMS errors, using an estimated RMS error at each measured point of 2.4 Gauss, are:

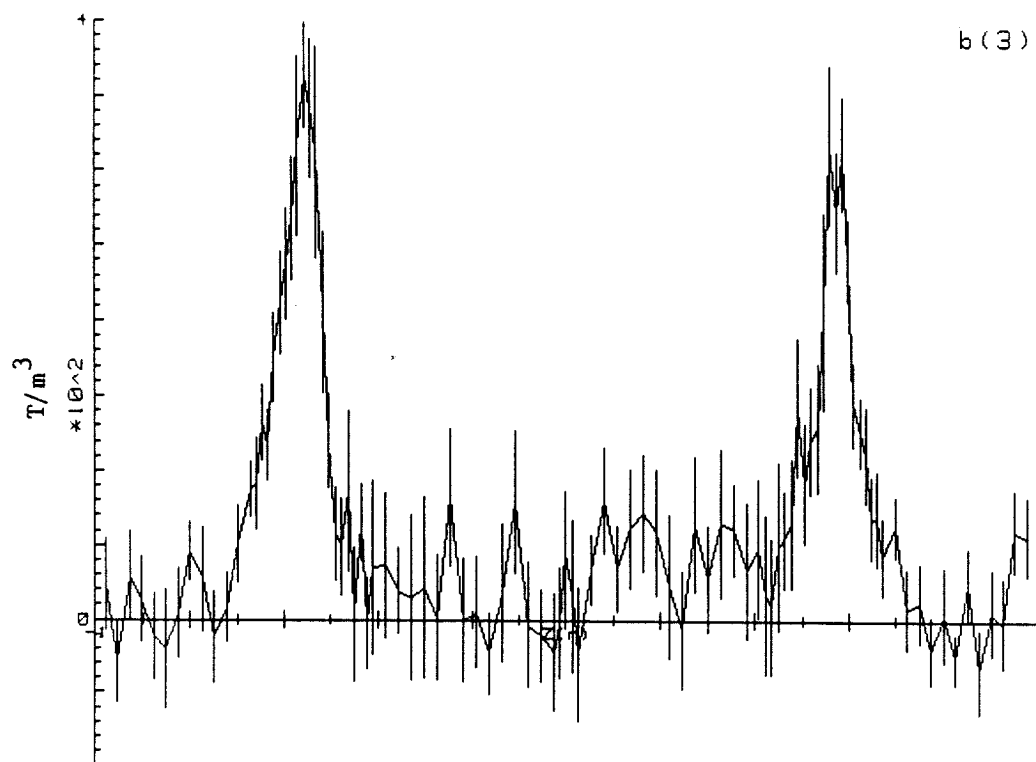
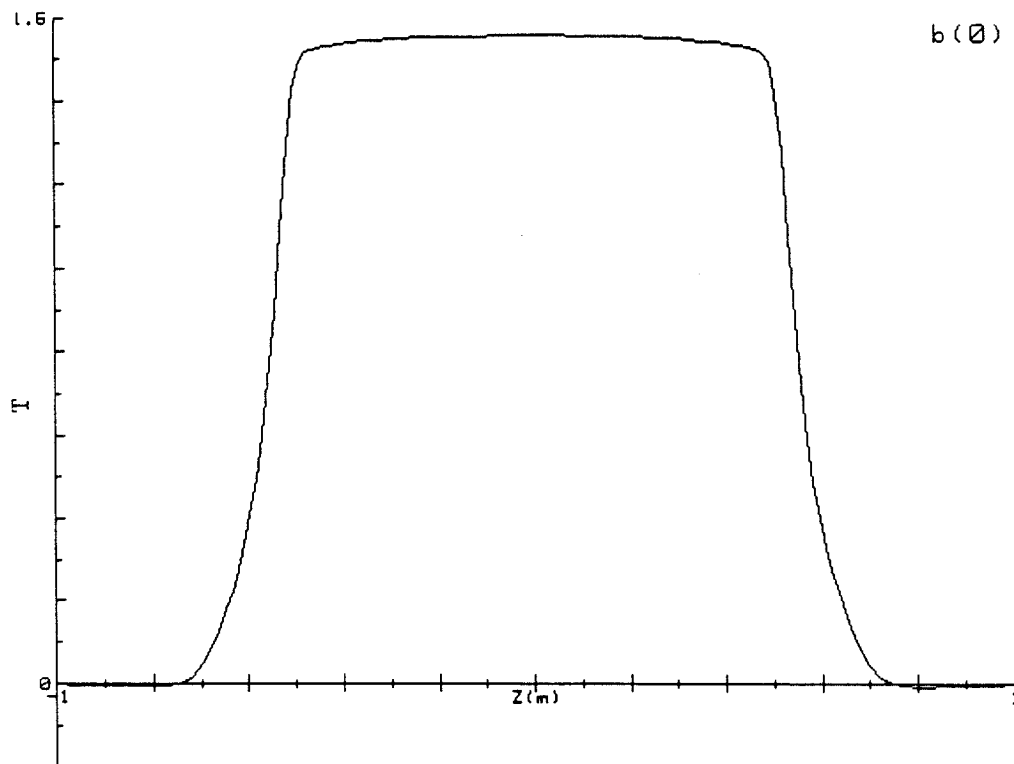
```
b(0)= +1.7449E-01+/- 2.9744E-07 T-m  
b(1)= +3.6049E-03+/- 1.2800E-05 T-m/m  
b(2)= -1.9178E-01+/- 1.3137E-03 T-m/m^2  
b(3)= +8.4180E+00+/- 4.0690E-02 T-m/m^3  
b(4)= -1.0588E+03+/- 6.1564E+00 T-m/m^4
```

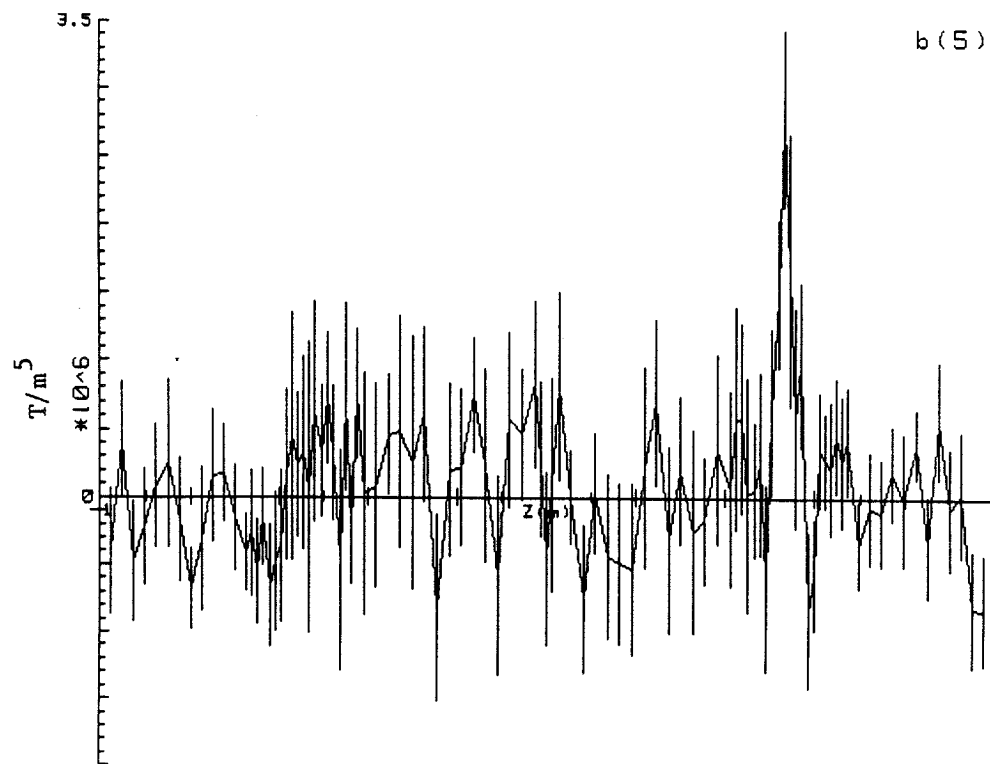
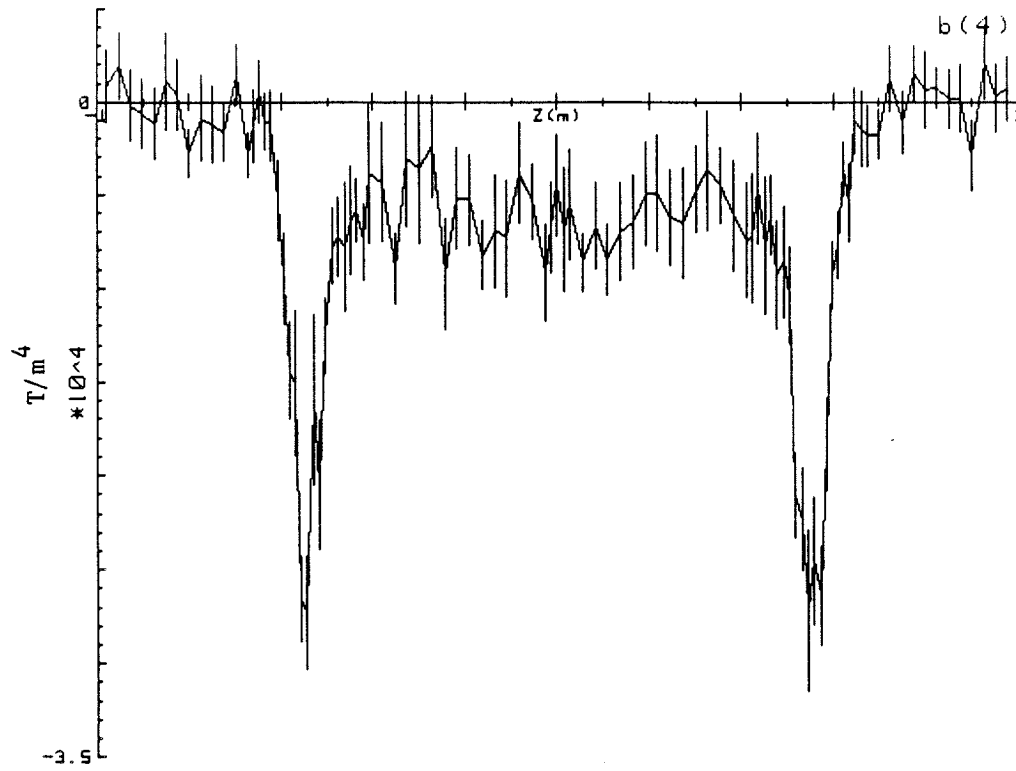
The coefficients*i!* and RMS errors for the CENTRAL field equal to the above coefficients divided by the effective length of 1.141 m are:

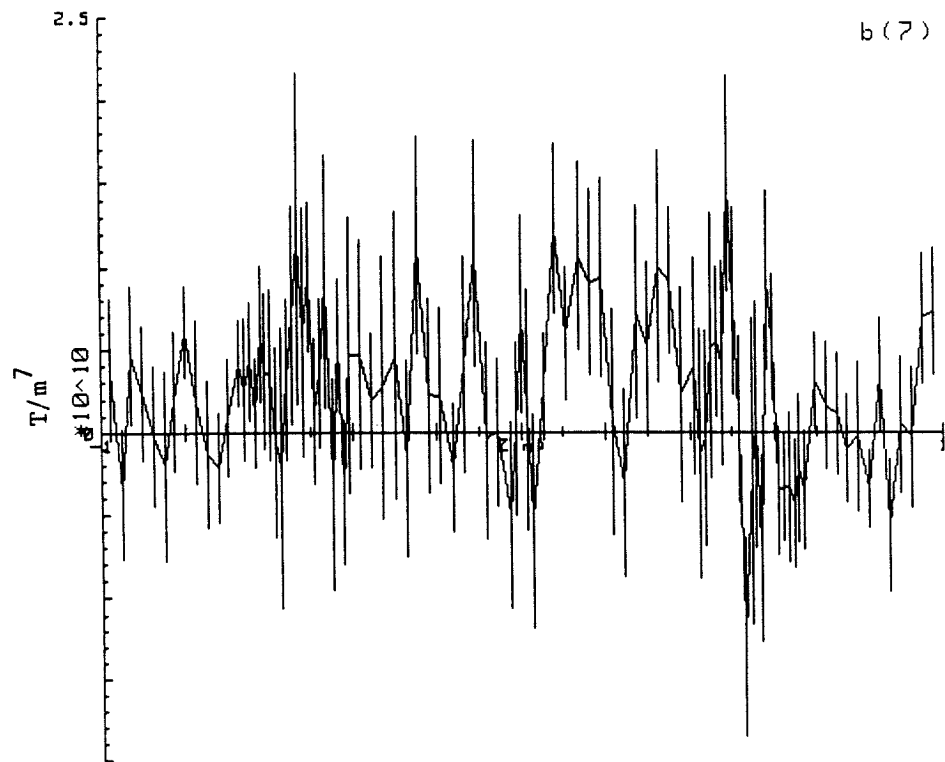
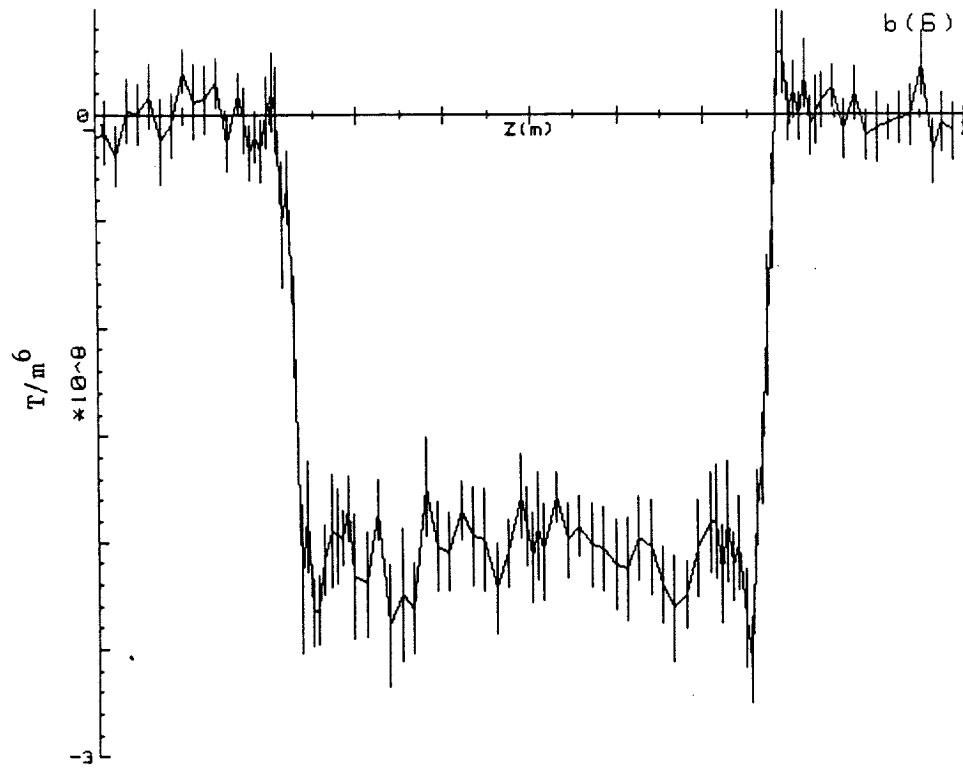
```
b0(0)=+1.5292E-01+/- 2.6067E-07 T  
b0(1)=+3.1592E-03+/- 1.1217E-05 T/m  
b0(2)=-1.6807E-01+/- 1.1513E-03 T/m^2  
b0(3)=+7.3774E+00+/- 3.5660E-02 T/m^3  
b0(4)=-9.2790E+02+/- 5.3954E+00 T/m^4
```

Sigma= .2886 Gauss

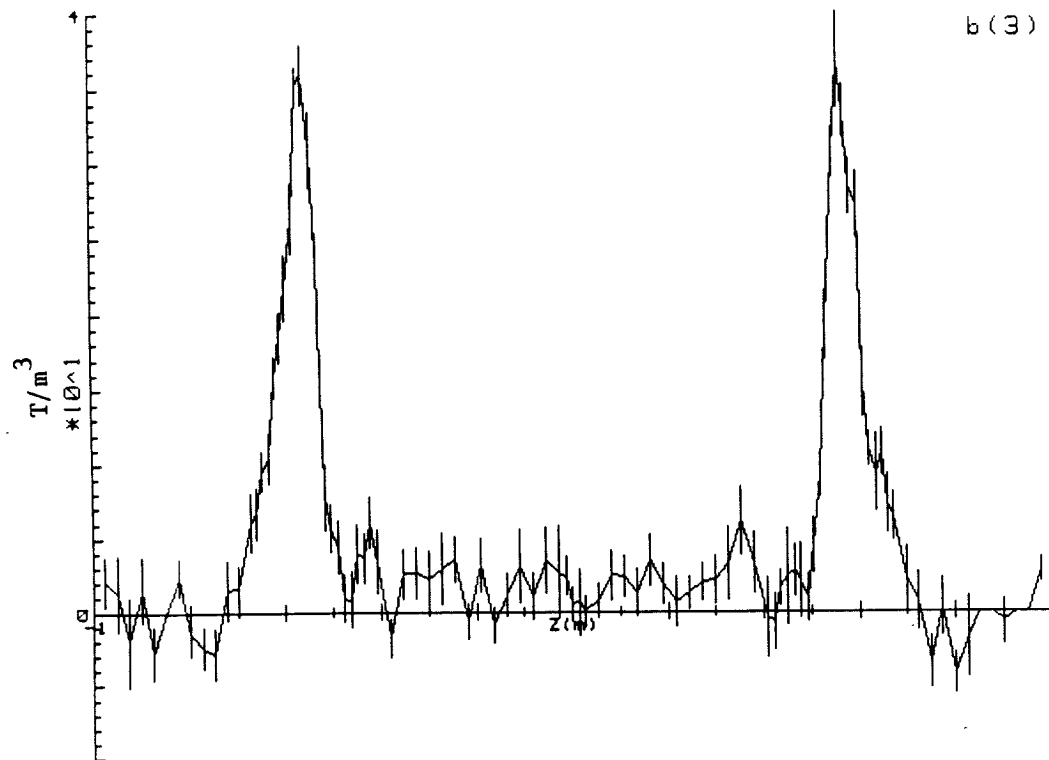
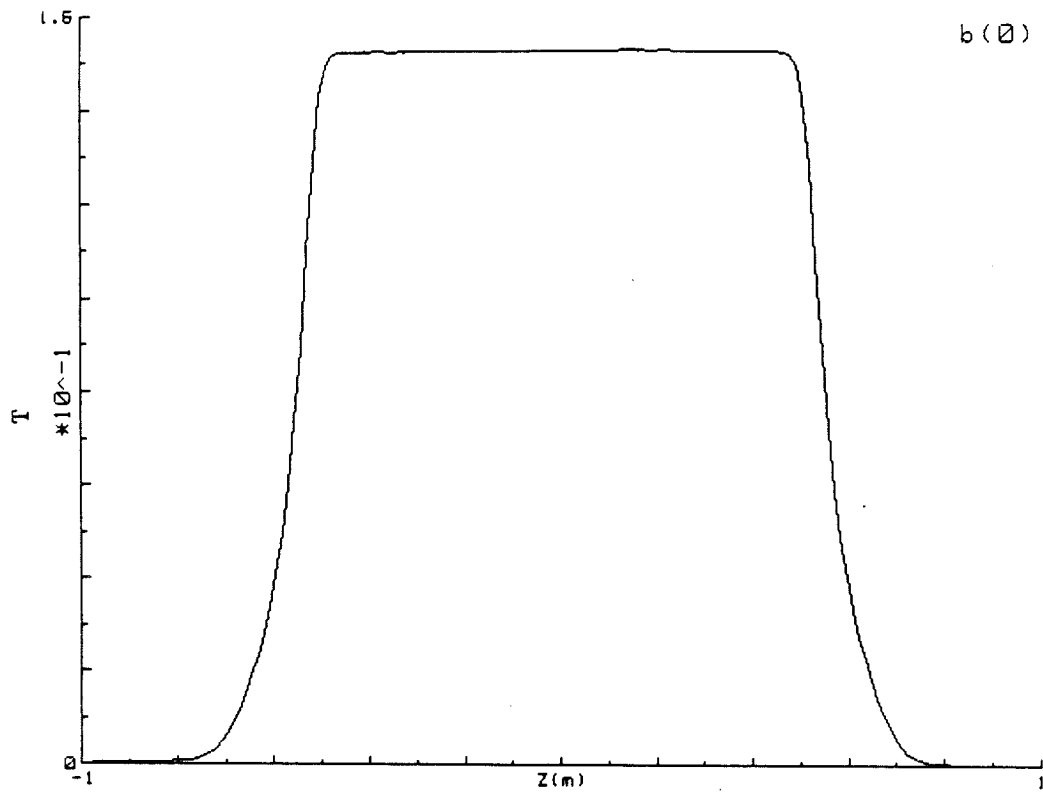
IX.B. Plots of coefficients vs Z at 1000 MeV.

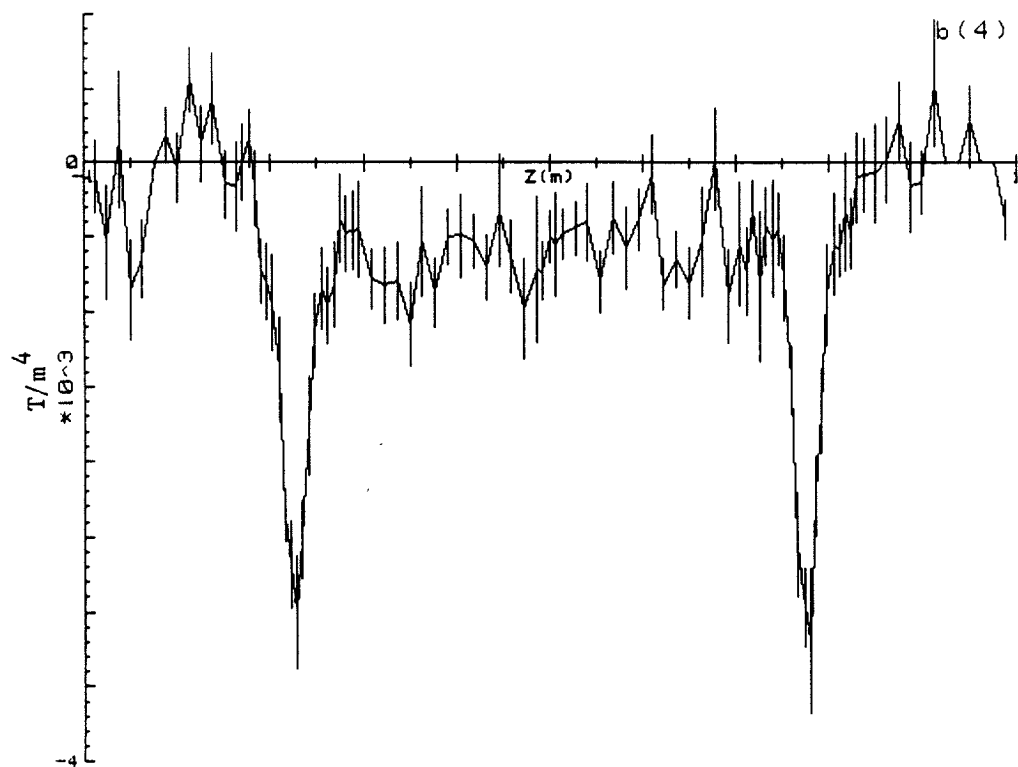






IX.C. Plots of coefficients vs Z at 100 MeV.





X. Vertical midplane.
A. Calculated locations at all scan points.

The following is a list of the data in a TANGENT line section of the scan:

X (in)	Z(in)									
	L(in)= 17.000	L(in)= 16.000	L(in)= 15.000	L(in)= 14.000	L(in)= 13.000	L(in)= 12.000	L(in)= 11.000	L(in)= 10.000	L(in)= 9.000	L(in)= 8.000
-3.000	.0078	.0078	.0074	.0074	.0074	.0074	.0074	.0074	.0074	.0074
-2.500	.0078	.0078	.0074	.0074	.0074	.0074	.0074	.0074	.0074	.0074
-2.000	.0078	.0078	.0074	.0074	.0074	.0074	.0074	.0074	.0074	.0074
-1.750	.0078	.0078	.0074	.0074	.0074	.0074	.0074	.0074	.0074	.0074
-1.500	.0078	.0078	.0074	.0074	.0074	.0074	.0074	.0074	.0074	.0074
-1.250	.0078	.0078	.0074	.0074	.0074	.0074	.0074	.0074	.0074	.0074
-1.000	.0078	.0078	.0074	.0074	.0074	.0074	.0074	.0074	.0074	.0074
0.000	.0078	.0078	.0074	.0074	.0074	.0074	.0074	.0074	.0074	.0074
0.250	.0078	.0078	.0074	.0074	.0074	.0074	.0074	.0074	.0074	.0074
0.500	.0078	.0078	.0074	.0074	.0074	.0074	.0074	.0074	.0074	.0074
1.000	.0078	.0078	.0074	.0074	.0074	.0074	.0074	.0074	.0074	.0074
1.250	.0078	.0078	.0074	.0074	.0074	.0074	.0074	.0074	.0074	.0074
1.500	.0078	.0078	.0074	.0074	.0074	.0074	.0074	.0074	.0074	.0074
1.750	.0078	.0078	.0074	.0074	.0074	.0074	.0074	.0074	.0074	.0074
2.000	.0078	.0078	.0074	.0074	.0074	.0074	.0074	.0074	.0074	.0074
2.500	.0078	.0078	.0074	.0074	.0074	.0074	.0074	.0074	.0074	.0074
3.000	.0078	.0078	.0074	.0074	.0074	.0074	.0074	.0074	.0074	.0074

X (in)	Z(in)									
	L(in)= 9.000	L(in)= 8.000	L(in)= 7.000	L(in)= 6.000	L(in)= 5.000	L(in)= 4.500	L(in)= 4.000	L(in)= 3.500	L(in)= 3.000	L(in)= 2.500
-3.000	.0074	.0074	.0074	.0074	.0074	.0074	.0074	.0074	.0074	.0074
-2.500	.0074	.0074	.0074	.0074	.0074	.0074	.0074	.0074	.0074	.0074
-2.000	.0074	.0074	.0074	.0074	.0074	.0074	.0074	.0074	.0074	.0074
-1.750	.0074	.0074	.0074	.0074	.0074	.0074	.0074	.0074	.0074	.0074
-1.500	.0074	.0074	.0074	.0074	.0074	.0074	.0074	.0074	.0074	.0074
-1.250	.0074	.0074	.0074	.0074	.0074	.0074	.0074	.0074	.0074	.0074
-1.000	.0074	.0074	.0074	.0074	.0074	.0074	.0074	.0074	.0074	.0074
0.000	.0074	.0074	.0074	.0074	.0074	.0074	.0074	.0074	.0074	.0074
0.250	.0074	.0074	.0074	.0074	.0074	.0074	.0074	.0074	.0074	.0074
0.500	.0074	.0074	.0074	.0074	.0074	.0074	.0074	.0074	.0074	.0074
1.000	.0074	.0074	.0074	.0074	.0074	.0074	.0074	.0074	.0074	.0074
1.250	.0074	.0074	.0074	.0074	.0074	.0074	.0074	.0074	.0074	.0074
1.500	.0074	.0074	.0074	.0074	.0074	.0074	.0074	.0074	.0074	.0074
1.750	.0074	.0074	.0074	.0074	.0074	.0074	.0074	.0074	.0074	.0074
2.000	.0074	.0074	.0074	.0074	.0074	.0074	.0074	.0074	.0074	.0074
2.500	.0074	.0074	.0074	.0074	.0074	.0074	.0074	.0074	.0074	.0074
3.000	.0074	.0074	.0074	.0074	.0074	.0074	.0074	.0074	.0074	.0074

The following is a list of the data in the ARC section of the scan:

X (in)	Z(in)									
	T(deg)= 15.000	T(deg)= 14.625	T(deg)= 14.250	T(deg)= 13.875	T(deg)= 13.500	T(deg)= 13.125	T(deg)= 12.750	T(deg)= 12.375		
-3.000	.0434	-.0029	-.0095	-.0122	-.0142	-.0140	-.0127	-.0130		
-2.500	-.1300	.0143	-.0006	-.0059	-.0036	-.0010	.0009	.0019		
-2.000	-.0507	.0593	-.0055	-.0026	.0014	.0113	.0301	.0310		
-1.750	-.0424	.1084	.0068	-.0021	.0026	.0153	.0348	.0348		
-1.500	-.0380	.2042	.0080	-.0027	.0028	.0184	.0392	.0525		
-1.250	-.0341	.4486	.0083	-.0026	.0024	.0186	.0459	.0605		
-1.000	-.0320	.6846	.0082	-.0025	.0031	.0198	.0452	.0859		
-.750	-.0300	.6844	.0085	-.0025	.0037	.0215	.0609	.0998		
-.500	-.0294	.6514	.0091	-.0023	.0033	.0223	.0583	.1142		
-.250	-.0282	.4886	.0088	-.0022	.0037	.0218	.0616	.1363		
0.000	-.0268	.4289	.0085	-.0014	.0039	.0210	.0627	.1281		
.250	-.0264	.3882	.0087	-.0015	.0051	.0231	.0642	.1339		
.500	-.0261	.3916	.0092	-.0007	.0052	.0260	.0628	.1301		
.750	-.0252	.3926	.0094	-.0004	.0059	.0270	.0665	.1299		
1.000	-.0255	.4362	.0095	.0004	.0064	.0298	.0651	.1094		
1.250	-.0263	.5382	.0097	.0007	.0078	.0308	.0602	.0872		
1.500	-.0266	.6831	.0103	.0010	.0090	.0315	.0545	.0704		
1.750	-.0285	.6829	.0106	.0019	.0101	.0309	.0456	.0522		
2.000	-.0308	.6805	.0109	.0029	.0118	.0303	.0256	.0268		
2.500	-.0400	.1305	.0107	.0041	.0126	.0227	.0256	.0268		
3.000	-.0555	.0523	.0079	.0043	.0086	.0104	.0109	.0102		

X (in)	Z(in)									
	T(deg)= 6.750	T(deg)= 6.000	T(deg)= 5.250	T(deg)= 4.500	T(deg)= 3.750	T(deg)= 3.000	T(deg)= 2.250	T(deg)= 1.500		
-3.000	-.0094	-.0093	-.0097	-.0108	-.0104	-.0128	-.0097	-.0084		
-2.500	.0044	.0041	.0033	.0026	.0035	.0006	.0047	.0054		
-2.000	.0442	.0261	.0250	.0257	.0260	.0241	.0294	.0314		
-1.750	.0425	.0436	.0436	.0452	.0441	.0406	.0479	.0475		
-1.500	.0356	.0407	.0407	.0431	.0421	.0368	.0472	.0474		
-1.250	.0397	.0404	.0401	.0431	.0425	.0368	.0472	.0474		
-1.000	.0328	.0399	.0399	.0431	.0425	.0368	.0472	.0474		
-.750	.0264	.0349	.0349	.0431	.0425	.0368	.0472	.0474		
-.500	.0248	.0328	.0328	.0431	.0425	.0368	.0472	.0474		
-.250	.0229	.0308	.0308	.0431	.0425	.0368	.0472	.0474		
0.000	.0217	.0293	.0293	.0431	.0425	.0368	.0472	.0474		
.250	.0207	.0287	.0287	.0431	.0425	.0368	.0472	.0474		
.500	.0198	.0277	.0277	.0431	.0425	.0368	.0472	.0474		
.750	.0188	.0267	.0267	.0431	.0425	.0368	.0472	.0474		
1.000	.0178	.0257	.0257	.0431	.0425	.0368	.0472	.0474		
1.250	.0168	.0247	.0247	.0431	.0425	.0368	.0472	.0474		
1.500	.0158	.0237	.0237	.0431	.0425	.0368	.0472	.0474		
1.750	.0148	.0227	.0227	.0431	.0425	.0368	.0472	.0474		
2.000	.0138	.0217	.0217	.0431	.0425	.0368	.0472	.0474		
2.500	.0128	.0207	.0207	.0431	.0425	.0368	.0472	.0474		
3.000	.0118	.0197	.0197	.0431	.0425	.0368	.0472	.0474		

Z(in)

X (in)	Z(in)									
	T(deg)= 6.750	T(deg)= 6.000	T(deg)= 5.250	T(deg)= 4.500	T(deg)= 3.750	T(deg)= 3.000	T(deg)= 2.250	T(deg)= 1.500		
-3.000	-.0002	-.0002	-.0002	-.0002	-.0002	-.0002	-.0002	-.0002		
-2.500	.0065	.0065	.0065	.0065	.0065	.0065	.0065	.0065		
-2.000	.0315	.0298	.0298	.0315	.0298	.0298	.0315	.0298		
-1.750	.0520	.0494	.0494	.0520	.0494	.0494	.0520	.0494		
-1.500	.0789	.0721	.0721	.0789	.0721	.0721	.0789	.0721		
-1.250	.1251	.1166	.1166	.1251	.1166	.1166	.1251	.1166		
-1.000	.1690	.1427	.1427	.1690	.1427	.1427	.1690	.1427		
-.750	.2220	.1880	.1880	.2220	.1880	.1880	.2220	.1880		
-.500	.2636	.2070	.2070	.2636	.2070	.2070	.2636	.2070		
-.250	.2967	.2304	.2304	.2967	.2304	.2304	.2967	.2304		
0.000	.3178	.2455	.2455	.3178	.2455	.2455	.3178	.2455		
.250	.3281	.2555	.2555	.3281	.2555	.2555	.3281	.2555		
.500	.3384	.2658	.2658	.3384	.2658	.2658	.3384	.2658		
.750	.3487	.2761	.2761	.3487	.2761	.2761	.3487	.2761		
1.000	.3590	.2864	.2864	.3590	.2864	.2864	.3590	.2864		
1.250	.3693	.2967	.2967	.3693	.2967	.2967	.3693	.2967		
1.500	.3796	.3070	.3070	.3796	.3070	.3070	.3796	.3070		
1.750	.3899	.3173	.3173	.3899	.3173	.3173	.3899	.3173		
2.000	.3999	.3276	.3276	.3999	.3276	.3276	.3999	.3276		
2.500	.4099	.3379	.3379	.4099	.3379	.3379	.4099	.3379		
3.000	.4199	.3482	.3482	.4199	.3482	.3482	.4199	.3482		

Z(in)

The following is a list of the data in the ARC section of the scan:

X (in)	T(deg)= 0.000	T(deg)= -0.375	T(deg)= -0.750	T(deg)= -1.500	T(deg)= -2.250	T(deg)= -3.000	T(deg)= -3.750	T(deg)= -4.500
-3.000	-0.0098	-0.0114	-0.0115	-0.0139	-0.0149	-0.0155	-0.0127	-0.0122
-2.500	-0.0095	-0.0023	-0.0037	-0.0064	-0.0078	-0.0087	-0.0060	-0.0055
-2.000	-0.0127	-0.0111	-0.0091	-0.0035	-0.0006	-0.0008	-0.0013	-0.0036
-1.750	-0.0184	-0.0180	-0.0116	-0.0103	-0.0055	-0.0000	-0.0034	-0.0067
-1.500	-0.0284	-0.0298	-0.0205	-0.0194	-0.0081	-0.0022	-0.0090	-0.0034
-1.250	-0.0327	-0.0389	-0.0293	-0.0228	-0.0170	-0.0093	-0.0109	-0.0172
-1.000	-0.0516	-0.0621	-0.0366	-0.0311	-0.0185	-0.0033	-0.0212	-0.0200
-0.750	-0.0496	-0.0680	-0.0370	-0.0324	-0.0333	-0.0088	-0.0010	-0.0246
-0.500	-0.0742	-0.0783	-0.0371	-0.0402	-0.0334	-0.0127	-0.0168	-0.0443
-0.250	-0.0553	-0.0810	-0.0392	-0.0176	-0.0020	-0.0362	-0.0102	-0.0076
0.000	-0.0634	-0.0838	-0.0409	-0.0035	-0.0170	-0.0452	-0.0110	-0.0126
0.250	-0.0672	-0.0532	-0.0268	-0.0067	-0.0122	-0.0453	-0.0147	-0.0056
0.500	-0.0398	-0.0312	-0.0064	-0.0139	-0.0201	-0.0816	-0.0156	-0.0021
0.750	-0.0406	-0.0481	-0.0111	-0.0090	-0.0219	-0.0543	-0.0156	-0.0037
1.000	-0.0316	-0.0145	-0.0171	-0.0100	-0.0085	-0.0359	-0.0153	-0.0171
1.250	-0.0254	-0.0250	-0.0113	-0.0095	-0.0087	-0.0162	-0.0037	-0.0111
1.500	-0.0216	-0.0125	-0.0030	-0.0002	-0.0009	-0.0088	-0.0015	-0.0015
1.750	-0.0117	-0.0078	-0.0033	-0.0046	-0.0054	-0.0143	-0.0077	-0.0058
2.000	-0.0073	-0.0030	-0.0024	-0.0042	-0.0060	-0.0114	-0.0047	-0.0093
2.500	-0.0022	-0.0009	-0.0015	-0.0058	-0.0058	-0.0053	-0.0047	-0.0040
3.000	-0.0007	-0.0022	-0.0033	-0.0043	-0.0039	-0.0009	-0.0014	-0.0012

X (in)	T(deg)= -11.250	T(deg)= -11.625	T(deg)= -12.000	T(deg)= -12.375	T(deg)= -12.750	T(deg)= -13.125	T(deg)= -13.500	T(deg)= -13.875
-3.000	-0.0151	-0.0150	-0.0151	-0.0155	-0.0146	-0.0144	-0.0126	-0.0132
-2.500	-0.0066	-0.0068	-0.0065	-0.0078	-0.0079	-0.0072	-0.0076	-0.0093
-2.000	-0.0005	-0.0016	-0.0013	-0.0005	-0.0006	-0.0008	-0.0039	-0.0067
-1.750	-0.0038	-0.0090	-0.0068	-0.0043	-0.0019	-0.0008	-0.0032	-0.0063
-1.500	-0.0054	-0.0121	-0.0112	-0.0051	-0.0051	-0.0014	-0.0028	-0.0056
-1.250	-0.0036	-0.0249	-0.0169	-0.0088	-0.0070	-0.0003	-0.0027	-0.0050
-1.000	-0.0079	-0.0209	-0.0160	-0.0127	-0.0072	-0.0018	-0.0015	-0.0046
-0.750	-0.0053	-0.0356	-0.0188	-0.0117	-0.0049	-0.0005	-0.0015	-0.0042
-0.500	-0.0002	-0.0223	-0.0223	-0.0065	-0.0043	-0.0004	-0.0019	-0.0036
-0.250	-0.0167	-0.0344	-0.0260	-0.0009	-0.0091	-0.0009	-0.0018	-0.0032
0.000	-0.0146	-0.0269	-0.0145	-0.0005	-0.0013	-0.0015	-0.0010	-0.0032
0.250	-0.0446	-0.0121	-0.0045	-0.0062	-0.0023	-0.0014	-0.0014	-0.0029
0.500	-0.0535	-0.0067	-0.0097	-0.0186	-0.0077	-0.0039	-0.0016	-0.0026
0.750	-0.0617	-0.0182	-0.0265	-0.0303	-0.0060	-0.0034	-0.0018	-0.0025
1.000	-0.0580	-0.0385	-0.0280	-0.0371	-0.0124	-0.0051	-0.0017	-0.0028
1.250	-0.0467	-0.0318	-0.0291	-0.0274	-0.0124	-0.0031	-0.0027	-0.0029
1.500	-0.0268	-0.0197	-0.0200	-0.0259	-0.0159	-0.0060	-0.0025	-0.0030
1.750	-0.0244	-0.0177	-0.0193	-0.0242	-0.0140	-0.0055	-0.0030	-0.0034
2.000	-0.0139	-0.0152	-0.0131	-0.0168	-0.0127	-0.0058	-0.0038	-0.0037
2.500	-0.0084	-0.0092	-0.0075	-0.0084	-0.0053	-0.0050	-0.0033	-0.0036
3.000	-0.0035	-0.0037	-0.0025	-0.0031	-0.0021	-0.0017	-0.0006	-0.0017

X (in)	T(deg)= -14.250	T(deg)= -14.625	T(deg)= -15.000
-3.000	-0.0140	-0.0234	-0.0360
-2.500	-0.0107	-0.0221	-0.0866
-2.000	-0.0087	-0.0310	-0.2310
-1.750	-0.0072	-0.0402	-0.4140
-1.500	-0.0070	-0.0591	-0.6105
-1.250	-0.0068	-0.0452	-0.8081
-1.000	-0.0068	-0.0253	-0.9065
-0.750	-0.0055	-0.0159	-0.9047
-0.500	-0.0052	-0.0139	-0.8471
-0.250	-0.0053	-0.0079	-0.8041
0.000	-0.0053	-0.0067	-0.8037
0.250	-0.0048	-0.0021	-0.8036
0.500	-0.0048	-0.0031	-0.8031
0.750	-0.0054	-0.0042	-0.8040
1.000	-0.0048	-0.0069	-0.8040
1.250	-0.0045	-0.0076	-0.8037
1.500	-0.0044	-0.0044	-0.8043
1.750	-0.0046	-0.0157	-0.8043
2.000	-0.0047	-0.0349	-0.8042
2.500	-0.0038	-0.0163	-0.8041
3.000	-0.0021	-0.0017	-0.8025

X (in)	T(deg)= -5.250	T(deg)= -6.000	T(deg)= -6.750	T(deg)= -7.500	T(deg)= -8.250	T(deg)= -9.000	T(deg)= -9.750	T(deg)= -10.500
-3.000	-0.0125	-0.0129	-0.0135	-0.0140	-0.0144	-0.0164	-0.0160	-0.0157
-2.500	-0.0048	-0.0055	-0.0049	-0.0044	-0.0058	-0.0077	-0.0071	-0.0068
-2.000	-0.0020	-0.0039	-0.0039	-0.0072	-0.0069	-0.0051	-0.0039	-0.0015
-1.750	-0.0073	-0.0046	-0.0090	-0.0112	-0.0111	-0.0090	-0.0099	-0.0057
-1.500	-0.0117	-0.0093	-0.0159	-0.0213	-0.0167	-0.0141	-0.0142	-0.0043
-1.250	-0.0168	-0.0107	-0.0154	-0.0308	-0.0154	-0.0202	-0.0178	-0.0085
-1.000	-0.0244	-0.0216	-0.0206	-0.0387	-0.0327	-0.0192	-0.0271	-0.0111
-0.750	-0.0282	-0.0416	-0.0286	-0.0414	-0.0329	-0.0265	-0.0223	-0.0054
-0.500	-0.0219	-0.0080	-0.0289	-0.0716	-0.0412	-0.0287	-0.0430	-0.0248
-0.250	-0.0212	-0.0068	-0.0344	-0.0428	-0.0038	-0.0336	-0.0280	-0.0210
0.000	-0.0304	-0.0095	-0.0172	-0.0317	-0.0193	-0.0066	-0.0335	-0.0088
0.250	-0.0174	-0.0076	-0.0034	-0.0056	-0.0339	-0.0161	-0.0058	-0.0068
0.500	-0.0174	-0.0178	-0.0072	-0.0072	-0.0164	-0.0225	-0.0101	-0.0097
0.750	-0.0191	-0.0367	-0.0027	-0.0125	-0.0389	-0.0102	-0.0177	-0.0079
1.000	-0.0088	-0.0134	-0.0082	-0.0082	-0.0291	-0.0233	-0.0118	-0.0059
1.250	-0.0115	-0.0175	-0.0066	-0.0096	-0.0242	-0.0221	-0.0176	-0.0079
1.500	-0.0065	-0.0051	-0.0072	-0.0072	-0.0138	-0.0121	-0.0101	-0.0061
1.750	-0.0085	-0.0061	-0.0046	-0.0077	-0.0144	-0.0073	-0.0096	-0.0069
2.000	-0.0077	-0.0079	-0.0058	-0.0078	-0.0089	-0.0068	-0.0049	-0.0069
2.500	-0.0041	-0.0052	-0.0035	-0.0046	-0.0089	-0.0052	-0.0057	-0.0086
3.000	-0.0014	-0.0018	-0.0009	-0.0014	-0.0009	-0.0012	-0.0029	-0.0038

The following is a list of the data in the TANGENT line sections of the scan:

X (in)	Z(in)									
	L(in)=-5.000	L(in)=-4.500	L(in)=-4.000	L(in)=-3.500	L(in)=-3.000	L(in)=-2.500	L(in)=-2.000	L(in)=-1.500	L(in)=-1.000	L(in)=-.500
-3.000	.0904	.0752	.0508	.0217	.0086	-.0086	-.0233	-.0425	-.0694	-.0958
-2.500	.0384	.0332	.0207	.0207	-.0086	-.0233	-.0425	-.0694	-.0958	-.1298
-2.000	.0158	.0219	.0226	.0143	.0052	-.0127	-.0320	-.0549	-.0824	-.1182
-1.750	.0114	.0168	.0181	.0154	.0035	-.0127	-.0320	-.0549	-.0824	-.1182
-1.500	.0079	.0132	.0161	.0130	.0050	-.0085	-.0320	-.0549	-.0824	-.1182
-1.250	.0064	.0110	.0146	.0121	.0049	-.0083	-.0253	-.0477	-.0787	-.1064
-1.000	.0038	.0095	.0118	.0121	.0064	-.0047	-.0201	-.0364	-.0564	-.0787
-.750	.0040	.0077	.0112	.0143	.0053	-.0036	-.0149	-.0349	-.0549	-.0787
-.500	.0035	.0073	.0116	.0135	.0052	-.0036	-.0149	-.0349	-.0549	-.0787
-.250	.0036	.0072	.0124	.0141	.0066	-.0033	-.0121	-.0320	-.0549	-.0787
0.000	.0031	.0069	.0116	.0151	.0063	-.0031	-.0101	-.0300	-.0549	-.0787
.250	.0035	.0088	.0113	.0148	.0078	-.0040	-.0063	-.0332	-.0549	-.0787
.500	.0038	.0085	.0121	.0146	.0093	-.0053	-.0085	-.0311	-.0549	-.0787
.750	.0041	.0095	.0126	.0143	.0093	-.0053	-.0085	-.0311	-.0549	-.0787
1.000	.0040	.0095	.0130	.0134	.0099	-.0059	-.0082	-.0328	-.0549	-.0787
1.250	.0047	.0097	.0126	.0133	.0099	-.0059	-.0082	-.0328	-.0549	-.0787
1.500	.0047	.0092	.0124	.0121	.0085	-.0054	-.0054	-.0235	-.0549	-.0787
1.750	.0044	.0092	.0120	.0108	.0074	-.0047	-.0050	-.0202	-.0549	-.0787
2.000	.0050	.0101	.0116	.0108	.0070	-.0042	-.0042	-.0217	-.0549	-.0787
2.500	.0058	.0097	.0093	.0075	.0037	-.0023	-.0023	-.0234	-.0549	-.0787
3.000	.0048	.0087	.0080	.0048	.0021	-.0006	-.0006	-.0243	-.0549	-.0787

X (in)	Z(in)									
	L(in)=-12.000	L(in)=-13.000	L(in)=-14.000	L(in)=-15.000	L(in)=-16.000	L(in)=-17.000	L(in)=-18.000	L(in)=-19.000	L(in)=-20.000	L(in)=-21.000
-3.000	.3700	-.1897	.6848	.0048	.0052	.0052	.0052	.0052	.0052	.0052
-2.500	.3223	.6511	.6846	.6430	.6388	.6388	.6388	.6388	.6388	.6388
-2.000	.6554	.6530	.6481	.6025	.4995	.4970	.4970	.4970	.4970	.4970
-1.750	.6842	.6530	.6061	.5824	.6849	.6849	.6849	.6849	.6849	.6849
-1.500	.6553	.6842	.6844	.6844	.6844	.6844	.6844	.6844	.6844	.6844
-1.250	.6841	.6541	.6499	.6032	.6403	.6403	.6403	.6403	.6403	.6403
-1.000	.6841	.6841	.6498	.6844	.6844	.6844	.6844	.6844	.6844	.6844
-.750	.6839	.6552	.6511	.6511	.6511	.6511	.6511	.6511	.6511	.6511
-.500	.6839	.6558	.6558	.6558	.6558	.6558	.6558	.6558	.6558	.6558
-.250	.6839	.6557	.6557	.6557	.6557	.6557	.6557	.6557	.6557	.6557
0.000	.4104	.5115	.5319	.6465	.5011	.6370	.6370	.6370	.6370	.6370
.250	.6836	.6569	.6518	.6518	.6518	.6518	.6518	.6518	.6518	.6518
.500	.6834	.6579	.6531	.6531	.6531	.6531	.6531	.6531	.6531	.6531
.750	.6834	.6579	.6531	.6531	.6531	.6531	.6531	.6531	.6531	.6531
1.000	.6834	.6579	.6531	.6531	.6531	.6531	.6531	.6531	.6531	.6531
1.250	.6834	.6579	.6531	.6531	.6531	.6531	.6531	.6531	.6531	.6531
1.500	.6834	.6579	.6531	.6531	.6531	.6531	.6531	.6531	.6531	.6531
1.750	.6834	.6579	.6531	.6531	.6531	.6531	.6531	.6531	.6531	.6531
2.000	.6834	.6579	.6531	.6531	.6531	.6531	.6531	.6531	.6531	.6531
2.500	.6834	.6579	.6531	.6531	.6531	.6531	.6531	.6531	.6531	.6531
3.000	.6834	.6579	.6531	.6531	.6531	.6531	.6531	.6531	.6531	.6531

X (in)	Z(in)									
	L(in)=-4.500	L(in)=-5.000	L(in)=-5.500	L(in)=-6.000	L(in)=-6.500	L(in)=-7.000	L(in)=-7.500	L(in)=-8.000	L(in)=-8.500	L(in)=-9.000
-3.000	-.2873	-.2199	-.0709	.0569	.1358	.1958	.2981	.4298	.5107	.6429
-2.500	-.2163	-.1888	-.0861	.0411	.1241	.1803	.3047	.4367	.5107	.6429
-2.000	-.1547	-.1759	-.0916	.0284	.1168	.1801	.3470	.4527	.5107	.6429
-1.750	-.1444	-.1592	-.0919	.0221	.1037	.1919	.3548	.4527	.5107	.6429
-1.500	-.1307	-.1476	-.0937	.0202	.0965	.1782	.3586	.4527	.5107	.6429
-1.250	-.1204	-.1404	-.0905	.0141	.0814	.1626	.3586	.4527	.5107	.6429
-1.000	-.1088	-.1346	-.0894	.0137	.0840	.1510	.3586	.4527	.5107	.6429
-.750	-.0994	-.1250	-.0873	.0088	.0847	.1642	.3586	.4527	.5107	.6429
-.500	-.0910	-.1186	-.0854	.0084	.0846	.1599	.3586	.4527	.5107	.6429
-.250	-.0842	-.1135	-.0842	.0089	.0842	.1599	.3586	.4527	.5107	.6429
0.000	-.0798	-.1108	-.0811	.0094	.0799	.1299	.3586	.4527	.5107	.6429
.250	-.0735	-.1076	-.0801	.0075	.0763	.1530	.3586	.4527	.5107	.6429
.500	-.0685	-.1009	-.0788	.0074	.0762	.1389	.3586	.4527	.5107	.6429
.750	-.0630	-.0983	-.0760	.0070	.0763	.1243	.3586	.4527	.5107	.6429
1.000	-.0580	-.0912	-.0763	.0070	.0763	.1143	.3586	.4527	.5107	.6429
1.250	-.0580	-.0932	-.0731	.0069	.0763	.1213	.3586	.4527	.5107	.6429
1.500	-.0557	-.0983	-.0726	.0093	.0723	.1317	.3586	.4527	.5107	.6429
1.750	-.0547	-.0954	-.0701	.0104	.0735	.1221	.3586	.4527	.5107	.6429
2.000	-.0538	-.0928	-.0701	.0109	.0735	.1250	.3586	.4527	.5107	.6429
2.500	-.0523	-.0889	-.0676	.0115	.0666	.1313	.3586	.4527	.5107	.6429
3.000	-.0542	-.0791	-.0661	.0154	.0777	.1220	.3586	.4527	.5107	.6429

X.B. Fit coefficients on each radial scan.

Scan #	A(0) (mm)	A(1) (mm/mm) *10 ⁻²	Sigma (mm)	Scan #	A(0) (mm)	A(1) (mm/mm) *10 ⁻²	Sigma (mm)
1	-3.6487	-2.320	4.6565	49	+0.9435	-.325	.5244
2	-2.8345	+5.109	5.4613	50	+0.9966	-.673	.6850
3	-3.5696	+1.701	8.6994	51	+0.5350	-.582	.3978
4	-6.5728	+.659	7.2880	52	+0.2467	-.714	.3295
5	-5.7294	-.639	8.3241	53	+0.0648	-.623	.3308
6	-5.3514	+5.489	4.2867	54	-0.5168	-.829	.6065
7	-2.8604	+2.022	1.4086	55	-0.0119	-.499	.2581
8	-2.0952	+1.750	.4537	56	+0.1450	-.742	.3173
9	-1.3341	+1.071	.2148	57	+0.1238	-.799	.3435
10	-0.7462	+1.002	.1356	58	-0.0617	-.793	.2781
11	-0.6720	-.142	.0527	59	+0.1733	-.716	.2969
12	-1.5440	-1.618	.0874	60	+0.3699	-1.136	.5238
13	-1.4325	-2.475	.3904	61	+0.0008	-1.276	.4913
14	-0.8752	-1.932	.4432	62	+0.1120	-.959	.3743
15	-0.4372	-1.252	.4294	63	+0.2277	-.887	.4684
16	-0.1820	-1.075	.2760	64	-0.7069	-1.541	.5928
17	-0.2432	-.624	.2159	65	-0.4988	-1.333	.4764
18	+0.0134	-.190	.1333	66	+0.0778	-1.250	.4528
19	+0.0136	+.078	.0760	67	-0.0244	-1.101	.3432
20	+0.0326	+.127	.0484	68	-0.2058	-1.058	.2511
21	-0.1088	+.146	.0194	69	-0.0606	-.581	.1265
22	-0.4603	+.274	.0325	70	-0.0732	-.148	.0373
23	-0.7877	+.404	.1219	71	-0.0567	+.009	.0207
24	+0.7474	-.318	13.6543	72	-0.0990	+.083	.0201
25	+0.2242	+.098	.0136	73	-0.1436	+.085	.0144
26	-0.0249	+.130	.0178	74	-0.7155	+4.222	3.6409
27	+0.1317	+.220	.0261	75	+0.1668	-.286	.0952
28	+0.5906	+.438	.0348	76	+0.1402	-.158	.0705
29	+1.3463	+.692	.2743	77	+0.2642	-.170	.0806
30	+2.3102	+1.097	.8973	78	+0.3400	-.151	.0607
31	+3.2594	+1.247	1.6822	79	+0.3437	-.062	.0304
32	+2.8908	+.791	1.4291	80	+0.1796	+.125	.0371
33	+2.6271	+.976	1.1692	81	+0.0142	+.677	.0510
34	+3.8848	+1.572	2.2383	82	-0.3185	+1.303	.1435
35	+4.0970	+1.487	2.2931	83	-1.2651	+2.282	.3075
36	+4.0145	+.774	2.6150	84	-2.2565	+2.585	.2747
37	+3.1967	+.507	1.7535	85	-2.9480	+2.107	.1806
38	+3.3720	+.557	2.0430	86	-2.0757	+.611	.0304
39	+3.7059	+.263	2.3061	87	+0.2995	-.351	.1135
40	+3.4366	+.228	1.9207	88	+2.1623	-.930	.1427
41	+3.5250	-.143	2.1628	89	+3.7499	-1.583	.2589
42	+3.7467	+.105	2.2530	90	+5.6841	-2.721	.8462
43	+3.5602	+.286	2.0595	91	+8.5665	-1.046	1.9435
44	+3.6849	+.341	2.3030	92	+13.3298	-5.823	3.2516
45	+3.6142	-.035	2.1109	93	+15.5338	-3.078	2.4864
46	+3.7933	+.006	2.3098	94	+14.8072	-5.583	6.2300
47	+3.1634	-.105	2.0034	95	+9.9370	+.049	9.2788
48	+2.2481	-.906	1.4246	96	+7.7571	-2.721	9.2932
				97	+4.4383	-4.950	9.8897

X.C. Plot of coefficients vs Z.

